

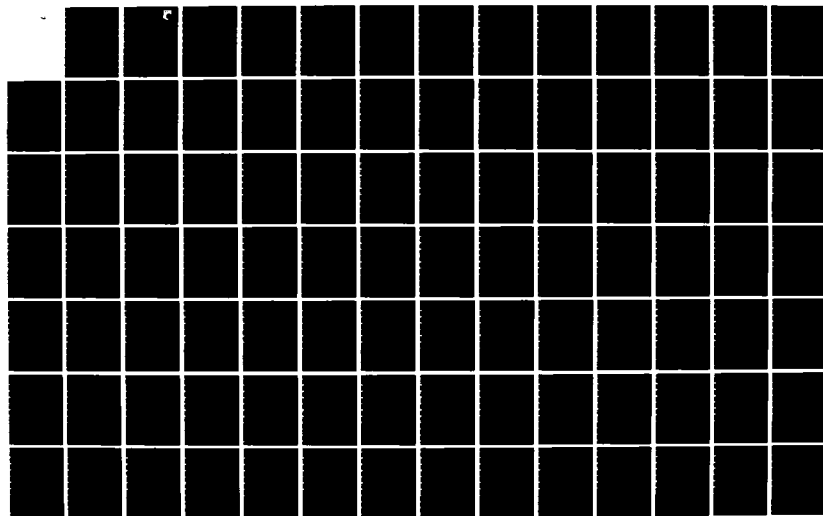
AD-A138 865

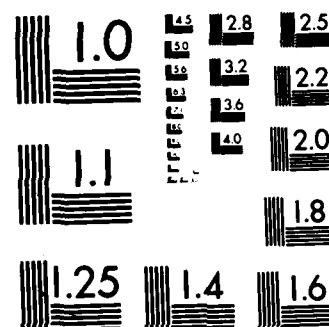
AN EXPERIMENTAL AND ANALYTIC STUDY OF THE FLOW SUBSONIC
WIND TUNNEL INLET. (U) NOTRE DAME UNIV IN DEPT OF
AEROSPACE AND MECHANICAL ENGINEERING. S M BATILL ET AL.
OCT 83 AFMNL-TR-83-3109 F33615-81-K-3008 F/G 20/4

1/2

UNCLASSIFIED

NL





MICROCOPY RESOLUTION TEST CHART
NATIONAL BUREAU OF STANDARDS-1963-A

AD A1 38865

AFWAL-TR-83-3109

(12)



AN EXPERIMENTAL AND ANALYTIC STUDY OF THE FLOW IN SUBSONIC
WIND TUNNEL INLETS

Dr. Stephen M. Batill
Mr. Michael J. Caylor
Mr. Joseph J. Hoffman
Department of Aerospace and Mechanical Engineering
University of Notre Dame
Notre Dame, Indiana 46556

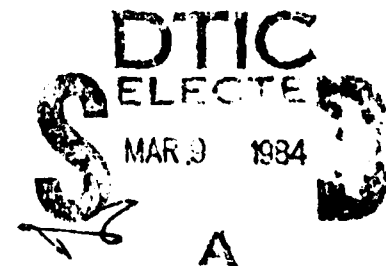
October 1983

Final Report for Period January 1981 - June 1983

Approved for public release; distribution unlimited.

DTIC FILE COPY

FLIGHT DYNAMICS LABORATORY
AIR FORCE WRIGHT AERONAUTICAL LABORATORIES
AIR FORCE SYSTEMS COMMAND
WRIGHT-PATTERSON AFB, OHIO 45433




84 03 09 003

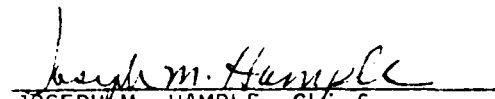
NOTICE

When Government drawings, specifications, or other data are used for any purpose other than in connection with a definitely related Government procurement operation, the United States Government thereby incurs no responsibility nor any obligation whatsoever; and the fact that the government may have formulated, furnished, or in any way supplied the said drawings, specifications, or other data, is not to be regarded by implication or otherwise as in any manner licensing the holder or any other person or corporation, or conveying any rights or permission to manufacture, use, or sell any patented invention that may in any way be related thereto.

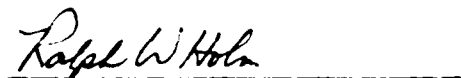
This technical report has been reviewed and is approved for publication.

Publication of this report does not necessarily constitute Air Force approval of the report's findings and conclusions. It is published only for the stimulation and exchange of ideas.


WILEY D. WELLS
Project Engineer


JOSEPH M. HAMPLE, Chief
Experimental Engineering Branch
Aeromechanics Division

FOR THE COMMANDER:


RALPH W. HOLM, Colonel, USAF
Chief, Aeromechanics Division
Flight Dynamics Laboratory

"If your address has changed, if you wish to be removed from our mailing list, or if the addressee is no longer employed by your organization please notify AFWAL/FIMN, W-PAFB, OH 45433 to help maintain a current mailing list."

Copies of this report should not be returned unless return is required by security considerations, contractual obligations, or notice on a specific document.

Unclassified

SECURITY CLASSIFICATION OF THIS PAGE (When Data Entered)

REPORT DOCUMENTATION PAGE		READ INSTRUCTIONS BEFORE COMPLETING FORM
1. REPORT NUMBER AFWAL-TR-83- 3109	2. GOVT ACCESSION NO. A138863	3. RECIPIENT'S CATALOG NUMBER
4. TITLE (and Subtitle) AN EXPERIMENTAL AND ANALYTIC STUDY OF THE FLOW IN SUBSONIC WIND TUNNEL INLETS		5. TYPE OF REPORT & PERIOD COVERED Final Jan. 1981 - June 1983
		6. PERFORMING ORG. REPORT NUMBER
7. AUTHOR(s) Stephen M. Batill Michael J. Caylor Joseph J. Hoffman		8. CONTRACT OR GRANT NUMBER(s) F33615-81-K-3008
9. PERFORMING ORGANIZATION NAME AND ADDRESS Department of Aerospace and Mechanical Engr. University of Notre Dame Notre Dame, IN 46635		10. PROGRAM ELEMENT, PROJECT, TASK AREA & WORK UNIT NUMBERS 61102F 2307-NH-47
11. CONTROLLING OFFICE NAME AND ADDRESS		12. REPORT DATE October 1983
		13. NUMBER OF PAGES 172
14. MONITORING AGENCY NAME & ADDRESS (if different from Controlling Office) FLIGHT DYNAMICS LABORATORY (AFWAL/FIMN) AIR FORCE WRIGHT AERONAUTICAL LABORATORIES (AFSC) WRIGHT-PATTERSON AIR FORCE BASE, OH 45433		15. SECURITY CLASS. (of this report) UNCLASSIFIED
		15a. DECLASSIFICATION, DOWNGRADING SCHEDULE
16. DISTRIBUTION STATEMENT (of this Report) Approved for public release: Distribution unlimited.		
17. DISTRIBUTION STATEMENT (of the abstract entered in Block 20, if different from Report)		
18. SUPPLEMENTARY NOTES		
19. KEY WORDS (Continue on reverse side if necessary and identify by block number) Wind Tunnel Design Three-Dimensional Internal Flows Smoke Flow Visualization		
20. ABSTRACT (Continue on reverse side if necessary and identify by block number) → This report documents an experimental and numerical study of the aerodynamic behavior of three dimensional subsonic wind tunnel inlets. The purpose of the study was to develop a rational procedure for the aerodynamic design of high contraction ratio, subsonic wind tunnel inlets. Of particular concern were those factors associated with the inlet design which would influence the use of smoke flow visualization techniques.		

2.7

This three-phased study included the following tasks:

- (1) The development and assessment of aerodynamic calculation techniques suitable for subsonic wind tunnel inlet flow-field predictions. Both a surface panel technique and a finite difference field solution were developed.
- (2) The design and fabrication of an indraft tunnel inlet which could be used to visualize the flow within the inlet. Measurement of field velocities, wall pressure and turbulence with the inlet for correlation with the prediction techniques.
- (3) The development of design criteria based on the numerical prediction techniques for three dimensional inlets with contraction ratios in a range of 10-40. Four basic parameters were used to characterize the inlet flow fields and a series of design charts are presented for matched cubic wall geometries.



Accession For	
NOTE: CHAS	
100-101	
100-101-101	
100-101-101	
By	
Available for	
Dist	Notes
A1	

PREFACE

The work documented in this report was performed by the Department of Aerospace and Mechanical Engineering, University of Notre Dame, for the Department of the Air Force, Air Force Wright Aeronautical Laboratories (AFSC), Flight Dynamics Laboratory, Wright-Patterson Air Force Base, Ohio under Contract F-33615-81-K-3008. The Principal Investigator on the project was Dr. Stephen Batill.

The authors wish to acknowledge the contributions of the University of Notre Dame's Computing Center and Department of Aerospace and Mechanical Engineering for the partial support of the graduate research assistants who participated in this effort and for most of the computing resources used during this program. They also wish to thank those members of the Supersonic Tunnel Association and the Subsonic Aerodynamic Testing Association who responded to an informal survey conducted during the early phases of this work. The authors also would like to thank Drs. Terrence Akai and Alan Cain of the Department of Aerospace and Mechanical Engineering, University of Notre Dame, for their valuable comments with regard to various aspects of the numerical studies performed during this study. Mr. Wiley C. Wells was Project Engineer for this effort, and his helpful assistance is also acknowledged.

The report documents work conducted from January 1981 to June 1983. The final report was submitted in July 1983.

TABLE OF CONTENTS

<u>Section</u>	<u>Page</u>
I	INTRODUCTION.
	1
	Wind Tunnel Inlets
	2
	Project Overview
	13
II	FLOW FIELD ANALYSIS
	14
	Previous Work.
	14
	Source Panel Method.
	19
	Finite Difference Method
	32
III	EXPERIMENTAL PROGRAM.
	40
	Objectives of Experimental Program
	43
	30:1 Contraction Ratio Inlet
	46
	Exit Flow Uniformity
	47
	Pressure Gradients and Separation.
	48
	Turbulence
	49
	Boundary Layer Behavior.
	52
	Influence of Damping Screens
	52
	Effect of Screen Step.
	55
	Effect of Noise.
	56
	Flow in the Corner Region.
	59
	Proximity Effects.
	60
	Comparison of Numerical Experimental Results . .
	61
	Final Thoughts
	62
IV	INLET DESIGN DATA
	64
	Inlet Geometry
	65
	Design Parameters.
	67

TABLE OF CONTENTS (cont.)

<u>Section</u>	<u>Page</u>
Inlet Design Charts.	71
V CONCLUSIONS AND RECOMMENDATIONS	75
References	80

LIST OF ILLUSTRATIONS

<u>Figure</u>	<u>Title</u>	<u>Page</u>
1	Schematic of Two-Dimensional Inlet Geometry - Matched Cubic	84
2	Schematic of Three-Dimensional Inlet Geometry	85
3	Two-Dimensional Panel Solution, Inlet 1, CR = 7.43	86
4	Two-Dimensional Panel Solution, Inlet 2, CR = 3.0	87
5	Exit Plane Velocity Distribution, Two-Dimensional Panel Solution	88
6	Three-Dimensional Paneling Results, Panel Scheme #3	89
	a. Paneling	89
	b. Leakage	89
	c. Pressure Coefficients	90
7	Three-Dimensional Paneling Results, Panel Scheme #5	91
	a. Paneling	91
	b. Leakage	91
	c. Pressure Coefficients	92
8	Three-Dimensional Paneling Results, Panel Scheme #6	93
	a. Paneling	93
	b. Leakage	93
	c. Pressure Coefficients	94
9	Exit Plane Velocity Profile Dependence on Sink Panel Location	95
10	Entrance Plane Velocity Profile Dependence on Upstream Paneling	96
11	Entrance and Exit Plane Velocity Profiles	97
12	Pressure Coefficients $C_{p_{u_e}}$, for Finite Difference Solution	98

LIST OF ILLUSTRATIONS (cont.)

<u>Figure</u>	<u>Title</u>	<u>Page</u>
13	Pressure Coefficient, $C_{p_{u_i}}$, for Finite Difference Solution	99
14	Leakage Calculation, Finite Difference Solution	100
15	Finite Difference Solution Convergence, Volume Flux Calculation	101
16	Flow Visualization Inlet Wall Contour	102
17	Photograph of Experimental Facility	103
18	Five-hole Probe and Hot-wire Data Locations	104
19	Five-hole Probe Data, Port 5	105
20	Lateral Wall Pressure Coefficients	106
21	Experimental Wall Centerline Velocity Ratios	107
22	Experimental Corner Region Velocity Ratios	108
23	Flow Visualization of Entrance Plane Wall Discontinuity ("Step")	109
	a. Entire Inlet	109
	b. Close-up	109
24	Experimental Axial Turbulence Intensities	110
25	Experimental RMS Velocities	111
26	Turbulence Frequency Spectra	112
	a. Station 1	112
	b. Station 4	112
27	Smoke Flow Visualization Along Inlet Wall	113
	a. Screens Flush	113
	b. Screen Step	113

LIST OF ILLUSTRATIONS (cont.)

<u>Figure</u>	<u>Title</u>	<u>Page</u>
28	Five-Hole Probe Data, Port 1	114
	a. Velocities	114
	b. Pitch Angles	114
29	Effect of Screens on Centerline Velocities	115
30	Axial Turbulence Intensities, Variation with Additional Screens	116
31	RMS Velocities, Variation with Additional Screens	117
32	Turbulence Frequency Spectra	118
	a. 0 Screens, Station 11	118
	b. 1 Screen, Station 1	118
33	Flow Visualization of Turbulence Screen Influence	119
	a. 2 Screens	119
	b. 4 Screens	119
	c. 11 Screens	119
34	Five-Hole Probe Velocity Measurements, Port 4	120
35	Five-Hole Probe, Pitch Angles, Port 4	121
36	RMS Velocities at Station 1	122
37	RMS Velocities at Station 4	123
38	Turbulence Frequency Spectra, Station 4	124
	a. $V_{TS} = 53.0$ fps	124
	b. $V_{TS} = 150$ fps	124
39	Turbulence Frequency Spectra, Station 4	125
	a. 0 Screens, $V_{TS} = 150$ fps	125
	b. 11 Screens, $V_{TS} = 141$ fps	125

LIST OF ILLUSTRATIONS (cont.)

<u>Figure</u>	<u>Title</u>	<u>Page</u>
40	Velocities Near Inlet Wall	126
41	Comparison of Experimental and Numerical Results, Wall Centerline	127
42	Comparison of Experimental and Numerical Results, Corner Region	128
43	Comparisons of Experimental and Numerical Results, Downstream Pressures	129
44	Comparison of Experimental and Numerical Velocity Profile	130
45	Pressure Distribution, CR = 10	131
	a. $L/H_i = 0.80, X = 0.20$	131
	b. $L/H_i = 0.80, X = 0.80$	132
	c. $L/H_i = 1.40, X = 0.20$	133
	d. $L/H_i = 1.40, X = 0.80$	134
46	Pressure Distributions, CR = 40	135
	a. $L/H_i = 0.80, X = 0.20$	135
	b. $L/H_i = 0.80, X = 0.80$	136
	c. $L/H_i = 1.40, X = 0.20$	137
	d. $L/H_i = 1.40, X = 0.80$	138
47	Inlet Design Charts, CR = 10, H/W = 1.0	139
	a. \tilde{u}_i vs X	139
	b. \tilde{u}_e vs X	140
	c. C_{p_i} vs X	141
	d. C_{p_e} vs X	142
48	Inlet Design Charts, CR = 25, H/W = 1.0	143
	a. \tilde{u}_i vs X	143

LIST OF ILLUSTRATIONS (cont.)

<u>Figure</u>	<u>Title</u>	<u>Page</u>
	b. \hat{u}_e vs X	144
	c. C_{p_i} vs X	145
	d. C_{p_e} vs X	146
49	Inlet Design Charts, CR = 25, H/W = 1.20	147
	a. \tilde{u}_i vs X	147
	b. \hat{u}_e vs X	148
	c. C_{p_i} vs X	149
	d. C_{p_e} vs X	150
50	Inlet Design Charts, CR = 25, H/W = 1.67	151
	a. \tilde{u}_i vs X	151
	b. \hat{u}_e vs X	152
	c. C_{p_i} vs X	153
	d. C_{p_e} vs X	154
51	Inlet Design Charts, CR = 40, H/W = 1.0	155
	a. \tilde{u}_i vs X	155
	b. \tilde{u}_e vs X	156
	c. C_{p_i} vs X	157
	d. C_{p_e} vs X	158

LIST OF SYMBOLS

C_{p_i}, C_{p_e}	Inlet Design Parameters (Eqns. 11)
$C_{p_{u_i}}, C_{p_{u_e}}$	Pressure coefficients based on mean entrance and exit plane velocities (Eqns. 7 and 8)
CR	Contraction Ratio = $(H_i W_i)/(H_e W_e)$
h	Local height along inlet axis
H_i	Inlet height at entrance plane
H_e	Inlet height at exit plane
L	Inlet length
PSD	Power Spectral Density (turbulence spectra)
V_{max}	Maximum velocity within the inlet
V_{min}	Minimum velocity within the inlet
U_{m_e}	Mean axial velocity at exit plane
U_{m_i}	Mean axial velocity at entrance plane
\tilde{u}_e	Exit plane velocity variation (Eqn. 9)
\tilde{u}_i	Entrance plane velocity variation (Eqn. 9)
u'^2	Root mean square of fluctuating velocity component
V	Local value of velocity (specific axial location)
V_c	Wall velocity at entrance plane, centerline
V_{cor}	Wall velocity at entrance plane, corner
W_i	Inlet width at entrance plane
W_e	Inlet width at exit plane
x, y, z	Cartesian coordinates
x_m	Axial location of cubic polynominal match point
X	Non-dimensional match point = x_m/L

LIST OF SYMBOLS (cont.)

α	Angle between the component of velocity in the x-z plane and the x axis
β	Angle between the component of velocity in the x-y plane and the x axis
ξ, η, ζ	Transformed spacial coordinates
ϕ	Velocity potential

Subscripts

e	Value associated with the exit plane
i	Value associated with the entrance plane
ℓ	Value associated with the inlet centerline
TS	Value associated with the test section

SUMMARY

This report documents an experimental and numerical study of the aerodynamic behavior of three-dimensional, subsonic wind tunnel inlets. The purpose of the study was to develop a rational procedure for the aerodynamic design of high contraction ratio, subsonic wind tunnel inlets. Of particular concern were those factors associated with the inlet design which would influence the use of smoke flow visualization techniques.

This three-phased study included the following tasks:

- (1) the development and assessment of aerodynamic calculation techniques suitable for subsonic wind tunnel inlet flow-field predictions. Both a surface panel technique and a finite difference field solution were developed.
- (2) the design and fabrication of an indraft tunnel inlet which could be used to visualize the flow within the inlet. Measurement of field velocities, wall pressure and turbulence within the inlet for correlation with the prediction techniques.
- (3) the development of design criteria based on the numerical prediction techniques for three-dimensional inlets with contractions ratios in a range of 10-40. Four basic parameters were used to characterize the inlet flow fields and a series of design charts are presented for matched cubic wall geometries.

SECTION I

INTRODUCTION

There has been surprisingly little effort expended by the aeronautical engineering community towards the aerodynamic design of one of their most valuable tools, the wind tunnel. To quote from Bradshaw and Pankhurst (Ref 1), "Wind tunnel design lies somewhere between an art and a science, with occasional excursions into propitiatory magic." This is not to say that most current wind tunnel facilities are not well-designed, or operate in a less than satisfactory manner, but on occasion the development of these facilities has been a painful trial and error procedure.

There are two good reasons for this current state of affairs. First, the aerodynamics of the wind tunnel itself are quite complex. There have been numerous studies directed at inlet, fan and diffuser design as well as techniques developed for turning and conditioning the flow in a wind tunnel. Each of these areas address some of the most challenging of current problems in fluid mechanics such as three-dimensional flows, unsteady and separating boundary layers and the structure and management of turbulence. These are all very sophisticated problems which will present challenges to aerodynamicists for years to come. A second, more subtle reason, is that often the facility designer is somewhat inexperienced with the many phases of tunnel design since most organizations do not regularly design and fabricate wind tunnels. The designer, therefore, must often rely on other's experience and proven methods and for that reason there has been little revolution, and only a minor amount of evolution, in tunnel

design in recent years. (The authors wish to stress this is not universally true. There have been numerous significant advances in tunnel designs, particularly in the areas of high speed, or high Reynolds number facilities. The authors' comments are directed towards the class of "conventional," subsonic tunnels.)

This report is directed toward aspects of the aerodynamic design of high contraction ratio, subsonic wind tunnel inlets. Any future reference in the report to inlets will be with regard to subsonic wind tunnels unless explicitly stated otherwise. The report documents a number of tasks whose goal was to better understand those factors which influence the inlet performance and to develop a rational procedure whereby a designer could arrive at a reasonable design of a subsonic wind tunnel inlet. As will be discussed in depth later in the report, the emphasis was on three-dimensional inlets whose contraction ratio (entrance to exit area ratio) was greater than 10. Inlets of this size are generally referred to as high contraction ratio inlets and are found on many types of subsonic tunnel designs.

Wind Tunnel Inlets

The purpose of the wind tunnel inlet is to align and accelerate the fluid into the test section so that proper and controllable test conditions can be generated. The contraction section is often considered in conjunction with any flow conditioning devices such as screens, gauze or honeycomb. Both the conditioning devices and the area reduction associated with the contraction have significant influence on the flow within the wind tunnel. They must be considered independently since their effects are quite different. The management of spatial and

temporal irregularities in the flow field, both small scale (turbulence) and large scale (swirl) and the elimination of such irregularities are influenced in part by the inlet design.

Before discussing the role of the inlet in the tunnel performance, some attention must be directed toward the type and purpose of the wind tunnel facility. There are two basic types of subsonic wind tunnels, the open-circuit type and the closed-circuit type. These may range in size from the table top demonstration tunnel to the largest of the government and industry facilities. A more complete description of the types as well as details on other aspects of the tunnel design can be found in Reference 1.

The function of the inlet in each type of tunnel is somewhat different. In the indraft tunnel (open circuit with fan downstream of test section), the air is entrained from the region around the inlet and therefore, can be influenced by wind, objects, motion, etc. in the vicinity of the entrance to the inlet. Some of these factors can be controlled and some cannot. The inlet serves the purpose of aligning and accelerating the air and it must be able to cope with various types of upstream conditions. This is often accomplished through the use of various flow management devices but the aerodynamics of the inlet, the surrounding fluid and the flow management devices are closely coupled. The contraction ratios on this type of tunnel are usually rather high with some recent designs using contractions as high as 150⁽²⁾.

The inlet on the blowdown tunnel (i.e., an open circuit tunnel with the fan upstream of the inlet and test section) and on the closed circuit tunnel encounters different inflow conditions. The disturbances

created by the fan, diffuser, turning vanes and all other hardware that is upstream of the inlet are present at the entrance to the inlet. The inlet is not intended to eliminate these disturbances and in certain cases can actually amplify their influence. There are numerous studies associated with the influence of area contractions on the development or decay of grid or isotropic turbulence (3-6) but in all cases these have dealt with cases in which the scale of the turbulence was much smaller than the scale of the region of the flow. The effect of the inlet on the large scale disturbances is still a matter for future research.

Inlet design on all subsonic facilities must be approached from the point of view that a well designed inlet will not compensate for problems associated with other sections of the tunnel but an inadequately designed inlet can create significant problems and degrade the tunnel performance. The impact of the influence of the inlet design on overall tunnel performance seems to vary with both the type of facility and with personal experience. Opinions seem to range from those who believe that almost any inlet contour which is "reasonable" will perform in an adequate fashion, (and obviously the term reasonable is very experience oriented) to the comments made in Reference 10 in which the authors state, "the contraction is perhaps the most critical of the various subsections from the design point of view."

Prior to a more detailed discussion of some aspects of the physics of the flow in wind tunnel contraction sections, it is useful to consider how the inlet design influences or is influenced by the overall facility design. The tunnel design will most likely start with decisions relative to the type of testing and the size of the test

section which will be required for certain types of models. Since subsonic tunnels often deal with scale model flight vehicles, the matching of important scaling parameters, such as Reynolds number, will influence the size and maximum speeds required in the test section. The selection of tunnel type, either open or closed circuit, is often dictated by the type of testing to be conducted, power requirements and, quite often, by the overall size of the facility. It is not unlikely for the overall length and width of a wind tunnel to be an order of magnitude greater than the respective length, width and height of the test section. It is at this point where the inlet begins to influence the basic design of a tunnel. The selection of the inlet contraction ratio, where typically bigger is considered better, will significantly influence the overall size of the tunnel as well as set performance parameters, such as velocities in the plenum or stilling chambers, and subsequent power requirements. The remaining inlet parameters which must then be determined are length, cross-sectional geometry and finally, wall contour. How does the selection of these parameters influence the tunnel performance? Before this can be determined one needs to establish what inlet parameters influence the wind tunnel performance characteristics and which of the inlet parameters are most important.

The primary function of the inlet is to modify the velocity within the tunnel through a reduction in cross-sectional area. In a subsonic wind tunnel inlet, the presence of the contraction is felt both upstream and downstream of the inlet. Consider the case of a closed circuit tunnel with a plenum of constant cross-sectional area upstream of the

inlet. In the plenum, the desired situation is for uniform, low velocity flow. This is where screens and honeycomb are located so that low velocities are required to maintain small pressure drops across the screens and thus minimize power requirements. The fluid in the center of the section "senses" the upcoming area reduction and begins to accelerate. In order to satisfy conservation of mass, the flow near the walls decelerates in the constant or even mildly decreasing area region near the entrance to the inlet. The resulting decrease in velocity brings about an adverse pressure gradient along the walls and particularly in the corners of the inlet. The boundary layer developing along the walls is then subjected to an adverse pressure gradient and, depending upon the velocity distribution in the boundary layer and the strength of the adverse pressure gradient, separation may occur. The separation can result in unsteady free shear layers and recirculating regions which can effectively alter the geometry of the inlet. This type of inlet separation can be intermittent and thus bring about significant unsteadiness in the test section.

As the flow continues to accelerate into the inlet, the fluid near the wall encounters large convex curvature and, near the exit plane of the inlet, the velocity along the wall can become greater than the mean exit velocity. This fluid near the wall must then be decelerated as it enters the test section which brings about another region of adverse pressure gradient and provides another opportunity for boundary layer separation. These problems are increased in three-dimensional inlets where the streamwise curvature in the corner region is greater than the curvature along either of the walls themselves. The magnitude of the

adverse pressure gradients can be reduced by lengthening the contraction but this leads to increased boundary layer growth, reduced boundary layer stability and increased tunnel size and cost.

The nonuniformity of the velocity near the entrance plane of the inlet also creates difficulty with respect to the design and function of the screens and honeycomb upstream of the inlet. Nonuniformity at the exit plane influences the length of the test section and possibly the allowable model locations. The inlet is often characterized by a length to height (L/H) or a length to effective diameter (L/D) ratio. This ratio has shown to have an influence on the turbulence reduction associated with both the screens and the inlet. Some of the other problems which must be considered when designing the inlet are:

- (1) influence on the acoustic environment within the tunnel;
- (2) the development of longitudinal (Goertler) vortices within the regions of concave curvature;
- (3) the influence of changing cross sectional geometry (i.e. circular to rectangular, square to hexagonal, etc.) on the wall boundary layer.

Each of these will be influenced by the inlet design. Currently there is little information available which can be directly applied by the facility designer, whereby the influence of these effects on the performance of a particular facility can be predicted. Probably the typical situation is one in which the designer "hopes" such effects will not be significant and if problems arise subsequent to the construction of the facility, he must then resort to a number of traditional fixes.

As a part of the research program documented in this report, a

survey of users and designers of wind tunnel facilities was conducted. This survey was distributed through the member organizations of the Subsonic Aerodynamic Testing Association (SATA) and the Supersonic Tunnel Association (STA). Although the survey and its results will not be presented in detail within this report, the responses to the survey were extremely helpful in developing certain aspects of the research program, as well as indicating a strong interest in the development of improved design techniques. The authors have taken the liberty of attempting to summarize some of the survey comments without reference to particular opinions of individuals or organizations. The survey was directed towards techniques used in the inlet design and problems encountered in facility development related to the inlet.

Many different techniques have been used to design the inlets for the subsonic tunnels in use today. These techniques range from "sketching" a smooth curve to detailed three dimensional flow field calculations and extensive model and prototype testing. There appears to be no consensus as to the "best" methods available. Later in the report a brief overview of some of the analytic techniques which have been used will be discussed, but in almost all cases mentioned in the survey responses, the results of an analysis were tempered by the experience of the designer.

The influence of the inlet on the overall facility design was obviously dependent upon the experience of the particular user. Numerous organizations had encountered no "problems" in the operation of their facility. Some, often those with older facilities, knew little of their tunnel's inlet characteristics and were pleased with the

performance of their tunnels. Others, particularly those who had made very detailed measurements of test section flow quality such as steadiness, uniformity and angularity were more concerned about the possible influence of the inlet on these characteristics. When turbulence levels were of primary concern, much more emphasis was given to the contraction design. Often the concern was directed towards the three dimensional boundary layer development within the inlet. The extreme cases were those experienced by designers, who after completion of a facility, were forced to redesign and rebuild an inlet in order to correct performance problems. The dominant problems were those associated with large scale separation within the inlet and the resulting unsteadiness and velocity nonuniformity within the test section. One final item resulting from an evaluation of the survey responses, indicated a lack of experimental data available on wind tunnel inlet performance.

These responses were prepared by users of a wide range of facilities, from automotive tunnels to detailed calibration facilities. This diversity in application resulted in the diversity of responses. The purpose of this study, though general in its focus on the development of methods for predicting inlet flow fields, was specific with regard to the class of special wind tunnels for which the methods were to be applied. There has been significant effort at the University of Notre Dame over the last forty years directed towards the development of facilities and techniques for smoke flow visualization (2, 11, 12). The work of Brown, and the success and failures of others who have developed smoke visualization tunnels, has demonstrated the importance

of the inlet design for this special class of subsonic wind tunnels. The most successful type of smoke visualization in use today utilizes the indraft subsonic wind tunnel with a high contraction ratio (≈ 20) inlet and numerous turbulence management devices. The smoke is generated outside of the tunnel and introduced upstream of the inlet in the region of very low velocity flow. Other techniques in other types of tunnels, such as the smoke-wires or smoke wands are much more limited with respect to their applicability due to limitations on speed, interference effects and smoke quantity. In the past few years, there has been a renewed interest in the use of smoke visualization for many different aerodynamics applications.⁽¹⁴⁻¹⁵⁾ This interest has brought about the design and fabrication of a number of new facilities. Most current flow visualization tunnels are relatively small in scale with test sections on the order of 2' x 2'. There is interest in extending these techniques to significantly larger facilities ⁽¹⁶⁾ as well as to much higher velocities.⁽²⁾ For these larger facilities, the designer must be much more sensitive to the inlet design. Larger contraction ratios result in larger overall facilities and associated installation and operation costs. More importantly, the larger the tunnel, the longer the residence time of the smoke filaments in the inlets. These smoke filaments are then allowed to diffuse or be disturbed for a longer period of time and this increases the difficulty associated with introducing coherent smoke streaklines into the desired locations within the test section. The design criteria related to the inlet on a smoke visualization tunnel are, therefore, different and often more demanding than those for other types of facilities. The effects of the inlet and

the turbulence management devices on an indraft tunnel are not easily separated. Although this report will focus on the inlet design, this fact must be recognized.

The designer eventually needs to be able to establish a set of criteria to guide his design decisions as well as a method for quantifying those criteria. Terms such as adequate, good, reasonable, etc. are typically useless in the design process. The following are the criteria upon which inlet designs can be based:

1. Size
 - a) Height
 - b) Width
 - c) Length
2. Quality of Flow
 - a) Steadiness
 - b) Uniformity
 - c) Angularity
 - d) Turbulence level and content
 - e) Susceptibility to separation
 - f) Boundary layer growth
 - g) Maintain coherent smoke streaklines (*Special facility requirement)
3. Cost
4. Ease of construction

The geometric criteria (height, length, width) are easily quantified and upper bounds on allowable values are often set by the buildings which will house the facility. The question of "how small?" then becomes

critical and will have an influence on cost and manufacturing.

The criteria associated with flow quality are more complex. They are related to the size and in some cases can be quantified in the form of velocity profiles, turbulence intensities and spectra and pressure distributions. There are actually only a few parameters which the designer can select from to achieve these design criteria. They are:

- a) Contraction ratio
- b) Cross-sectional geometry
- c) Length
- d) Wall contour

With so few parameters to select, it appears as if it should be a rather straightforward problem. Unfortunately there exists no direct correspondence between each of the design parameters and the design criteria. Two methods which have been used in the past involve a direct and an indirect approach. The indirect approach involves the definition of certain flow field parameters, most commonly the axial velocity distribution, and an attempt is made to determine the wall contour required to yield that velocity field. Depending upon the way in which the velocity field is defined there may or may not be a contour which provides satisfactory results. The direct approach involves the selection of a contour and then the subsequent determination of the flow field parameters. Such a method could be repeated until an acceptable design is achieved with respect to the selected criteria. A problem occurs in that there is an infinite number of possible cross sectional shapes and wall contours which could describe the geometry of the walls between the entrance and exit of the

inlet. The obvious solution is to select a particular family of wall contours, for which there are a reasonable number of parameters which describe the contour and then limit the inlet design to this family. This is the procedure adopted in this report. It is therefore limited by the suitability of the selected family of contours as well as by the ability to include and quantify all the appropriate design criteria.

PROJECT OVERVIEW

The goals of the research documented in this report were threefold. The phases of the study were: (I) identify a suitable aerodynamic prediction technique for analyzing the flow in fully three dimensional wind tunnel inlets; (II) design and fabricate a three-dimensional inlet to provide a "data point" for evaluation of the analysis methods as well as a facility for studying the physics of the inlet flow field; and (III) using the most appropriate prediction procedure, identified in Phase I and verified in Phase II, to develop a rational design procedure for a family of three-dimensional inlets. The following sections of the report discuss the results of each of these phases. Specific details of both the analysis methods and experimental procedures are not included because conventional techniques were used, and the methods are detailed in the appropriate references. The purpose of this effort was not so much to develop new analysis procedures or techniques, but to apply existing methods to enhance the understanding of an important engineering problem. Although the stated objective is to help define specific design guidelines for subsonic, three-dimensional wind tunnel inlets, it is recognized that the work only represents a small contribution to the further understanding of this complex design process.

SECTION II

INLET FLOW FIELD ANALYSIS

In order to develop an aerodynamic design of an inlet for a specific wind tunnel application, one would like to be able to predict the performance of the inlet and be able to evaluate that performance against a set of defined criteria. There are a number of current aerodynamic prediction methods which appear suitable for fully three dimensional, subsonic wind tunnel inlets. Two of these methods were evaluated as a part of this research program. Computer programs were developed using both a source panel, distributed singularity approach and a finite difference potential flow solution of Laplace's equation for inlets of arbitrary rectangular cross sections.

This section will discuss in a brief overview some earlier analytic work related to wind tunnel inlet aerodynamics and describe the application of the two methods to a particular family of inlet geometries. Both methods are discussed in some detail since each presents certain promise for use in future studies. The finite difference procedure was eventually selected for use in the development of the design data which will be presented in Section IV. The relative advantages of each approach will be presented in the discussion. It should be noted that these methods are not new, their applicability to this type of flow field has been demonstrated in the past but they have not been used to systematically study the parameters which influence the inlet flow fields.

Previous Work

The aerodynamic design of wind tunnel contraction cones has evolved over the years as somewhat of an inexact science. Around 1940 the first serious attempts were made at developing methods for the design of wind tunnel inlets. Much of the work at that time focused on solving the equation for incompressible, inviscid, and irrotational flow (i.e. the two-dimensional or axisymmetric form of the Laplace equation). The general solution method was to specify a centerline velocity distribution in terms of axial distance 'x' and then find a solution for the stream function in series form ⁽¹⁾. Tsien was the first to publish work based on this design philosophy ⁽¹⁷⁾. He proposed the design of an axisymmetric contraction with a monotonically increasing axial velocity. Szczeniowski solved the Stokes-Beltrami equation using a different axial velocity distribution. The resulting streamlines turned out to be functions of Bessel functions ⁽¹⁸⁾. In a similar method, Batchelor and Shaw examined the theoretical flow through an axisymmetric contraction by using a relaxation method for solving the governing differential equation ⁽¹⁹⁾. They were particularly interested in minimizing the adverse pressure gradients which occur in the inlet and exit regions of a contraction.

At about this same time Smith and Wang proposed an interesting technique for the design of a two-dimensional or axisymmetric contraction cone with a high degree of exit flow uniformity ⁽²⁰⁾. They made use of the exact analogy between the magnetic field that is created by two coaxial and parallel coils carrying electric current and the velocity field that is created by two corresponding ring vortices.

Several of the inlets that are in current use at the Notre Dame Aerospace Laboratory were designed using Smith and Wang's technique. These large, three-dimensional inlets were constructed by joining together walls with the same Smith and Wang two-dimensional wall contour. These inlets have proven very successful in providing the test section flow quality necessary for smoke flow visualization though there are problems in using smoke near walls or in corner regions of these tunnels (11).

Very few papers on wind tunnel contraction design were written in the ensuing years. It was not until the mid-70's that interest in contraction design was renewed. Recently several independent pieces of work have been published on the problem of inlet design with the aid of large scale computing machinery. These current works have attempted to overcome some of the deficiencies of the earlier work by adding more practical constraints to the inlet flow solutions. Many of the earlier design methods assumed potential flow in contractions of infinite length and gave little attention to real flow phenomena such as boundary layer growth along the inlet walls.

In one of the more recent works, Chmielewski specified a streamwise acceleration distribution. He used two parameters to choose the shortest contraction that avoided boundary layer separation. His two-dimensional study carried contraction design methodology beyond that of previous investigations by including a quantitative consideration of boundary layer behavior (21).

Borger used a polynomial of the fifth degree to describe the contraction contour. The coefficients of the polynomial were chosen to

produce the minimum length contraction that avoids boundary layer separation at both the inlet and exit and provides uniform flow at the exit plane. Borger's design calls for a slight expansion at the exit to improve exit flow uniformity (22).

The work of Mikhail and Rainbird was based on the hypothesis that it is possible to control the wall pressure development and the flow nonuniformity by controlling the wall curvature distribution. By optimizing this distribution, a short contraction can be used that keeps both the adverse pressure gradients and flow non-uniformity within tolerable ranges. They considered the optimum contraction to be the shortest one that satisfied specified flow quality requirements in the test section (23).

The papers by Chmielewski, Borger, and Mikhail and Rainbird have presented more reasonable requirements on exit flow uniformity and the influence of the boundary layer on the inlet flow field. Two of the more significant of these later works, however, are those of Morel (24,25). Morel also viewed design as a search for the optimum wall shape leading to the minimum nozzle length required for a given purpose. He formulated a set of design criteria to judge flow qualities. Morel felt, like most other designers, that obtaining exit flow uniformity and avoiding separation were the two primary goals of the contraction design. In addition, he specified minimum contraction length and minimum exit boundary layer thickness as secondary goals to be satisfied. This set of criteria was used by Morel to develop his practical design technique.

Morel's two-dimensional and axisymmetric design methods are based

on the results of numerical solutions which were incorporated into a set of design charts which could be used in actual design studies. The contraction contours are formed by two cubic arcs joined at a common point called the match point. This match point is the single parameter used in defining Morel's family of wall shapes. The design charts are used to determine the required contraction length and the position of the match point in terms of allowable pressure coefficients used to indicate the susceptibility of the inlet to boundary layer separation. These pressure coefficients are determined by boundary layer and flow uniformity requirements. The match point, the contraction ratio, and the contraction inlet height are the three values needed to completely define the geometry of one of the matched cubic inlets.

All of the methods that have been reviewed have dealt with the design of two-dimensional or axisymmetric contraction cones. In reality, however, most practical inlets are three-dimensional with square or rectangular cross-sections. Expanding a two-dimensional design technique to account for three-dimensional flow effects in wind tunnel contractions has proven to be a difficult task, even with today's advanced computing capabilities. The most significant problems in three-dimensional inlets with non-circular cross sections occur in the corner regions. In contractions of polygonal cross-sections, severe secondary flows can exist in the boundary layer near the corners. Even if such crossflows can be avoided, as in a "two-dimensional" contraction, the boundary layers in corner regions will be more susceptible to separation than the boundary layers near planes of symmetry (25).

To compromise between the difficulties of the construction of axisymmetric inlets and the undesirable boundary layer effects in the corners of rectangular contractions, some contractions have been built with octagonal cross-sections (26). For design purposes, it was assumed that both the potential flow and the boundary layer behave as in a contraction of circular cross-section. This design philosophy, however, is only a compromise. What is needed is a methodology for the design of three-dimensional contractions, regardless of cross-sectional shape. The underlying purpose of the current study was to work towards this goal by carrying out a combined analytical and experimental investigation to evaluate the performance of three-dimensional wind tunnel inlets.

Source Panel Method

The method of source panels is a surface paneling technique whereby the given body is replaced by a series of "source panels." These panels consist of a continuous distribution of uniform sources. Once the body is "paneled," a set of linear simultaneous equations is established by applying boundary conditions on each panel. From these equations the unknown source strength for each panel can be determined.

There are three reasons for choosing the method of source panels to calculate the flow-fields in wind tunnel inlets. First, panel methods have long been known to be very successful in modeling complex external flows, such as the flow about an entire airplane. Second, the method of source panels is well-suited to modeling arbitrary geometries. Finally, the boundary conditions associated with the source panel method are easy to apply. Even the boundary conditions at the entrance plane

for the indraft inlet can be modeled with relative ease.

There are disadvantages to the source panel method as applied to internal flows. The computer time required is not always justified by the quality of the results obtained. Also, there is the problem of "leakage" which appears to be unique to internal flow applications of the source panel method. The term "leakage" is used to describe the difficulty associated with satisfying the conservation of mass for a closed boundary, internal flow. The solid wall boundary condition is only satisfied at a finite number of points along the inlet wall, called control points which allows for the possibility for fluid to have a normal component to the wall between control points.

Most of the available literature describing source panel theory is restricted to external flows (27-31). Few works describe the source panel method as it is applied to internal flows (32-35). Hess and Smith (32) provide a detailed account of the theory associated with the source panel method. They also include a discussion of the internal flow case.

The purpose of the present work was to develop computer codes in two and three dimensions based on the source panel method (36). These programs were used to calculate the flow-fields in high contraction ratio inlets. The two-dimensional code was developed first to obtain experience in working with the method. The remainder of the work then focused on the development of the three-dimensional computer code. Once the programs were developed they were used to determine if the method of uniform source panels could be accurately applied to internal flows in wind tunnel inlets, and to establish the limitations of the method. Application of the program provided insight into the peculiarities of

the method itself, and allowed determination of the accuracy of the results. The computer program developed here was not used in parametric studies of design criteria for three-dimensional, high contraction ratio inlets, for reasons to be discussed later.

It is important to note that there are currently computer codes available which are significantly more sophisticated than the uniform quadrilateral source panel used in this study. Unfortunately these codes were not available during the study documented in this report and the results presented in this section are not indicative of the full capabilities of such paneling methods. Details of the development of the codes used in this work are presented in Reference 36.

As mentioned both two and three-dimensional programs were developed using the source panel method. The purpose of the two dimensional development was to gain experience with the use of panel methods for internal flow applications. The matched cubic family of wall contour's was used in both applications. Schematics of matched cubic contours with definition of some of the basic geometry used in this study are shown in Figures 1 and 2. The tunnel contours are defined using the following expressions.

$$H = H_e + (H_i - H_e) [1 - x^3/(X^2L^3)] \quad (1)$$

$$\text{for } x/L \leq X$$

and

$$H = H_e + (H_i - H_e) (1 - x/L)^3 / (1 - X)^2 \quad (2)$$

$$\text{for } x/L \geq X$$

Constant area sections extend upstream and downstream of the inlet. For the panel solution, the downstream end of the "test section" was

replaced with a series of uniform "sink" panels. These panels were used to drive the flow (such as done by the uniform flow in an external flow application). The strengths of the sinks are defined in order to satisfy uniform flow conditions at the sink panels. The applications of both programs, with emphasis upon the methods of paneling and significance of the results will be discussed in the following paragraphs.

The two-dimensional program provided information regarding the flow-field velocities, pressure coefficients, volume flux, and exit flow angularities for any two-dimensional wind tunnel inlet. The program input included specification of the inlet contour, the desired exit velocity, and the panel geometry.

The pressure coefficients are used to identify regions where adverse pressure gradients exist (i.e. regions of possible separation) as well as regions of flow acceleration. The two-dimensional program was used for the inlets shown in Figures 3 and 4. The plots of the pressure coefficient versus distance along the inlet centerline are also included on these figures. Note that the acceleration along the wall lags the acceleration at the centerline. Inlet 1 (Figure 3) has a very small adverse pressure gradient along the wall, as is illustrated by its smooth pressure coefficient plot. Inlet 2 (Figure 4) illustrates the effect of paneling sharp concave and convex corners. Near the concave corner ($x = 3.0$ inches) in Figure 4, the wall pressure coefficients increase noticeably in response to the concave corner, whereas the centerline pressure coefficients continue to decrease uniformly. Near the convex corner ($x = 5.0$ inches) the wall pressure coefficients

actually "overshoot" and the pressure coefficients become negative. The centerline pressure coefficients continue to decrease uniformly to the expected value of zero at the exit of this inlet.

Since the boundary conditions were only enforced at the control points on each panel there was no guarantee that the normal velocity was zero at other points on the panel. The net effect was that some of the flow "leaked" out of the inlet between the control points. The influence of satisfying the boundary conditions at only the control points was evaluated by determining if the volume flux through the inlet remained constant. This was accomplished by choosing two locations in the inlet and integrating the velocity profile over the cross-sectional area at each section. Results of such a test revealed that the largest percent difference between influx and outflux for the two-dimensional inlets was less than one percent for the inlets tested. This result was insensitive to the quality of the paneling scheme used, assuming that a "reasonable" number of panels were used to model the inlet. Between 60 to 200 panels were found to be "reasonable" for the two-dimensional inlets analyzed here. For the two-dimensional case the leakage problem was apparently not significant because even a small number of panels provided good definition of the wall geometry. However, it will be seen that leakage posed a substantial problem in the three-dimensional application.

An important part of the flow-field in a wind tunnel inlet occurs in the exit plane, since this is the flow that enters the test section. The preferred exit flow would be uniform and parallel to the test section axis. Most wind tunnel tests assume that these conditions

exist. The program developed here allowed for a detailed analysis of the flow angularities at the contraction exit. The u- and v-components (x and y directions, respectively) were known at the exit, allowing the calculation of the angle which the flow made with the horizontal in the exit plane. Figure 5 shows the velocity and direction of the flow in the exit plane of Inlet 1 (Figure 3).

Figure 5 also serves to illustrate the tendency of the flow to overspeed following a convex corner. The flow near the walls has a greater velocity than the flow at the centerline. If a straight channel (such as a test section) was then attached, the velocity profile would be expected to become uniform, implying that the velocity along the walls must decelerate. This velocity reduction would be accompanied by an adverse pressure gradient and possible separation.

The two-dimensional program described here was merely a foundation for the three-dimensional program. The two-dimensional program was effective in demonstrating that the source panel method can be used to calculate the flow-fields in two-dimensional wind tunnel inlets. The extension to three-dimensional inlets is considered next.

The extension to three-dimensions, though conceptually straightforward, required the development of a completely new code (36). The paneling schemes and input data definition became much more complex and though the data definition was simplified by the symmetry of the inlet, the actual computations were performed for a complete inlet.

Six tests were performed with the three-dimensional program to determine the effect of the paneling scheme and the accuracy of the results. The inlet used in these tests was a square cross-section

inlet whose wall geometry was defined by a matched cubic profile. This inlet was chosen in conjunction with the experimental investigation of the same inlet geometry. The six tests were divided into three groups of two. The first group had a constant x spacing, representing an inefficient paneling scheme. The second group had a variable x spacing, with the number of divisions in the x-direction being few. The third group also had variable x spacing, but in this case the number of divisions was large. The third case represented the most efficient paneling scheme. The first test in each group had few divisions in the y and z directions. The second test had more divisions in the y and z directions, resulting in a more refined paneling scheme. The tests are summarized in the following table.

PANELING TESTS

Test #	Paneling Scheme Used	Number of Panels
1	constant x spacing, few panels	160
2	constant x spacing, many panels	252
3	coarse, variable x spacing, few panels	160
4	coarse, variable x spacing, many panels	252
5	fine, variable x spacing, few panels	372
6	fine, variable x spacing, many panels	704

These tests were selected because they provided a wide range of paneling schemes with a minimal number of cases. The results for tests 3, 5 and 6 are included in Figures 6-8. The plots are in sets of three for each

test. The first plot in each set is the paneled first quadrant of the inlet. The second plot contains the percent leakage in the inlet as a function of longitudinal distance away from the exit plane. The third plot shows the pressure coefficients at the wall centerline and the inlet centerline versus the distance along the inlet centerline. These results will be discussed in detail below.

Figures 6a-8a show the paneling scheme for half of one face of the inlet. Only one face is included here because the inlet had a square cross-section. The paneling on the sink panel was automatically determined by the paneling of the inlet walls. The panel boundaries for the walls of the inlet were used as the boundaries for the sink panels. The panel method is "nominally exact" in that the inlet can be modeled perfectly if an infinite number of panels (i.e. a continuous distribution) could be used to represent the inlet surface ⁽³⁷⁾. Such a case would be computationally impossible. The limit is defined by the capabilities of the computer. There is no absolute maximum number of panels. The computing time is a function of the number of panels used, the size of the spacing in the x, y, and z directions when computing the flow-field velocities, and the accuracy with which the leakage in the inlet is calculated. Changing any of these variables alters the computing time. Although 704 panels was the maximum number of panels used in these tests, it is generally regarded that at least 1600 panels are needed to sufficiently describe an internal flow ⁽³⁸⁾. This is comparable to the detail achieved in the two-dimensional case when approximately 60 panels are used.

For the six tests described above, the sink panel plane was located

at a distance equal to 100 percent of the length of the inlet away from the exit plane. Velocities in regions near the sink panels, away from the control points, were highly irregular. This assumption was then analyzed by varying the length to the sink panels from 20 to 100 percent of the inlet's length. The exit plane velocities were then compared to determine what effect the sink panel plane location had on the exit flow. The results are plotted in Figure 9. This Figure illustrates the trends in the exit plane velocity with different distances to the sink panel.

It was expected that the velocities in the exit plane would converge as the sink panel distance approached infinity. It can be seen that the velocities for locations in the exit plane up to $y < 1.609$ inches away from the centerline of the inlet were convergent. For distances greater than this a relative degree of convergence was not observed until the sink panel location had reached 80 to 100 percent of the length of the inlet away from the exit plane. Based on these findings, a distance of greater than 100 percent of the length of the inlet could be used. The value of 100 percent was adequate for the present application. It should be noted that the value determined here may not be absolute. The amount of downstream section required for the sink panel plane may be dependent upon the geometry of the inlet and the specific application.

A similar argument to the one for the sink panel plane may be made with regard to the entrance to the contraction section. The addition of a straight section upstream of the inlet was investigated. Figure 10 illustrates the effect that adding an upstream channel, with a length

equal to 100 percent of the inlet length had on the flow velocities in the entrance plane. These values were compared to the entrance plane velocities for the case where there is no upstream channel. It can be seen from the Figure that the upstream section significantly altered the character of the flow-field near the wall in the entrance plane. The upstream section did not appreciably alter the flow velocities in the exit plane, though. The largest deviation in the velocity in the exit plane was less than 0.1 percent with the addition of the upstream channel. The six tests were executed without the upstream section. Again, this result only applies to the inlet used here. Other inlets may require an upstream section.

If the prediction technique is to provide useful information for inlet design studies, one must be able to compute accurate wall pressure distributions for subsequent evaluation of the boundary layer behavior. Determining detailed wall surface pressures is complicated with the panel method since the wall boundary conditions are satisfied only at panel control points and must be approximated between control points.

The wall pressure coefficients were determined by extrapolating the velocity to the wall assuming a linear velocity distribution near the wall. The velocity near the wall where two panels intersect at a convex angle tends to infinity. Therefore, if the two points used in the extrapolation were too close to a panel edge, their velocities might not have been truly representative of the values which would have actually existed at those locations. The resulting extrapolated velocity would then be invalid. A finer paneling scheme would reduce this effect by providing a more refined estimate for the velocities used in the

extrapolation. The general criterion is that a velocity should not be calculated within fifty percent of the distance defined by the characteristic dimension of the panel. The characteristic dimension is taken as the length of the longest diagonal. A velocity calculated at a distance away from the panel which is less than fifty percent of the length of the longest diagonal may not reflect the true velocity at that point. The effect of finer paneling is to reduce the characteristic dimension of each panel and increase the range of applicability of the extrapolation procedure (29).

The results shown in the plots confirm the above discussion. In each case, except Test 6, it is seen that there was one region where the wall pressure coefficients became irregular. The values did not decrease uniformly as expected. There was a sharp drop in the pressure coefficient followed by a sharp rise, and then resumption of the predicted uniformly decreasing pattern. In each instance this anomaly can be traced to regions near panel intersections where the inlet curvature was large. The subsequent experimental results indicated that the numerical solution in these regions was not correct, and in these regions the extrapolation technique was not valid.

The two-dimensional program predicted a downstream region where the velocities "overshoot" the expected values. This region was also predicted by the three-dimensional program. In Figure 8c it can be seen that the pressure coefficients became negative at about $x \approx 49.2$ inches, slightly past the end of the region of greatest convex curvature in the inlet. These results are consistent with the two-dimensional program. In the region between $x = 30.0$ inches and $x = 35.1$ inches there

appeared to be a slight adverse pressure gradient along the wall. As the centerline velocity increased in this region, the wall velocities were at the same time decreasing as they approached the region of high curvature. The result was an adverse pressure gradient. This adverse pressure gradient became less prominent as the paneling scheme became more refined.

The problem of leakage is the one factor which usually limits the results from the three-dimensional source panel program for internal flows. Leakage is the term used to describe the variation in volume flux in the inlet due to the "porous" nature of the source panels which model the inlet. The flow normal to the source panels is zero only at the control point on each panel. At all other points on the panel there may be flow through the panel, causing the volume flux to change. Figures 6b-8b are plots of the percent leakage in the inlet. The reference value was taken to be the volume flux in the exit plane, since this was the location where the exit velocity was prescribed. The negative values for the leakage indicated that the reference value had less volume flux than the point to which it was being compared. These plots clearly show that there is a serious leakage problem, since the magnitude of the leakage was on the order of fifty percent.

The regions of local minima evident on each plot occur at regions very near panel intersections. At panel intersections the velocities asymptotically approach zero or infinity, depending on whether the intersection results in a concave or convex corner, respectively.

The maximum percent leakage of the two-dimensional case was found to be approximately one percent. Leakage calculations for the three-

dimensional case showed that the maximum leakage in the inlet varied from sixty percent for the most inefficient paneling scheme, to thirty percent for the most "efficient" paneling scheme. The leakage problem is a serious one for the three-dimensional application of the source panel method to internal flows. The magnitude of the leakage can be controlled to some degree by the number of panels used as well as by the quality of the paneling scheme.

The problem of leakage was one of the primary motivating factors in the development of the so-called "higher-order" panel methods. In these methods, the source strengths are allowed to vary over the source panel. Also, more complex paneling schemes are used to obtain greater accuracy in modeling the inlet. Entire studies have been dedicated to the geometry problem alone (39). The discussion in this section demonstrates the importance of the paneling scheme on the flow-field calculations for a three-dimensional, high contraction ratio, wind tunnel inlet. The pressure coefficients and the leakage are directly dependent upon the quality of the paneling scheme used to represent the inlet. In turn, the quality of the paneling scheme is directly dependent upon the experience of the user and the limitations of the computing system.

The purpose for the development of the analysis procedures was to have a way in which both detailed field velocities and surface pressures could be predicted. Unless extreme panel detail is used or possibly higher order panels incorporated, the current procedure appeared inadequate. It still had the benefit of straight-forward implementation of the boundary conditions, particularly the inflow condition for the

inlet. This allowed for application to both indraft and closed circuit inlet concepts. Although no further development of the panel method was performed during this study, this work and that of others (2,27) has shown its' suitability for wind tunnel design and performance analysis. In an attempt to develop a reasonably efficient and accurate prediction scheme for a systematic study of a family of inlets, the panel method was not selected. The next section documents the development of a finite difference, field solution for the wind tunnel inlet flow.

Finite Difference Method

As an alternate to the source panel method previously discussed, a finite difference field solution to the incompressible inlet flow was developed. As in the case of the panel method, there are certain advantages and disadvantages to the finite difference approach. A number of the advantages are:

- (1) Complete field information is determined as a result of the calculation. This allows for easy determination of velocity profiles and wall pressures.
- (2) The symmetric nature of the three-dimensional inlet geometry is compatible with numerous transformation schemes which allow for simplification of the computational domain.
- (3) Although three-dimensional, the expected solution does not present strong gradients in field parameters so excessive grid detail, and thus computer storage, is not necessary.
- (4) There is a wealth of experience associated with the "numerical" aspects of the difference solutions.

There were also a number of anticipated disadvantages.

- (1) More detailed specification of the upstream and downstream boundary conditions are required in a manner much different from the panel approach. This appears to limit direct applicability to certain types of indraft configurations.
- (2) If spatial transformations were used to simplify the computational grid, it would complicate the simple field equation (Laplace's equation) and increase the computation times.
- (3) Computation times for the three-dimensional inlets could be significantly greater than the surface paneling techniques.

The decision to select one of the two analysis techniques was based on an evaluation of accuracy and computational efficiency. The following section describes the development of the finite difference method which was subsequently used to develop the inlet design criteria.

A number of pilot methods were investigated during the development of the final "production" code. Each code was based on the same basic concept, this was to describe the flow field in terms of a velocity potential which must satisfy Laplace's equation (Equation 3)

$$\phi_{xx} + \phi_{yy} + \phi_{zz} = 0 \quad (3)$$

everywhere in the fluid domain and predescribed conditions on either the potential or its derivatives on all boundaries of the domain. The potential function was selected because of its suitability to three dimensional flows. The velocity field components are determined from the gradients of the potential

$$u = \phi_x, \quad v = \phi_y, \quad w = \phi_z \quad (4)$$

and the magnitude of the velocity at a point in the inlet, V , defined as

$$V = (u^2 + v^2 + w^2)^{1/2} \quad (5)$$

One has a choice of either attempting to solve for the potential field in the real domain (x, y, z) as illustrated in Figure 2 or to transform this region into a space which will either simplify the field equation or boundary conditions. For the problem at hand, the field equation is as simple as it can be but the curved wall boundaries do create difficulties. These curved walls, coupled with the large area change between the entrance and exit sections of the inlet, present significant problems if one attempts to solve the field equation in the real space. In the early stages of the program, a two dimensional code was developed which utilized a nonuniform grid in the real space and special curved wall boundary conditions. Although this approach yielded reasonable results for the two dimensional case, the anticipated complexity associated with the coding in three dimensions did not warrant further development.

The method selected for the three-dimensional analysis is presented in detail in Reference 40. This approach uses a transformation based on the local width and height of the inlet to transform the variable area region to one of constant cross section. The transformation takes the

form

$$\xi = x, \quad \eta = y/w(x), \quad \zeta = z/h(x) \quad (6)$$

The use of this transformation results in a much more complex form of the field difference equation but the ease with which the boundary conditions can be applied outweighs these difficulties. Extensive numerical experimentation was conducted during this project and the results agree well with the experiences cited in Reference 40.

Initially a non-conservative finite difference method was used which demonstrated problems with both convergence and accuracy. Due to the nature of the transformation, the field equations for a center differenced non-conservative solution lacked diagonal dominance of the resulting set of linear equations for the potential field. This required the use of special iterative schemes to resolve the numerical convergence problems but still resulted in somewhat inaccurate and very slowly converging solutions.

The fully conservative field form of Reference 40 was also developed and yielded good results. This same method was used for a detailed study of German-Dutch low speed tunnel (40) and it appears to provide a reasonable, though not computationally inexpensive solution, to the inlet flow field problem. The computational scheme is extended into constant area sections upstream and downstream of the inlet. Derivative boundary conditions are applied on the solid walls and on planes of symmetry. The length of the upstream and downstream sections, and the type of boundary conditions applied on these planes are

decisions which must be made for a particular inlet geometry. A number of numerical experiments were performed during this study and, for all the results presented, the upstream and downstream constant area sections were one half the length of the inlet. A uniform velocity condition was imposed at the upstream and downstream planes. Modeling the inlet flow field in this manner is quite suitable for closed circuit tunnel applications but has obvious limitations for indraft tunnels. The definition of the upstream boundary condition for an indraft tunnel would require matching the interior flow to some exterior solution or using a transformation to handle the semi-infinite upstream region. With the addition of screens in an actual tunnel, the upstream conditions for either the indraft or closed circuit tunnel are different from those considered in this report. The screens alter the mean flow but, since the subsequent design studies were intended to demonstrate trends in performance, there was no attempt made to incorporate the influence of the screens in the computations. Only future research can clearly define the interaction between the screens and the inlet.

The results of the computation for a specific inlet are values of the velocity potential at a discrete number of grid points within the inlet. From the gradients of the potential, velocities and thus pressures can be computed. Since the solutions are linear, they depend only on the geometry of the inlet and results can be presented in terms of velocity ratios or non-dimensional pressure coefficients.

The computational grid was defined in such a manner so that values of the potential were computed at points one half a grid space from f planes of symmetry or walls. For most of the computations made in

developing the design charts presented in Section IV, a 10 x 10 x 40 grid was used to define the inlet. Only a single quadrant of the inlet was modeled, with symmetry conditions being applied along vertical and horizontal centerline planes. The constant area upstream section was modeled with a 10 x 10 x 10 grid, the inlet with a 10 x 10 x 20 grid (the finer resolution in the streamwise direction) and the constant area downstream section was a 10 x 10 x 10 grid. Using this grid spacing, the values of velocity and pressure referred to in this report as "centerline" are computed at values of $\eta = \zeta = 0.05$ and the "corner" values are at positions with $\eta = \zeta = 0.95$.

A set of results are given in Figures 11-14 for the same inlet geometry discussed in the previous section on the panel method. Figure 11 shows the velocity distribution at the centerline plane and along the wall at the entrance and exit planes. Figure 12 is a pressure distribution along the centerline and corner.

$$C_{p_{u_e}} = 1 - \left(\frac{V}{U_{m_e}} \right)^2 \quad (7)$$

This pressure distribution is based on the mean velocity at the exit plane (U_{m_e}) and appears constant over the upstream section of the inlet. Non-dimensionalizing the pressure in this manner is adequate for the downstream regions of the inlet, but significant detail is lost in the upstream region. For this region, an "upstream" pressure coefficient

$$C_{p_{u_i}} = 1 - \left(\frac{V}{U_{m_i}} \right)^2 \quad (8)$$

is also used where Um_1 is the mean velocity at the inlet entrance plane and is shown in Figure 13. These two figures illustrate the critical adverse pressure regions near the walls at both the entrance and exit planes. The volume flux along the inlet was also computed, by a simple numerical integration, and is shown in Figure 14, in a form similar to that for the panel method. The percent of leakage is based on the volume flux at the exit plane and the maximum variation was only 2.6%, which occurred at the entrance plane. This shows a significant improvement over the panel solution procedure.

The solution of the field equations was iterative and convergence was particularly slow. Using the fully conservative difference scheme, the solution was convergent for all geometries considered but for the $10 \times 10 \times 40$ grids (4000 field points) convergence to a variation in potential of less than 10^{-5} was only possible with computation times on the order of one hour on the IBM 370/168. (This is consistent with Ref. 40.) Such slow convergence, and excessive computer times would make it impractical to perform flow calculations for numerous geometries so a study was performed to determine an approximation to a converged solution. Figure 15 is a plot of maximum volume flux variation for various computation times. Based on these results, 20 minutes was selected as an "adequate" computation time and this value was used in all design studies. These results were for a CR-25 inlet with a match point, $X = 0.5$, but should be indicative of the results achieved for the range of inlets considered in this study.

Based on these results, the finite difference method was selected

for use in the development of the design data presented in Section IV. It is an approximate technique, which is somewhat costly from a computation point of view, but it does yield reasonable results. Comparison with the experimental results, presented in the next section, added confidence to the use of this technique.

SECTION III

EXPERIMENTAL PROGRAM

As a parallel effort with the analytic program development, an experimental program was pursued which was intended to provide both improved understanding for the physics of the inlet flow field and a benchmark for evaluation of the analysis procedures. Unlike in the analysis, where the inlet can be effectively "isolated" from the performance of the remainder of the tunnel components, in the experimented study the interaction between the inlet and turbulence screens became important. The emphasis in this phase of the study was directed towards indraft subsonic tunnels with flow visualization applications.

Surprisingly, little experimental work has been done to evaluate existing inlet designs. A few papers have been published which discuss experimental work carried out to examine individual aspects of contraction design. Most of these have focused on the effect of the inlet on the turbulence level in the test section. Uberoi tested the effect of contraction ratio on isotropic turbulence by conducting experiments in three square contractions of different contraction ratios (3). Klein and Ramjee studied the effect of contraction geometry on non-isotropic turbulence by using eight circular nozzles of different geometries all with the same contraction ratio (5). Ribner and Tucker employed a spectrum concept to study the selective effect of the contraction on the components of turbulent velocity fluctuations (4).

Almost all practical wind tunnels have damping screens or honeycombs upstream of the contraction to straighten the flow and reduce

the scale of the turbulence. The use of screens is particularly essential in obtaining low turbulence levels in the test section. Numerous studies have been conducted to determine the effect of damping screens in reducing wind tunnel turbulence. They include a variety of experiments to examine the effect of screen wire size, mesh solidity, spacing, and positioning in the settling chamber (41-43).

The work done to explore various effects on wind tunnel turbulence has provided valuable results. The turbulence in an inlet, however, is just one aspect to be considered and researched. Very little experimentation has been done to tie together all the important aspects of a contraction design, i.e. pressure gradients, exit flow quality, boundary layer behavior, turbulence levels, etc. Also, few experiments have been performed to correlate real inlet flows with theoretical predictions.

Many design techniques have been proposed in an effort to obtain a high quality flow in the test section. A good inlet design should consider all of the following performance and physical specifications:

- (1) a high degree of exit flow uniformity
- (2) no flow separation or unsteadiness
- (3) minimal boundary layer growth
- (4) reduction in turbulence intensity
- (5) shortest possible contraction length.

In reality, an "ideal" inlet which meets all of the above specifications is difficult, if not impossible, to achieve. Often trade-offs and compromises must be made in order to design a satisfactory contraction for a given application.

Many early design concepts were concerned primarily with obtaining an axially aligned, uniform flow at the contraction exit plane. This was, and still is, the most important function of the contraction section. Aerodynamic measurements in the test section could be adversely affected if the oncoming air stream is misaligned or possesses a non-uniform velocity distribution.

Later design work was also concerned with the presence of adverse pressure gradients and the possibility of boundary layer separation. Minimizing the boundary layer growth along the inlet walls is advantageous for two reasons. First, the smaller the boundary layer thickness the less likely are the chances of separation in regions of adverse pressure gradients. Second, the boundary layer in the contraction continues to grow as it enters the tunnel working section. The presence of a relatively large boundary layer can effectively modify the geometry of the inlet and alter the exit plane velocity distribution. Also, the boundary layer can affect measurements in the test section by directly interfering with the model, pitot tube, hot-wire probe, etc.

Early NACA work in various wind tunnels demonstrated that turbulence could also affect measurements on airfoil models (44). Research has been conducted by Mueller and Pohlen to study the effects of turbulence on low Reynolds number airfoil performance in wind tunnels (45). These sets of experiments have indicated the need to reduce the amount of turbulent fluctuations in the air stream. Ideally, the flow in the test section should practically be turbulence free in order to simulate the conditions of atmospheric flight.

The wind tunnel contraction section serves to modify the turbulence levels in the flow in the test section. The degree of turbulence in the air flow is specified by the turbulence intensity - the ratio of the fluctuating velocity component to the mean velocity. The turbulence intensity is reduced as it passes through the length of the contraction. The length of the inlet serves to decrease the turbulence levels in the test section by providing a finite distance over which the turbulence is allowed to decay. The area reduction of a contraction tends to stretch the vortex filaments associated with turbulence (3). Several experimental studies have shown that contractions exhibit a selective effect on the three components of turbulent fluctuations. Prandtl was the first to point out that a sharp decrease in the cross-sectional area of a pipe with a consequent increase in the mean speed of the flow tends to smooth out flow irregularities (3). Thus, the contraction reduces the turbulence intensity level by increasing the mean flow speed. The scale of the initial turbulence can be reduced through the use of damping screens upstream of the inlet. Smaller scale fluctuations tend to decay more quickly than larger ones (8).

Reducing the physical size of the contraction cone has obvious advantages. A shorter inlet would require smaller support facilities and would cost less to construct. This is sometimes not a concern for inlets to be used with small wind tunnels, but for larger tunnels, like the 40' x 80' tunnel at NASA Ames, the length of the contraction is important.

Objectives of Experimental Program

The primary objectives of the experimental phase centered on the

evaluation of the aerodynamic performance of an inlet designed using Morel's two-dimensional method (25). Morel's technique was chosen because two inlets designed earlier by his method performed satisfactorily. The two inlets, a 75:1 contraction and a 150:1 contraction, were built in 1980 for use with a transonic smoke flow visualization wind tunnel (2). Such radically high contraction ratios were necessary to allow for flow visualization in the test section and to avoid excessive pressure losses through the screens. Morel's method was chosen because his design charts made the method relatively simple to use in practical design applications. Some of his charts had to be extrapolated to accommodate the higher contraction ratios. The design concept was expanded to the three-dimensional case by matching four contraction walls of the same contour; the resulting inlets each had square cross-sections. Using a similar approach a contraction ratio of 30:1 inlet was built specifically for this experimental investigation for use with a subsonic wind tunnel currently in operation at the University of Notre Dame.

Several aspects of contraction performance were examined during the experimental phase. In particular, Morel's design was evaluated in terms of: (1) exit flow uniformity, (2) adverse pressure gradients and wall separation, (3) effect of contraction on turbulence, and (4) boundary layer behavior. Also, other experiments were performed to examine: (5) the effect of damping screens on flow quality, (6) the effect of a wall discontinuity at the contraction entrance (this "step" was formed when the inner edges of the screen frames were not flush with the inlet lip of the contraction), and (7) the effect of obstructions in

the proximity of the contraction entrance.

The investigation of the inlet flow required performing four separate sets of experiments. Quantitative measurements were taken using wall static pressure ports, a five-hole pressure probe, and a single wire hot-wire anemometer. A qualitative analysis of the flow in the wind tunnel inlets was aided by smoke flow visualization techniques.

The wall pressure measurements were taken to examine the strength of the adverse pressure gradients near the inlet and exit of the contraction. Pressure measurements were also taken in the corner regions to explore the severity of the secondary flows. Results obtained from the wall pressure data were compared with predicted results from the analytical methods.

The five-hole pressure probe and the hot-wire anemometer were used to make flow field measurements at points in the interior of the inlets. The five-hole probe was used to measure mean flow speed and flow angularity. Data from probe measurements was used to provide velocity profiles at several axial locations. Proximity effects and the effect of wall discontinuities were also investigated with the five-hole probe.

Turbulence measurements along the centerline of the inlet were made with the hot-wire anemometer. The hot-wire was used primarily to study the effects of the contraction and screens on local axial turbulence levels. For specific cases, it was also used to acquire data for frequency content analysis.

Smoke visualization techniques were used to supplement the quantitative measurements. The 30:1 contraction ratio inlet was specially built with clear side walls to allow viewing of the inlet

interior, even when the damping screens were in place. This capability enabled the observation of phenomena such as flow separation and entrained secondary flows in the boundary layer.

The current inlet research serves only as a starting point for future work. The experimental techniques and procedures that have been developed provide a foundation for a more complete and in-depth investigation of wind tunnel inlets. Reference 46 gives details of the experimental program discussed in this report. The experimental results that have been presented will be used to evaluate the inlet in terms of more specific flow characteristics: (1) exit flow uniformity, (2) adverse pressure gradients and wall separation, and (3) effect of the contraction on turbulence. Several other aspects of the inlet flow including the effect of damping screens and the effect of the screen step will also be discussed.

30:1 Contraction Ratio Inlet

The experiments of this phase centered on a single inlet designed using Morel's two-dimensional approach and having a matched cubic wall geometry. The inlet was designed using conservative values for the inlet and exit wall pressure coefficients (46). The 30:1 contraction ratio inlet was constructed for use on either of two subsonic wind tunnels. The contraction is 56.6" long and the inlet and exit heights are 47.0" and 8.58" respectively. The match point was located at $X = 0.71$ (i.e. 40.2 inches from the entrance plane). The top and bottom of the contraction were constructed from sheets of 1/8" masonite and the sides were formed from clear sheets of Lexan. The Lexan was flexible enough to form the wall contour and also possessed the optical quality

needed for flow visualization work. The structure was supported externally so as not to interfere with the flow in the interior of the inlet. Particular care was taken to allow viewing of the corner regions. A special test section and diffuser unit was built to make the inlet compatible with existing wind tunnel facilities. The wall contour of the flow visualization (FV) inlet is plotted in Figure 16 and a photograph of the complete tunnel is shown in Figure 17. The damping screens were made of two types of mesh. Five screens were made of a multistrand nylon mesh grid with a 0.002" diameter strand in a 26 per inch grid. The six screens attached upstream of the nylon screens were made of an aluminum mesh with a 0.009" diameter aluminum wire in a 18 per inch grid. The location of the five-hole probe and hot-wire probe measurements are shown in Figure 18.

Exit Flow Uniformity

The five-hole probe data at the exit plane (Figure 19) indicates that the contraction exit flow is uniform and aligned for the 11 screen case. The pitch and yaw angles at all points in the profile are within plus or minus 1 degree of 0 degrees. The precision of these results corresponds well with the accuracy level of the five-hole probe system. In Figure 19a the velocity is shown to decrease near the wall. A velocity profile taken with the hot-wire, however, did not indicate this decrease, even at points closer to the wall. The discrepancy in the results was probably caused by boundary interference on the measured probe pressures. If the probe is placed within 5 probe head diameters of a wall the calculated velocities could be as much as 4% low (47). The data point in question in Figure 19a was located 0.3 inches from the

wall; this is just 2.4 probe diameters. The wall pressure coefficient data in Figure 20 indicates a non-uniform lateral velocity distribution at $x/L = 0.95$. At this axial location the wall velocity varies by 2.5% from the centerline to the port one inch from the corner. The lateral velocity profile suggests that a non-uniform wall velocity distribution may exist at the contraction exit plane.

Pressure Gradients and Separation

In a two- or three-dimensional contraction, regions of adverse pressure gradient will occur along the wall at both the inlet and exit of the contraction. The wall pressure measurements indicate that the damping screen configuration directly affects the wall pressure gradient in the upstream portion of the contraction. Figures 21 and 22 show the wall velocity gradients in the upstream section of the FV inlet for 3 different screen cases. For the optimum screen configuration (all 11 screens flush with the inlet lip) no adverse gradient was detectable. The sharpest negative velocity gradient occurred for the case of the screen step. For this case the wall velocity slowed by almost 70% over a distance about equal to $0.23L$. The longest adverse gradient occurred when no damping screens were used; in this case a negative velocity gradient existed over a distance of about $0.3L$. Note that the wall velocities for all of the cases are almost the same at the most downstream data location.

Pressure measurements in the inlet showed no evidence of an adverse pressure gradient along the contraction walls near the exit plane. Since the constant area exit region of the inlet is very short, an adverse pressure gradient would also take place over a very short

region. Additional pressure taps on the test section wall just upstream and downstream of the contraction exit would have been helpful in examining the behavior of the adverse pressure gradient. The inability to detect the adverse gradients in the inlet was due to an insufficient number of static ports near the exit. The external support structure of the inlet made it difficult to instrument the inlet with extra pressure taps.

Separation along the walls of a contraction could occur if a positive pressure gradient is severe enough. Smoke flow visualization was used to look for regions of separated flow in the inlet. With the screens flush, no separation was observed. When the step configuration was used, however, a separation bubble near the inlet lip was clearly evident. This phenomena is pictured in Figures 23a and 23b. A positive pressure gradient was formed when the inlet flow encountered an effective area increase on the downstream side of the separation bubble causing the flow velocity near the wall to decrease. This same type situation probably exists for the 0 screen case as well, except the separated region is larger and not as well defined (pictures could not be taken of this case because the streamtubes break up quickly unless screens are used).

Turbulence

The effect of the contraction on turbulence levels is best shown by examining data shown in Figures 24 and 25. The local turbulence intensities in the inlet are shown to decrease toward the contraction exit. The fluctuating velocities, u' , on the other hand, increase through the contraction, especially in the region of greatest area

reduction. The u' velocities at station 4 ($x/L = 1.0$) were not plotted because they were about an order of magnitude greater than those at stations 1 and 2.

From Figure 24, the influence of the contraction seems to depend on the magnitude or content of the initial turbulence. The experiments show that for higher initial turbulence intensities the percent reduction in the intensities was greater. When one screen is used, the intensity at the contraction exit is less than $1/3$ its initial value. For the 11 screen case, however, the reduction in turbulence intensity is only about 40%. Using turbulence intensities as a means of evaluating the effectiveness of the contraction in reducing turbulence is misleading because the intensities are referenced to the local mean velocity. Another way of assessing the effect of the contraction on turbulence is to look at the behavior of the rms velocities for the different screen combinations. When only one screen was in place the magnitude of u' increased about 6 times through the length of the contraction. When all 11 screens were used, u' at the exit plane was found to be almost 20 times its upstream value. This big jump is attributed more to acoustic excitation than to the effect of the contraction (the effect of noise will be discussed later). Nevertheless, the magnitude of the fluctuating component of velocity continuously increases through the inlet for all combinations of screens.

Comparing these experimental results with those of Uberoi (3) and Klien and Ramjee (5) shows that the effect of the contraction on turbulence depends on the contraction ratio and the nature of the turbulent fluctuations. Uberoi examined the effect of contraction ratio

on isotropic turbulence. He used 3 square inlets with contraction ratios of 4:1, 9:1, and 16:1. For the two smaller inlets Uberoi's results agreed with predictions from linear theory for isotropic turbulence, i.e. the magnitude of u' decreases through the contraction. For the 16:1 contraction, however, u' first decreased and then increased to a final value which was 1.2 times the initial value. Since the inlets currently being studied have such high contraction ratios, the increase in u' through the inlets may be due to high contraction ratio effects.

Klien and Ramjee studied the effects of contraction geometry on non-isotropic turbulence. They found that the contraction ratio was the governing parameter and not the wall geometry. Their results showed that, for a contraction ratio of 10, the magnitude of u' increased 6-fold through the contraction while the turbulence intensity continuously decreased to about 1/5 of its initial value. These results compare favorably with those obtained in the inlet. In most practical applications the turbulence in front of the contraction is non-isotropic; damping screens have also been shown to produce non-isotropic turbulence (4). The degree of anisotropy in the inlet was not measured because only a single wire hot-wire probe was used in the experiments.

Pre- and post-contraction frequency spectra were measured for both inlets. Two spectra taken in the inlet (Figure 26) best illustrate the effect of the contraction on the longitudinal component of the fluctuating velocity. The spectra were taken at stations 1 and 4. The spectral densities indicate that the contraction tends to attenuate the lower frequencies, i.e. the higher frequencies (greater than 5 Hz) at

station 4 have greater relative power than those at the upstream station. Although the nature of the turbulence in the inlet is still not completely defined, its spectra compare in form with Uberoi's spectra for u' . For Uberoi's 9:1 contraction, the post-contraction spectrum is shifted to higher wave numbers (higher frequencies) with less power at the lower wave numbers. His results indicate less of an effect on the downstream spectrum when the 16:1 contraction was used.

Boundary Layer Behavior

An attempt was made to survey the boundary layer at the exit of the inlet, but the manual hot-wire traversing mechanism that was used could not provide the resolution necessary for such measurements. The probe was lowered to within a tenth of an inch from the wall with no noticeable decrease in velocity. This indicated a relatively small boundary layer at the contraction exit.

Smoke flow visualization also proved useful in examining the boundary layer. Figure 27, though, shows an interesting flow phenomena along the walls of the FV inlet. In these two photographs, smoke streaklines are introduced as close as possible to the vertical, transparent wall of the inlet with and without the "step" caused by the screen placement. In the contracting region a cross-flow entrained in the boundary layer can be seen. The lateral motion of the entrained flow is away from the corners towards the wall centerline.

Influence of Damping Screens

The use of damping screens upstream of the contraction cone is known to improve the flow quality in the test section. Experiments were performed to examine the effect of the screens on the flow in the two

inlets. The results from these experiments will now be discussed with particular emphasis on flow uniformity and steadiness.

Five-hole probe measurements were used to compare the flow uniformity and angularity for the cases of 0 and 11 screens. Probe data at port 1 are shown in Figure 28. At this upstream port the damping screens tend to smooth out the irregularities in the mean flow velocity. Figure 28a shows the decrease in the flow speed due to the associated total pressure losses through the screens for a fixed fan speed. The velocities obtained with the five-hole probe at this port were repeatable to within 2.5% of the mean value. Hot-wire measurements made at stations 1 and 2 for various combinations of screens also show this characteristic of damping screens (Figure 29). Due to errors introduced during linearization at low speeds, the uncertainty in the flow velocities measured with the hot-wire was estimated to be about 4%. The effect of the screens in reducing flow angularity is very evident from Figure 28b. In the vicinity of the inlet wall the screens decrease the pitch angle of the flow by more than 10 degrees. At port 1, fluctuations in the measured pitch angles in the 0 screen case ranged up to 3 degrees from the mean value, whereas in the 11 screen case the deviation was approximately 2 degrees. The screens had similar effects on the yaw angularity of the flow, but the effects were not as pronounced due to the symmetric location of the data points (in the vertical centerplane).

The effect of damping screens on the exit plane flow quality is shown in Figure 19. The screens improve the flow quality in terms of both velocity uniformity and flow angularity. Figure 19c shows a bias

towards higher yaw angles at points away from the centerline. This trend in β is significantly reduced with the addition of damping screens.

An important function of damping screens is to reduce the turbulence level in the test section. Several experiments were run to examine the effect of the screens on turbulence. Measurements made at station 4 were used to investigate the influence of the screens on test section turbulence. Figures 30 and 31 present turbulence intensities and rms velocities for the test section velocity case of 53 fps. From Figure 30, it can be seen that the turbulence intensities tend to decrease with the addition of more damping screens. This effect is most pronounced at the most upstream station. At the contraction exit, station 4, very little effect is noticeable; this again is due to the higher reference velocity used in the definition of the local turbulence intensity. By increasing the number of screens the turbulence intensities become more uniform throughout the inlet, i.e. the effect of the contraction on turbulence is reduced. When just 1 screen is in place the turbulence intensities vary by as much as 0.95%, but when all 11 screens are used the intensities vary by no more than 0.13%. Using more than 7 screens seems to have little effect on the intensities measured in the inlet.

The fluctuating velocities in the inlet are shown in Figure 31. The same trends are evident. As extra screens are added ahead of the contraction, the u' velocities tend to decrease. The lowest rms velocities occur at the most upstream data station.

Frequency spectra data and flow visualization techniques provided additional information on the effect of damping screens on turbulence.

Spectra taken at station 1 in the FV inlet illustrate the influence of the screens on the frequencies of the turbulent fluctuations (Figure 32). With the addition of just one screen a noticeable increase in the relative power of the higher frequencies is observed. Interestingly, the addition of extra screens has little effect on the spectrum.

Some earlier flow visualization studies were conducted at Notre Dame to show the effect of the damping screens (2). All of the previous work, though, was concerned with the coherence of the streaklines in the test section. The advantage of the FV inlet is that it allows viewing of the streamtubes where they are the thickest, just downstream of the screens. Figure 33 shows the streamtubes in the inlet when 2, 4, and 11 screens were used. For the 2 screen case, the smoke began to break up within the first 20% of the inlet and had diffused by the time it reached the test section. When 4 screens were used the smoke tubes remained intact but still exhibited some signs of flow unsteadiness. The use of all 11 screens produced well defined, coherent streamtubes throughout the length of the inlet and into the test section.

Effect of the Screen Step

Unless care is taken when installing the damping screen frames, a step could result at the inlet lip. The step cases examined were for forward facing steps, i.e. there was an area decrease from the screen frames into the inlet. The effect of the screen step has already been discussed in terms of the adverse pressure gradient in the upstream portion of the inlet. This is probably the most notable of the effects of the screen step.

The effect of the step on the whole inlet flow field is shown in

Figure 23a. The streamtubes very near the center of the inlet are affected very little by the step. Turbulence measurements made at the centerline station 3 confirmed this. The turbulence intensities measured for the step case compared closely with the intensities that were measured when the screens were flush. Some of the streamtubes away from the centerline begin to diffuse in the contracting region. This could not be verified since hot-wire measurements were taken only at centerline stations. Figures 23 and 27 all show that the streamtubes close to the wall tend to break up after flowing over the step. These streamtubes have completely deteriorated by the time the flow enters the test section. Five-hole probe velocity measurements at port 4 ($x/L = 0.85$) indicate that the flow in the downstream sections of the inlet is affected by the step (Figure 34). For the same wind tunnel fan RPM, the mass flow in the step case is slightly higher because of the decreased pressure losses through the screens (slower screen velocities due to the larger area of the screen frames). Figure 35 shows that flow angularity is virtually unaffected by the step.

Effect of Noise

The discussion of the turbulence data has already mentioned the problems associated with noise in taking hot-wire measurements. The hot-wire sensor is sensitive enough to measure the small fluctuating velocities induced by acoustic excitation of the air particles. In their experiments, Dryden and Shubauer found that noise can considerably effect turbulence measurements (up to 25%) (41). They identified two major sources of noise in a wind tunnel: propeller noise and so-called drag noise produced by turbulence in the boundary layer at the tunnel

walls. Drag noise is more prevalent in closed-circuit type tunnels, but similar effects can exist in indraft type tunnels as well (e.g. separation in the diffuser section, seepage through seams in the test section, etc.). From their experiments with screens, Dryden and Shubauer also found that damping screens are partially responsible for the lower limit placed by sound; for the same RPM the propeller noise increased with each additional screen.

In the 30:1 contraction, the effects of noise were localized. The influence of the noise depended on the data point location and the speed of the wind tunnel fan. The u' velocities at stations 1 and 4 for three test section velocity cases are shown in Figures 36 and 37 respectively. At the upstream station, the rms velocities decrease as expected through the addition of the seventh screen. Extra screens seem to do little in reducing the level of the turbulence. For the two lower speed cases, the u' velocities appear to reach "bottom line" values. The measurements at station 4 indicate that three damping screens are optimum in reducing turbulence. The addition of extra screens appears to do nothing to improve flow steadiness. These results are contrary to the photographic data of Figure 33 which show that increasing the number of screens improves the quality of the streamtubes. This implies that adding screens improves the quality of the streamtubes and that adding screens either reduces the turbulence intensity in the inlet or somehow changes the structure of the turbulence. The discrepancies in the results can be explained by taking into account the effects of noise. While the data at station 1 indicates some acoustic interference, the effects are more obvious at station 4. Station 4 is more susceptible to

acoustic effects because it is located closest to the wind tunnel fan in a relatively narrow channel ($.05 \text{ ft}^2$). When the fan is turning at higher RPMs (higher test section velocities), the noise contribution to the local turbulence is greater. The wind tunnel operates noticeably louder at the higher speeds. In the highest velocity case, the rms velocities actually show an increase when more than 7 damping screens are used. These results concur with Dryden and Shubauer's findings which demonstrated that additional screens tended to amplify the effect of the propeller noise.

The sets of frequency spectra shown in Figures 38 and 39 provide more insight into the effects of noise on turbulence measurements. The spectra in Figure 38 were both taken at station 4 for two different fan RPMs. In the higher speed case the majority of the power is located at frequencies below 25 Hz; a roll-off in the power over the first 100 Hz is indicated in the lower speed case. Two dominant frequency spikes at about 7 and 15 Hz are evident in the high speed spectrum. These frequencies have been identified by Mueller and Pholen as subharmonics of the fan blade passage frequency (45). The frequency spike at 15 Hz can also be detected in Figure 39.

The frequency spectra in Figure 39 illustrate the effect of the damping screens on propeller noise. Figure 39a shows the spectrum when no screens are used (same case as Figure 38b), and Figure 39b shows the spectrum when all 11 screens are in place. In the 11 screen case, the relative magnitude of the frequency spike at 15 Hz is about 20 times that of the 0 screen case. Thus, it is clear that the addition of damping screens increases the effect of the noise of the wind tunnel

fan. The spectra of Figures 38 and 39 have also shown that noise can influence hot-wire turbulence measurements, especially at the stations nearest to the source of the noise.

Flow in the Corner Region

Wall pressure data and smoke flow visualization pictures provide some information on the behavior of the inlet flow in the vicinity of two adjoining walls. The corner flows are initially slower than the corresponding wall centerline flows. In the center of the acceleration region, however, the flow speeds in corners become faster than those at the wall centerline. The lateral variation of the wall pressure coefficients is presented in Figure 20. In the upstream portion of the inlet the velocities gradually decrease towards the adjoining wall. Figure 27a shows that secondary flows in this region of the contraction tend to draw the flow away from the corners. The flow speeds in the corners and at the wall centerline become about equal around $x/L = 0.80$. The data at $x/L = 0.84$ indicates interesting behavior in the transition regions. Five-hole probe velocity measurements at port 4 show a similar type profile when the screens are flush (Figure 34). Near the contraction exit the corner velocities are only slightly greater than those at the centerline.

The velocity ratios provided in Figure 22 indicate the severity of the adverse pressure gradient in the corners. All 3 of the cases examined show signs of a negative velocity gradient. With 11 screens flush no adverse gradient was noticeable along the centerline (Figure 22), but in the corner regions a small gradient does exist. The most severe gradient was exhibited for the case of the screen step. In this

case the wall velocity decreased by more than 75% in a distance less than $0.2L$. These results demonstrate why flow separation is most likely to occur in the corners of a square or rectangular contraction. Figure 27a shows the disturbed flow in one of the corners of the FV inlet.

Proximity Effects

In the experiments to evaluate the effect of obstructions on the inlet flow, all 11 screens were used to simulate the standard screen operating configuration. Only the data for one case (ceiling with two walls) is presented because it represents the "worst case" of those examined. The effects in the upstream section were measured at port 1. The velocities of Figure 40 show a lower mass flow near the wall in the obstruction case. This would be expected since the ceiling and walls restrict flow access to the upper portions of the inlet. The total mass flow of the wind tunnel is reduced by about 7% for the same fan RPM. The velocities for all 3 cases shown were about the same at data points below $y/h = 0.75$.

The proximity effects in the downstream portions of the inlet were investigated at port 4. Figure 34 shows that the velocity profile is altered slightly when obstructions are placed near the inlet. Again, the reduced mass flow is evident. The pitch angles of the flow at port 4 are shown in Figure 35 to be almost unaffected by the obstructions. At this data location the yaw angularity was essentially eliminated (to within the accuracy level of the probe).

Comparison of Numerical and Experimental Results

The experiments with the CR = 30 inlet did provide a benchmark for evaluation of the results of the numerical studies, though a direct comparison of calculated and predicted performance is difficult. The panel solution which would have been more appropriate in its application to the indraft tunnel due to the manner in which the upstream boundaries were modeled, proved unsuitable as discussed in Section II. The finite difference solution, though significantly more accurate is limited by the manner in which the upstream boundary conditions must be described. A computation was performed using a 10 x 10 x 40 grid, for the experimental FV inlet. Uniform axial flow conditions were prescribed at a distance equal to one half the total inlet length, upstream and downstream of the entrance and exit planes. These calculations are compared with the experimental results for both the 0 and 11 screen cases in Figures 41 - 44. In each case the results are non-dimensionalized in terms of either velocity ratios or pressure coefficients.

The entrance region wall pressures for the centerline plane and the corner region are presented in Figures 41 and 42. The comparison is good for the case in which all eleven antiturbulence screens are in place. The slight adverse pressure gradient is obvious, particularly in the corner region. It should be noted that the computational results are for grid points "close" to the wall. They were located at a position 5% of the local tunnel width from the wall. The experimental pressure taps were approximately 1 inch from the corner.

It is difficult to make accurate velocity or pressure measurements

near the entrance plane, for even with test section velocities near 200 ft/sec, the entrance velocities are near 7 ft/sec and the resulting pressure differences (static to total) are often less than 0.010 inches of water. The unsteadiness associated with the operation of the indraft tunnel without screens also created difficulties and may be responsible for the difference between the measured and calculated results.

Correlation in the downstream section of the inlet is again very good for the 11 screen case as shown in Figure 43 for the wall centerline. No adverse pressure gradient was evident near the exit plane but the most downstream pressure tap was located at $x/L = 0.95$ and any overspeeding near the wall would have occurred at a more downstream location. The velocity profiles at ports 1 and 5, which were discussed earlier and are presented in Figures 19 and 22 are repeated in Figure 44 and compared with the predicted profile. Although some general trends are comparable, the comparison with the prediction is not good. The velocities at both ports are referenced to the measured value at the point closest to the centerline. At port 1, this is the velocity at $y/h = 0.23$, due to length limitation of the probe. At port 5, the reference value was the centerline velocity. At the low speed end, port 1, the measurements were hampered by the use of the 5-hole probe and associated pressure measuring equipment at the very low speeds. At the high speed end, port 5, the measurements are within 1% of the mean and this too represents a limit on the velocity field measuring capabilities.

Final Thoughts

The experience gained in the experimental phase of the effort may

have generated more questions than it answered. The performance of the inlet is strongly influenced by the character of the incoming flow. The upstream conditions, both in analysis and experiments, influence the inlet flow field. In the analysis, the upstream conditions can be "controlled" in a different manner than in the experiment. Since one of the areas of concern of this effort was the performance of the high contraction ratio, indraft tunnel when used as a smoke visualization facility, experiment demonstrated that this inlet design, when coupled with adequate screening, would perform well. The screens are obviously vital and the role they play in effecting both velocity fields and turbulence levels is not fully understood. Trying to correlate the quality of the smoke streaklines with the hot-wire turbulence measurements is a difficult task and one which will require additional research. Both the inlet and the turbulence managing devices must be adequately designed for a tunnel to function properly.

SECTION IV

INLET DESIGN DATA

The final task in this research effort was to use the results of the analytic program development and the experimental studies to develop a set of practical guidelines for wind tunnel inlet design. This would become a formidable task unless one would limit the type and application of the tunnel facility for which the inlet is to be designed. The approach taken to develop the design data was to first characterize the inlet geometry with a relatively simple set of parameters and then to use the numerical prediction techniques to predict performance for a range of these parameters. The inlet performance was "measured" with a set of parameters related to flow field uniformity and adverse wall pressure gradients. The designer is then able to select a set of performance goals, and use the results of the numerical simulations which have been presented in chart form to select the required inlet size and shape parameters.

The application for the design data is again the relatively high contraction ratio tunnel of either indraft or closed circuit design. The numerical procedure has been demonstrated for cases in which the upstream boundary conditions were more characteristic of the closed circuit tunnel but the experimental studies demonstrated reasonable agreement for an indraft tunnel design. The range of contraction ratios considered (10 - 40) for both square and rectangular cross section inlets is suitable for subsonic tunnels which could operate over a relatively wide speed range. The low end of the range may be more suitable for closed circuit tunnels where the higher contraction ratios

are characteristic of values used in some recent indraft tunnel designs, particularly those designed for smoke flow visualization.

The development of the set of rational preliminary design guidelines or procedures required the:

- 1.) selection of a set of parameters which characterize the inlet geometry, and
- 2.) selection of a set of parameters which define the inlet performance.

The suitability of the subsequent design procedure depends on these two sets of parameters. Those selected were the result of the experience gained in the analytic work and experimental studies but in no way represent the "best" set. Future work in this area may indicate the need for other parameters.

Inlet Geometry

The inlet geometries considered are square or rectangular cross sections as shown in Figure 2. The basic geometric parameter is the area contraction ratio, $CR = (H_i W_i) / (H_e W_e)$. The ratio of height to width (H/W) sets an "aspect ratio" for the cross section. The length of the inlet can be scaled by the height (L/H) so that the basic size parameters are all non-dimensional. The H/W ratio could be a function of axial distance as would be the case in an inlet which would be used to transition from a square plenum to a rectangular cross section. This type of inlet was not considered but it is consistent with the prediction methods and, therefore, could be considered in the future. The following shows the range of the parameters used in developing the design charts.

<u>CR</u>	<u>L/H</u>	<u>H/W</u>
10	0.6 → 1.6	1.0
25	0.6 → 1.6	1.0 → 1.67
40	0.6 → 1.6	1.0

The selection of the wall geometry is a much more difficult task. There are obviously a large number of candidate wall geometries from arbitrary "smooth curves" to sophisticated high order polynomials. The matched cubic geometry was selected for this work for two reasons. First, it allows for a single parameter, $X = x_m/L$, the match point, to be used to completely define the wall geometry. Second, it had proven successful for a number of recent tunnel designs. From a practical consideration, it is realized that the curve formed by the matched cubic is more complex than some possible geometries such as those formed by circular arc and straight line segments. This does complicate fabrication but the fact that it satisfies two important "boundary" conditions and can be defined by a single parameter may outweigh the added complications. These boundary conditions are the zero wall slopes (i.e. alignment with the test section longitudinal axis) at the upstream and downstream end in the inlet. The need for zero wall slope at the downstream end is obvious, and recent experience ⁽²⁾ has shown benefits of zero wall slope at the inlet entrance, particularly with screens or other turbulence management devices present. The design studies presented in this report used values of $X = 0.2 \rightarrow 0.8$ which effectively spans the range of very rapid contractions with mild curvature in the downstream section to inlets with most of the area reduction in the downstream section.

Though the inlet geometry discussed may seem quite limited, there were 120 separate inlets studied using this set of parameters. This represents over 40 hours of computer processing time and, though expensive, was far more reasonable than the cost of fabricating 120 separate inlets and "testing" each.

Design Parameters

The result of each computer simulation was the complete potential field for each inlet. It was necessary to reduce this information to a set of parameters which could be used in evaluating the performance of each design.

An attempt was made to select a simple set of parameters which would be related as closely as possible to measures of "good" inlet performance. These parameters were then related to flow quality and susceptibility to flow separation.

Flow uniformity can be measured in terms of a maximum variation of velocity at a given cross section. Two parameters were defined.

$$\begin{aligned}\tilde{u}_i &= \left(\frac{V_{t_i} - V_{cor_i}}{U_{m_i}} \right) \times 100 \quad (\%) \\ \tilde{u}_e &= \left(\frac{V_{cor_e} - V_{t_e}}{U_{m_e}} \right) \times 100 \quad (\%) \end{aligned} \tag{9}$$

These represent the percent of maximum variation in velocity at the entrance and exit plane cross sections. At the entrance plane the greatest velocity occurs at the centerline (V_{t_i}) and the smallest velocity at the corner (V_{cor_i}). The opposite situation occurs at the

exit plane, with the greatest velocity occurring at the corner. The two parameters are expressed in terms of a percent variation from the mean velocity at the given cross section. The mean velocity was determined by computing the volume flux and dividing by the cross sectional area.

The exit plane uniformity is important due to its influence on the test section flow quality. Although the nonuniformity decays as the flow continues in the constant area test section, the degree of nonuniformity will influence the length of the test section and allowable model locations. The entrance plane uniformity, though not apparently as critical a parameter, can effect the selection of the turbulence management devices. Since \tilde{u}_1 can be greater than 100%, the variation in speed across the entrance plane can be quite large. This can effect the size and placement of screens or honeycomb or possibly set an upper limit on tunnel operating speed.

The second set of parameters selected to describe the inlet performance are related to the development of the wall boundary layers. It would be ideal to use the results of the numerical calculations to perform detailed calculations of the development of the boundary layers in order to predict separation or displacement thickness. This type of calculation is beyond the scope of a preliminary design study, but there are simpler techniques for predicting boundary layer behavior. It is important to eliminate the possibility of separation of the wall layer at any point in the inlet due to the influence separated regions have on the test section flow quality. The behavior of the boundary layer is dependent upon the character of the layer as the flow enters the inlet. This is dependent upon tunnel type and upon disturbances created

upstream of the inlet. The development of the layers within the inlet will be influenced by the pressure distribution imposed on the layer and by the wall roughness. The experiments and numerical studies have shown the presence of adverse pressure gradients near both the entrance and exit planes of the inlets whose walls are matched cubics. Figures 45 and 46 show the details of this adverse pressure gradient near the inlet entrance for a series of design parameters. The pressure coefficient C_p is based on the mean entrance plane velocity. Figure 45 shows the pressure at both the wall centerline and corner region for $CR = 10$ for a very short inlet $L/H = 0.8$ and a long inlet $L/H = 1.40$. For the match point forward in the inlet $X = 0.2$, there is a very strong adverse pressure region which begins well upstream of the inlet entrance plane and reaches a peak at $X/L \approx 0.1$. For the match point well downstream in the inlet, $X = 0.80$, the magnitude of the adverse region is much less but it extends over a greater length of the inlet. Figure 46 shows the same combination of inlet geometries for a contraction ratio of 40. Somewhat surprisingly, the results are very similar. The magnitudes and locations of the peaks are quite comparable indicating a very weak dependence on CR for this range of values.

The type of data shown in Figures 45 and 46 indicate the environment seen by the boundary layer but it does not indicate whether or not separation occurs. There are a few simple procedures available to help predict separation. One method which has been used in similar studies in the past is Stratford's turbulent boundary layer separation criteria (48). The Stratford criteria is straightforward and easy to apply. It shows that separation depends upon the strength of the

adverse pressure gradient and length of the developing turbulent boundary layer. Separation is predicted to occur at a point where

$$C_p (x \, dC_p/dx)^{1/2} = 0.39 (10^{-6} x R_e)^{1/10} \quad (10)$$

The constant (0.39) in equation (10) is changed to (0.35) for cases where for $(d^2p/dx^2 < 0)$. The distance x is measured from the "origin" of the turbulent boundary layer and the empirical relation is valid for Reynold's numbers (based on x) on the order of 10^6 . This criteria was applied to a group of inlet designs as will be discussed in the next section. The location of the origin of the boundary layer is usually not known in the inlet design problem, and the region of most severe adverse pressure is the corner, where the flow is highly three-dimensional. Although this criteria is useful in developing a "feel" for boundary layer behavior, a more detailed approach would be required for accurate prediction of separation.

Morel did show that the magnitude of the adverse pressure region could be correlated to two simple parameters (24). These two parameters are used to study the sensitivity of the pressure distribution on the inlet geometry. There is a simple parameter for the entrance region and one for the exit region.

$$\begin{aligned} C_{p_i} &= 1 - (v_{\min}/U_{m_i})^2 \\ C_{p_e} &= 1 - (U_{m_e}/v_{\max})^2 \end{aligned} \quad (11)$$

The values U_m and U_m are again the mean values at the entrance and exit planes respectively. The values V_{\max} and V_{\min} are the maximum and minimum speeds within the inlet. They occur along the corner and are characteristic of the magnitude of the adverse pressure gradient occurring near the inlet entrance and exit.

The four parameters \tilde{u}_i , \tilde{u}_e , C_{p_i} and C_{p_e} can be used to describe the aerodynamic performance of the inlet. A designer can select allowable values for each parameter and then determine the required tunnel geometry to achieve each.

Inlet Design Charts

Using the performance parameters discussed in the previous paragraphs, the results of a series of calculations were summarized into a set of design charts. These charts are shown for the complete set of parameters discussed earlier in Figures 47-51. Each figure has four parts representing the variation of each parameter, \tilde{u}_i , \tilde{u}_e , C_{p_i} and C_{p_e} , with match point and length to height ratio for a given contraction ratio. These curves can be used to select the preliminary inlet geometry for a given wind tunnel application.

As would be expected, the degree of entrance or exit plane uniformity are competing parameters. Entrance plane uniformity can be improved by moving the match point rearward, but this increases the exit plane nonuniformity. Both parameters are improved by increasing the inlet length. Entrance and exit plane pressure distributions, as reflected in the parameters C_{p_e} and C_{p_i} , are also competing parameters. Forward positions of the match point result in low values for C_{p_e} (small adverse pressure gradients in the downstream end of the inlet) but this

also results in large values for C_{p_i} . Again both parameters are reduced by increasing the inlet length.

Additional calculations were performed applying Stratford's criteria to the pressure distribution along the corner region and the results are included with C_{p_i} (part c of each figure). Assuming an effective origin of the turbulent boundary layer equal to 50% of the inlet height upstream of the entrance plane, the flagged symbols represent designs for which turbulent boundary layer separation is predicted. This seems to correlate very well with the parameter C_{p_i} and on each figure upper bound for C_{p_i} is shown. This upper bound does depend upon the selection of position of the virtual origin of the boundary layer and should therefore be used as only a rough estimate of a limit on C_{p_i} .

Similar calculations were not performed for the boundary layer near the exit plane. Since the history of this layer is so complex it was felt that it would be inappropriate to attempt to apply Stratford's criteria in this region. Allowable values for C_{p_e} will therefore have to be developed from experience or from more detailed boundary layer calculations.

The dependence of each parameter on contraction ratio can be determined by interpolating between the curves. \tilde{u}_i is not a strong function of CR where the other three parameters show a stronger dependence. The only calculations for rectangular cross section inlets were performed for CR = 25. The values for \tilde{u}_i and \tilde{u}_e decrease for increased H/W ratios. It appears that as H/W increases the inlet becomes more "two-dimensional" for a given contraction ratio, even

though the ratio of H/W remains constant along the inlet. The influence of the corners is not as strong. The parameter C_{pi} showed a decrease with increases in H/W as would be expected if the influence of the corners is reduced. This implies that a shorter rectangular inlet could be used rather than a square cross section for a similar contraction ratio. As an example in comparing Figures 48c and 49c, using the Stratford criteria as discussed earlier, the square cross section, $CR = 25$, inlet with $L/H = 1.0$ and $X = 0.6$ indicates separation at the upstream corner region where the same geometry with a rectangular cross section and $H/W = 1.2$ indicates no separation.

As an example in the use of these charts, consider the design of a $CR = 25$ inlet of square cross section, with the following target parameters:

- 1) $\tilde{u}_1 = 25\%$
- 2) $\hat{u}_e = 1.0\%$
- 3) $C_{pi} = 0.4$

(The selection of C_{pi} is somewhat arbitrary but seems reasonable for a closed circuit tunnel with a plenum whose length is approximately $1/2$ of the inlet height.) From Figure 48c, based on C_{pi} , the shortest inlet allowable appears to have a $L/H = 1.0$, with a $X = 0.8$ match point but referring to Figure 48b, this inlet would have a $\tilde{u}_e = 6.5\%$ which is far above the target value. A 1% value for \hat{u}_e could be achieved with $L/H = 1.2$ and $X = 0.57$, which would yield a value of $C_{pi} \approx 0.41$ and $\tilde{u}_1 \approx 15\%$ and $C_{pe} = 0.05$. Coincidentally this value of C_{pe} is that selected in the two-dimensional design of the inlet used in the experimental program and it is therefore in an acceptable range. This

would then provide a reasonable preliminary estimate of the wall geometry of the inlet and size of the inlet section. The design is highly dependent upon the selection of the target parameters. It will only be through experience and additional analysis that more confidence in acceptable values of these parameters can be achieved but the current study does provide direction for that future work.

SECTION V

CONCLUSIONS AND RECOMENDATIONS

This report documents the results of a combined numerical and experimental study of the aerodynamics of high contraction ratio, subsonic wind tunnel inlets. The inlet or contraction section of a wind tunnel facility has significant impact on the performance and operating characteristics of any subsonic wind tunnel. Although numerous studies have been directed at the development of methods for predicting wind tunnel performance almost all have been applied to two-dimensional geometries and are therefore limited in their applicability to "real" three-dimensional wind tunnel facilities. Previous studies demonstrated the possibilities of using numerical aerodynamic prediction methods such as surface paneling or field finite difference solutions to predict the inlet performance. These studies were conducted to evaluate the performance of specific inlets and they did not provide any general design trends for future wind tunnel facilities. It was the intent of this work to build on this previous experience and develop a set of guidelines for use in preliminary aerodynamic design of three-dimensional wind tunnel inlets. Of particular concern was a class of special purpose tunnels which can be used for smoke flow visualization. Previous studies had shown the importance of the inlet design to the successful use of smoke flow visualization techniques. These types of tunnels typically require large contraction ratios (20-150) and very short contractions to avoid dispersion of the smoke streaklines. This combination of large contraction ratio and minimum inlet length complicates the inlet design.

The numerical studies demonstrated both the potential and limitations of both the source panel method and the finite difference field solution methods as applied to the aerodynamic design of three dimensional contractions. The ease with which complex three-dimensional geometries can be defined is an asset of the source panel method. It also appears well suited for use with indraft tunnel configurations where the upstream conditions (air entering the inlet) are unknown. There were difficulties encountered with the application of the uniform source panel method related to "leakage" for internal flows. Such problems have been encountered in the past and the use of either greater paneling detail or a higher order panel could reduce this problem. The finite difference field solution proved to be the more accurate for this study. This did require the use of a fully conservative difference scheme and a transformation in order to apply the boundary conditions on the curved wind tunnel walls. There were difficulties associated with the upstream and downstream boundary conditions which limit the current results to inlet geometries similar to closed circuit tunnels. The leakage experienced with the panel method was significantly reduced but the resulting computer code was not particularly economical from a computational point of view and each of the "production runs" used for the subsequent development of the design data required approximately 20 minutes of IBM 370 CPU time. There are techniques available which could be used in future numerical studies to reduce some of the computational times but even then, future parameter studies would require significant computer resources. The greatest potential for an efficient but accurate computational method for inlet aerodynamic performance

predictions seems to lie with a combination of the surface singularity approach such as a source or vortex panel and a finite difference field solution. The panel method could be used to provide the inlet upstream boundary conditions in the form of values of the potential field. This would provide the upstream conditions for the finite difference field solution within the inlet, test section and possibly diffuser. This would allow for an accurate internal flow solution without the extreme panel detail required for the internal flow problem, as well as allow for the use with all types of tunnel configurations (i.e. indraft or closed circuit). Such an approach may also allow for the inclusion of the effect of the antiturbulence devices often placed at the entrance to the inlet. This would be extremely beneficial not only in the inlet design but also in the design of the turbulence management devices.

The experimental phases of the effort provided data on the performance of a single high contraction ratio inlet design. Velocity and pressure data were collected which allowed for the evaluation of the numerical methods. The ability to visualize the flow within the inlet provided insight into the three-dimensional character of the inlet flow field. The study of this inlet also helped in the determination of quantifiable inlet performance parameters which were subsequently used in the development of the inlet design data. The most important result of this phase of the effort was the reinforcement of the fact which had been noted in previous smoke tunnel studies that the design of the inlet and the antiturbulence devices are not independent. They must be complimentary. A poor or inadequate design of one component cannot be compensated for with the other and the interaction between the two

components is quite complex. The screens (or honeycomb) effect the velocity field and modify the turbulence. The inlet geometry obviously effects the velocity field as well as modifies the levels and content of the turbulence as the fluid passes through the inlet.

A set of preliminary design charts were developed using the finite difference field solution method which can be used for the aerodynamic design of high contraction ratio inlets in the range 10-40. The charts were developed for a family of wall contours defined by matched cubic polynomials. Although this represents only one of many possible wall geometries the resulting design charts should prove useful in basic sizing considerations such as length, aspect ratio and regions of maximum curvature. Associated with the development of the design charts was the selection of a parameter which could be used to measure inlet aerodynamic performance. These parameters are related to entrance and exit plane uniformity and adverse wall pressure gradients. It is the presence of the regions of adverse wall pressure gradients which brings about separation and unsteadiness in the inlet flow field. An approximate turbulent boundary layer separation prediction technique based on Stratford's criteria was used to examine the possibility of separation near the upstream end of the family of inlets studied. Additional work is needed before definitive separation criteria can be established. The design charts represent an attempt to provide a rational approach to the inlet design problem but the authors wish to stress that they are preliminary in nature. They represent the first time that a procedure has been developed which should aid in the design of true three-dimensional wind tunnel inlets. It is only through the

application and verification of this design data that it can be fully evaluated.

It is hoped that the work conducted during this project will provide direction and motivation for additional studies in this important area of aerodynamic design of wind tunnel facilities.

REFERENCES

1. Bradshaw, P. and Pankhurst, B. C., "The Design of Low-Speed Wind Tunnels," Progress in Aeronautical Sciences, Vol. 5, MacMillan Publishing Co., 1964.
2. Batill, S., Nelson, R. and Mueller, T., "High Speed Smoke Flow Visualization," AFWAL-TR-81-3002, March, 1981.
3. Uberoi, M. S., "Effect of Wind-Tunnel Contraction on Free-Stream Turbulence," Journal of Aeronautical Sciences, Vol. 23, pp. 754-764, August, 1956.
4. Ribner, H. S. and Tucker, M., "Spectrum of Turbulence in a Contracting Stream," NACA Technical Report 1113, 1953.
5. Klien, A. and Ramjee, V., "Effects of Contraction Geometry on Non-Isotropic Free-stream Turbulence," Aeronautical Quarterly, pp. 34-38, February, 1973.
6. Uberoi, M. S. and Wallis, S., "Small Axisymmetric Contraction of Grid Turbulence," J. Fluid Mechanics, Vol. 24, 1966.
7. Comte-Bellot, G. and Corrsin, S., "The Use of a Contraction to Improve the Isotropy of Grid Generated Turbulence," Journal of Fluid Mechanics, Vol. 25, 1966.
8. Ramjee, V. and Hussain, A., "Influence of the Axisymmetric Contraction Ratio on Free Stream Turbulence," Journal of Fluids Engineering, Vol. 98, 1976.
9. Tan-Atichat, J., "Effects of Axisymmetric Contractions on Turbulence of Various Scales," Ph.D. Dissertation, Illinois Institute of Technology, Chicago, Ill. May 1980.
10. Purtell, L. P. and Klebanoff, P. S., "A Low-Velocity Airflow Calibration and Research Facility," National Bureau of Standards Technical Note 989, March, 1979.
11. Mueller, T. J., "Smoke Visualization of Subsonic and Supersonic Flows (The Legacy of F.N.M. Brown)," Final Report UNDAS TN-34121-1, AFOSR-TR-78-1262, June, 1978.
12. Batill, S. M. and Mueller, T. J., "Visualization of the Laminar-Turbulent Transition in the Flow Over an Airfoil Using the Smoke-Wire Technique," AIAA Paper 80-0421-CP, 1980.
13. Mueller, T. J., "On the Historical Development of Apparatus and Techniques for Smoke Visualization of Subsonic and Supersonic Flows," AIAA Paper 80-0420, 11th Aerodynamic Testing Conference, March 1980.

14. Merzkirch, Wolfgang (Editor), "Flow Visualization II," Proceedings of the Second International Symposium on Flow Visualization, Bochum, West Germany, Hemisphere Publishing Corp., Sept. 1980.
15. Asanuma, T., (Editor), "Flow Visualization," Proceedings of the First International Symposium of Flow Visualization, Tokyo, Japan, Hemisphere Publishing Corp., Oct. 1977.
16. Wells, W. C. and Beachler, J. C., "The Subsonic Aerodynamic Research Laboratory (SARL): A New 10 x 7 foot Low-Turbulence Facility for Flow Visualization," SATA Presentation at Grumman Aircraft Co., April, 1983.
17. Tsien, H., "On the Design of the Contraction Cone for a Wind Tunnel," *Journal of Aeronautical Sciences*, pp. 68-70, February, 1943.
18. Szczeniowski, B., "Contraction Cone for a Wind Tunnel," *Journal of Aeronautical Sciences*, pp. 311-312, October, 1943.
19. Batchelor, G. K. and Shaw, F.S., "A Consideration of the Design of Wind Tunnel Contractions," Report ACA-4, March, 1944.
20. Smith, R. H. and Wang, C., "Contracting Cones Giving Uniform Throat Speeds," *Journal of Aeronautical Sciences*, pp. 356-360, October, 1944.
21. Chmielewski, G. E., "Boundary Layer Considerations in the Design of Aerodynamic Contractions," *Journal of Aircraft*, Vol. II, No. 8, August, 1974.
22. Borger, G. G., "The Optimization of Wind Tunnel Contractions for the Subsonic Range," NASA TRF-16899, March, 1976.
23. Mikhail, M. N. and Rainbird, W. J., "Optimum Design of Wind Tunnel Contractions," AIAA Paper 78-819, 1978.
24. Morel, T., "Comprehensive Design of Axisymmetric Wind Tunnel Contractions," *Journal of Fluids Engineering*, ASME Transactions, pp. 225-233, June, 1975.
25. Morel, T., "Design of Two-Dimensional Wind Tunnel Contractions," ASME Paper No. 76-WA/FE-4, pp. 1-7, December, 1976.
26. Cohen, M. J. and Ritchie, N.J.B., "Low Speed Three-Dimensional Contraction Design," *Journal of the Royal Aeronautical Society*, Vol. 66, pp. 231-236, April, 1962.
27. Hess, J. L., "Status of a Higher-Order Panel Method for Non-Lifting Three-Dimensional Potential Flow," McDonnell Douglas Report MDC J7714-01, August, 1977.

AD-A138 865

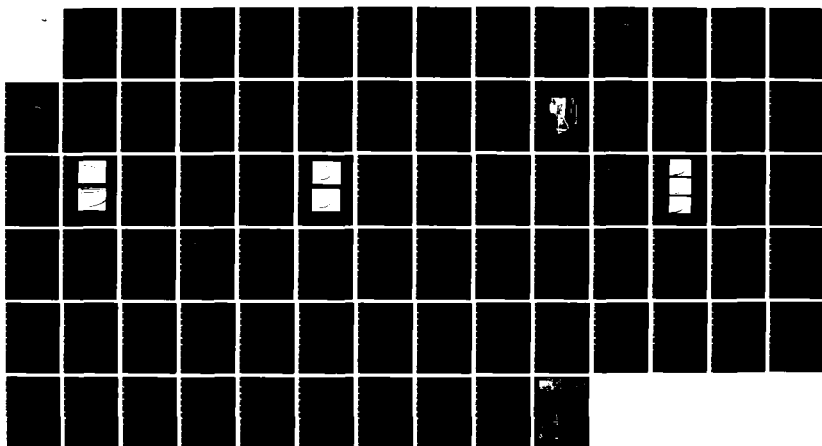
AN EXPERIMENTAL AND ANALYTIC STUDY OF THE FLOW SUBSONIC 2/2
WIND TUNNEL INLET. (U) NOTRE DAME UNIV IN DEPT OF
AEROSPACE AND MECHANICAL ENGINEERING S M BATILL ET AL.

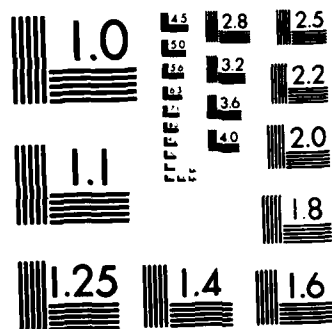
UNCLASSIFIED

OCT 83 AFWAL-TR-83-3109 F33615-81-K-3008

F/G 20/4

NL





MICROCOPY RESOLUTION TEST CHART
NATIONAL BUREAU OF STANDARDS 1963-A

28. Johnson, F. T. and Rubbert, P. E., "Advanced Panel-Type Influence Coefficient Methods Applied to Subsonic Flows," AIAA Paper 75-50, 1975.
29. Hess, J. L. and Smith, A.M.O., "Calculation of Non-Lifting Potential Flow About Arbitrary Three-Dimensional Bodies," Journal of Ship Research, Vol. 8, No. 2, September, 1964, pp. 22-44.
30. Johnson, F. T., "A General Panel Method for the Analysis and Design of Arbitrary Configurations in Incompressible Flows," NASA CR-3079, May, 1980.
31. Bristow, D. R., "Development of Panel Methods for Subsonic Analysis and Design," NASA CR-3234, February, 1980.
32. Hess, J. L. and Smith, A.M.O., "Calculation of Potential Flow About Arbitrary Bodies," Progress in Aeronautical Sciences, Vol. 8, 1967, pp. 1-138.
33. Renken, J., "Investigation of the Three-Dimensional Flow in a Duct With Quadrangular, Variable Cross-Section By Means of the Panel Method," Deutsche Forschungs -und Versuchsanstalt fur Luft -und Raumfahrt, Institut fur Luftstrahlantriebe, Cologne, West Germany, Report No. DLR-FB 75-46, February, 1976.
34. Hess, J. L., Mack, D. P. and Stockman, N.O., "An Efficient User-Oriented Method for Calculating Compressible Flow In and About Three-Dimensional Inlets - Panel Methods," NASA CR-159578, April, 1979.
35. Lee, K. D., "Numerical Simulation of the Wind Tunnel Environment by a Panel Method," AIAA Journal, Vol. 19, No. 4, April, 1980, p. 470.
36. Hoffman, J. J., "Development of a Computer Program Using the Source Panel Method to Analyze Subsonic Flow-Fields in High Contraction Ratio Wind Tunnel Inlets," Masters Thesis, Department of Aerospace and Mechanical Engineering, University of Notre Dame, Notre Dame, Indiana, June, 1983.
37. Hunt, B., "The Panel Method for Subsonic Aerodynamic Flows: A Survey of Mathematical Formulations and Numerical Models and an Outline of the New British Aerospace Scheme," in Computational Fluid Dynamics, Vol. 1, edited by Wolfgang Kollman, Hemisphere Publishing Corp., Washington, 1980, pp. 99-166.
38. "Applied Computational Aerodynamics," AIAA Recorded Lecture Series, Recorded 25-26 June, 1977, prior to the AIAA 10th Fluid and Plasmadynamics and 3rd Computational Fluid Dynamics Conference on 27-29 June, 1977.
39. Halsey, N. D. and Hess, J. L., "A Geometry Package for the Genera-

tion of Input Data for a 3-D Potential Flow Program (Final Report)," NASA CR-2962, June, 1978.

40. Sanderse, A. and van der Voreen, J., "Finite Difference Calculation of Incompressible Flows Through a Straight Channel of Varying Rectangular Cross-Section, With Application to Low Speed Wind Tunnels," NLR TR 77109 U, September, 1977.
41. Dryden, H. L. and Schubauer, G. B., "The Use of Damping Screens for the Reduction of Wind-Tunnel Turbulence," paper presented at the Aerodynamics Session, Fifteenth Annual Meeting, I.A.S., New York, January 28-30, 1947.
42. Schubauer, G. B., Spangenberg, W. G. and Klebanoff, P. S., "Aerodynamic Characteristics of Damping Screens," NACA TN 2001, National Bureau of Standards, Washington, D.C., January, 1950.
43. Loehrke, R. I. and Nagib, H. M., "Experiments on the Management of Free Stream Turbulence," AGARD Report No. 598, 1972.
44. Dryden, H. L. and Abbot, I. H., "The Design of Low-Turbulence Wind Tunnels," NACA Technical Report 940, 1949.
45. Mueller, T., Pohlen, L., et. al., "The Influence of Free-stream Disturbances on Low Reynolds Number Airfoil Experiments," Experiments in Fluids, Vol. 1, No. 1, pp. 3-14, 1983.
46. Caylor, J. J., "An Experimental Investigation of High Contraction Ratio Wind Tunnel Inlets," Masters Thesis, University of Notre Dame, Notre Dame, Indiana, January, 1983.
47. United Sensor and Control Corp., Calibration Data for Type DC-125 Probe, Bulletin DC, Watertown, Mass.
48. Stratford, B. S., "The Prediction of Separation of the Turbulent Boundary Layer," Journal of Fluid Mechanics, Vol. 5, 1959.

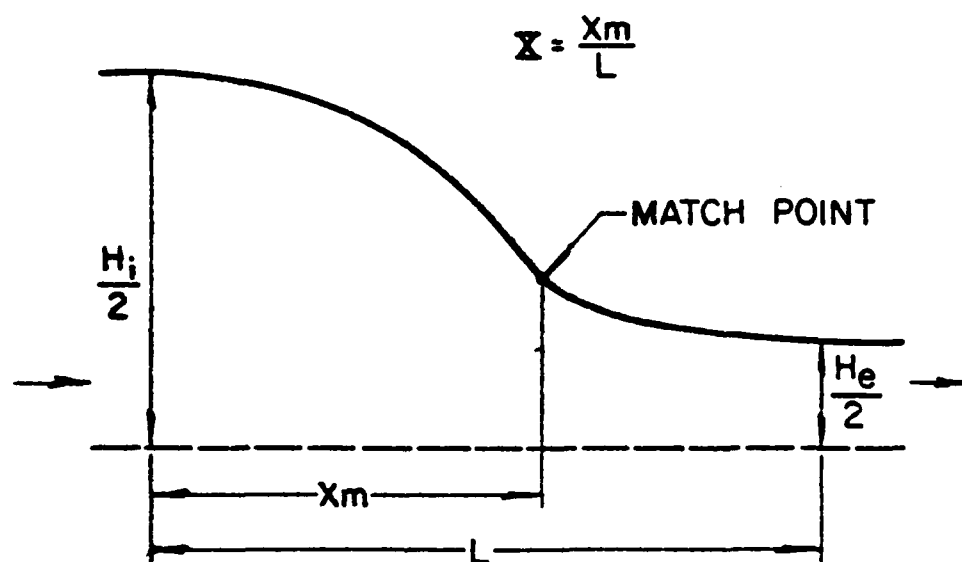


Figure 1. Schematic of Two-Dimensional Inlet Geometry - Matched Cubic

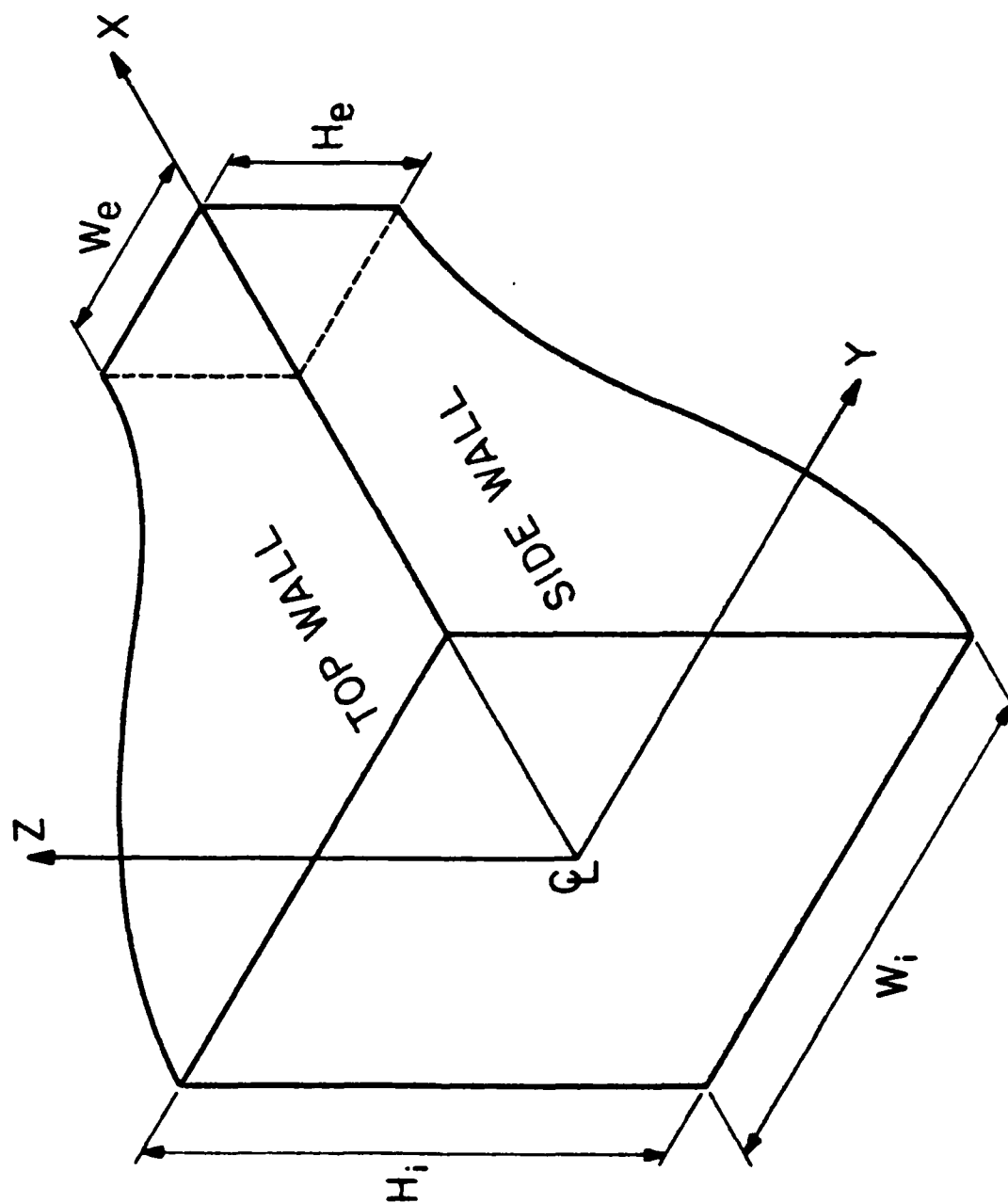
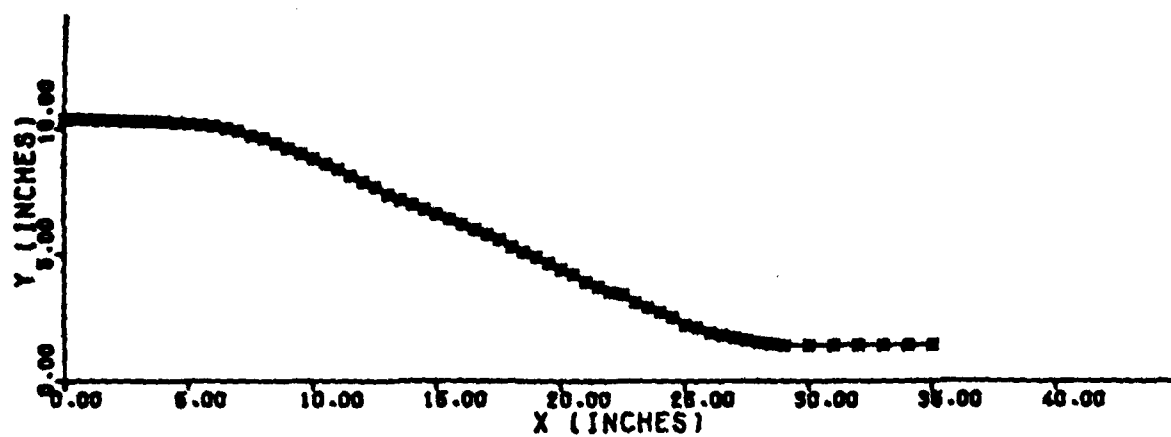
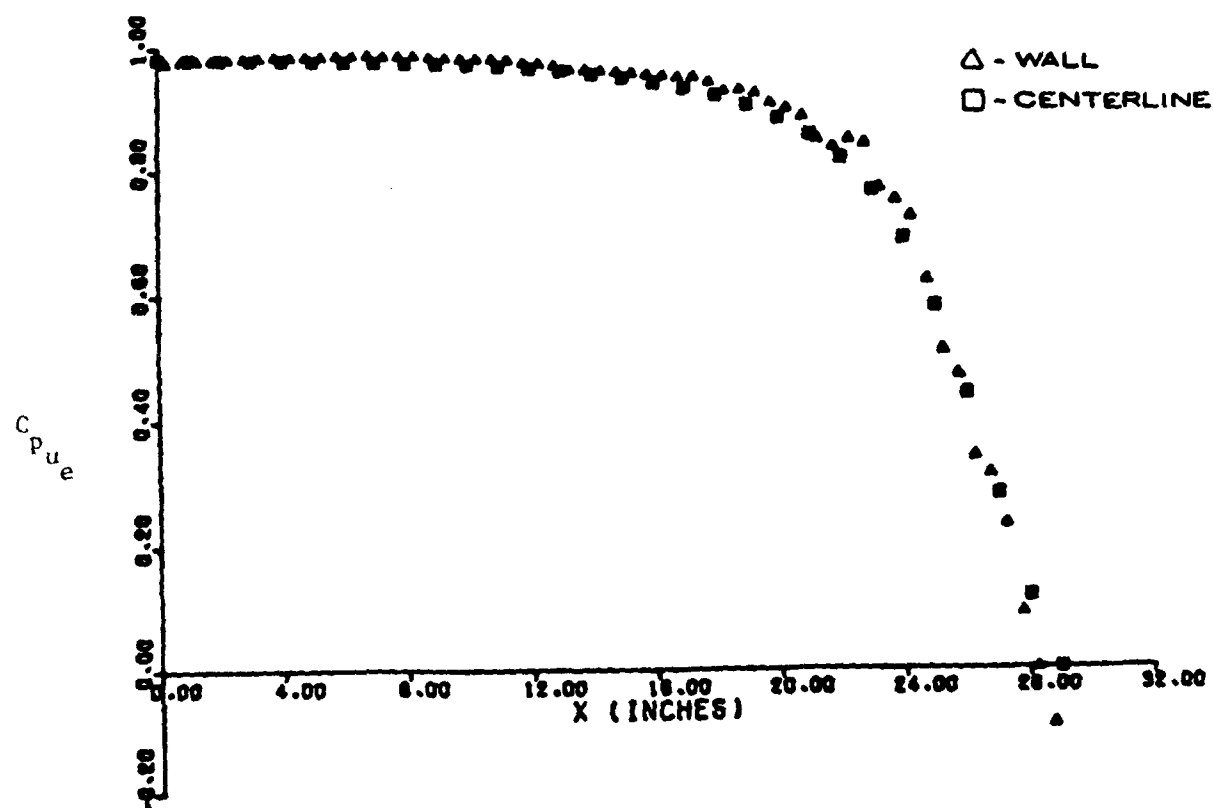


Figure 2. Schematic of Three-Dimensional Inlet Geometry

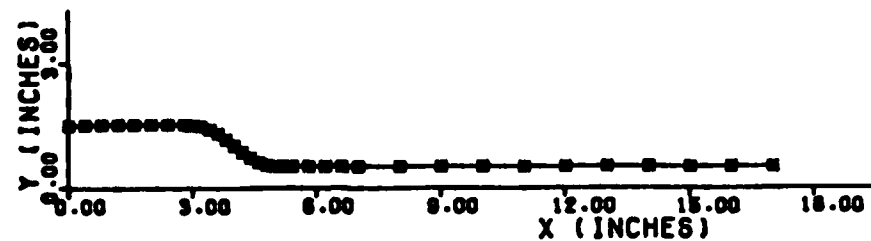


Paneling

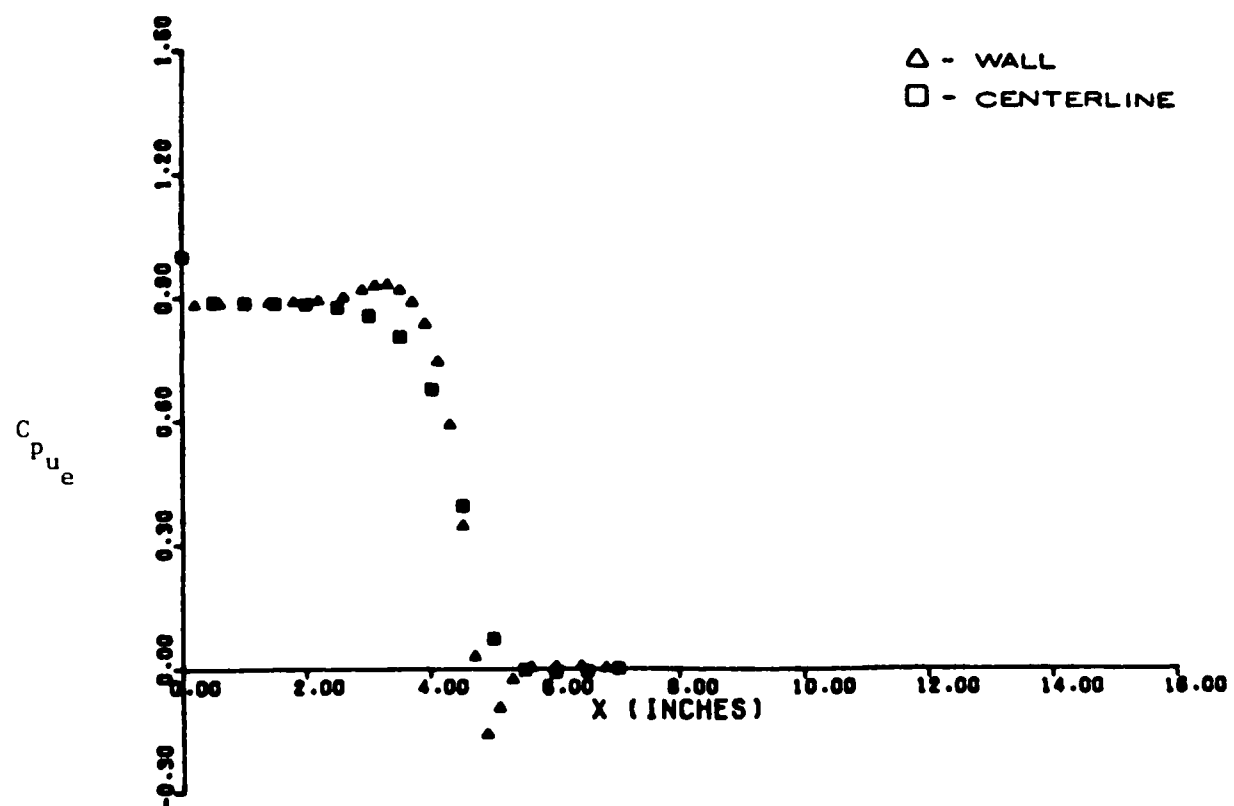


Pressure Coefficients

Figure 3. Two-Dimensional Panel Solution,
Inlet 1, CR = 7.43

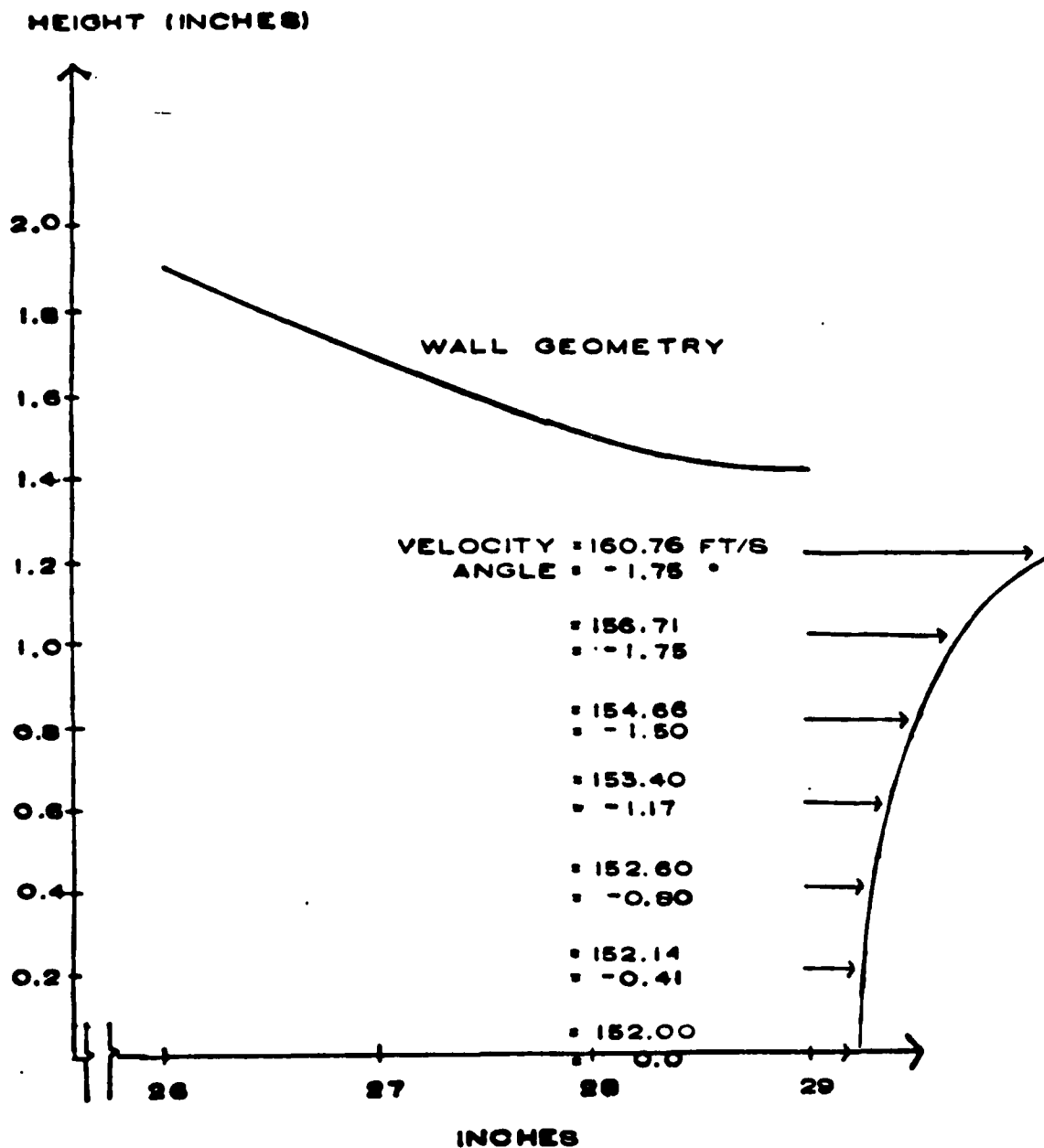


Paneling



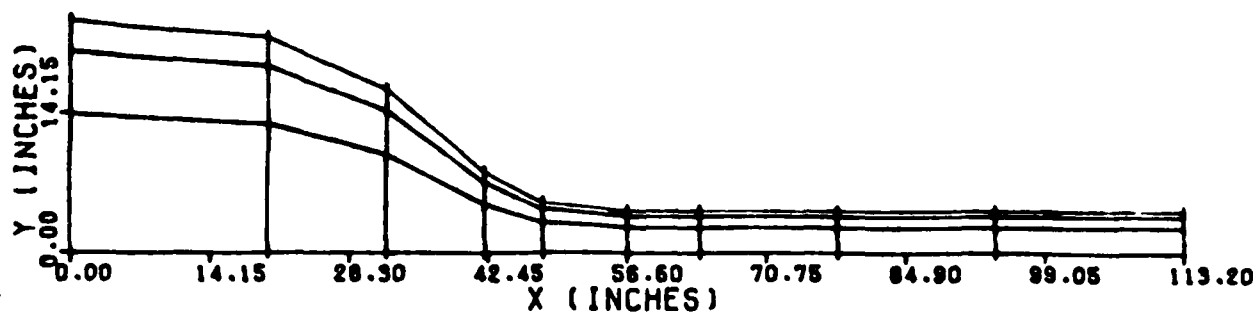
Pressure Coefficients

Figure 4. Two-Dimensional Panel Solution,
Inlet 2, CR = 3.0

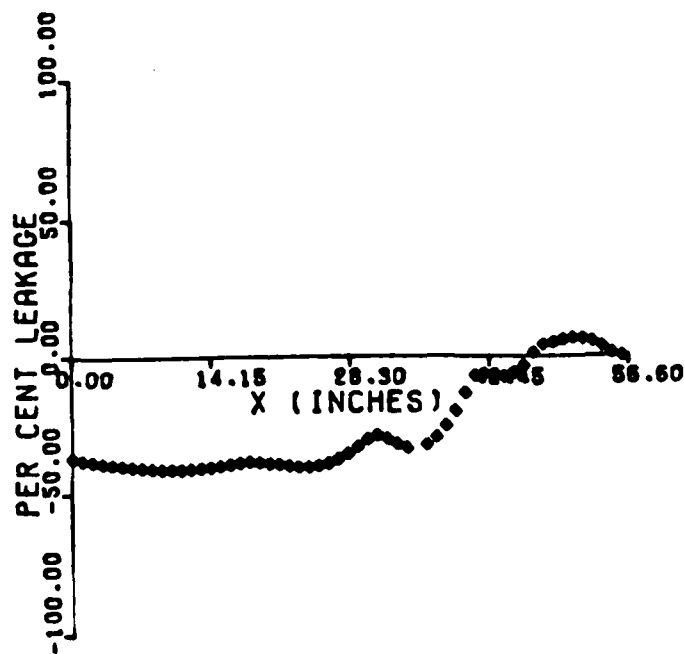


Exit Flow Angularities

Figure 5. Exit Plane Velocity Distribution, Two - Dimensional Panel Solution

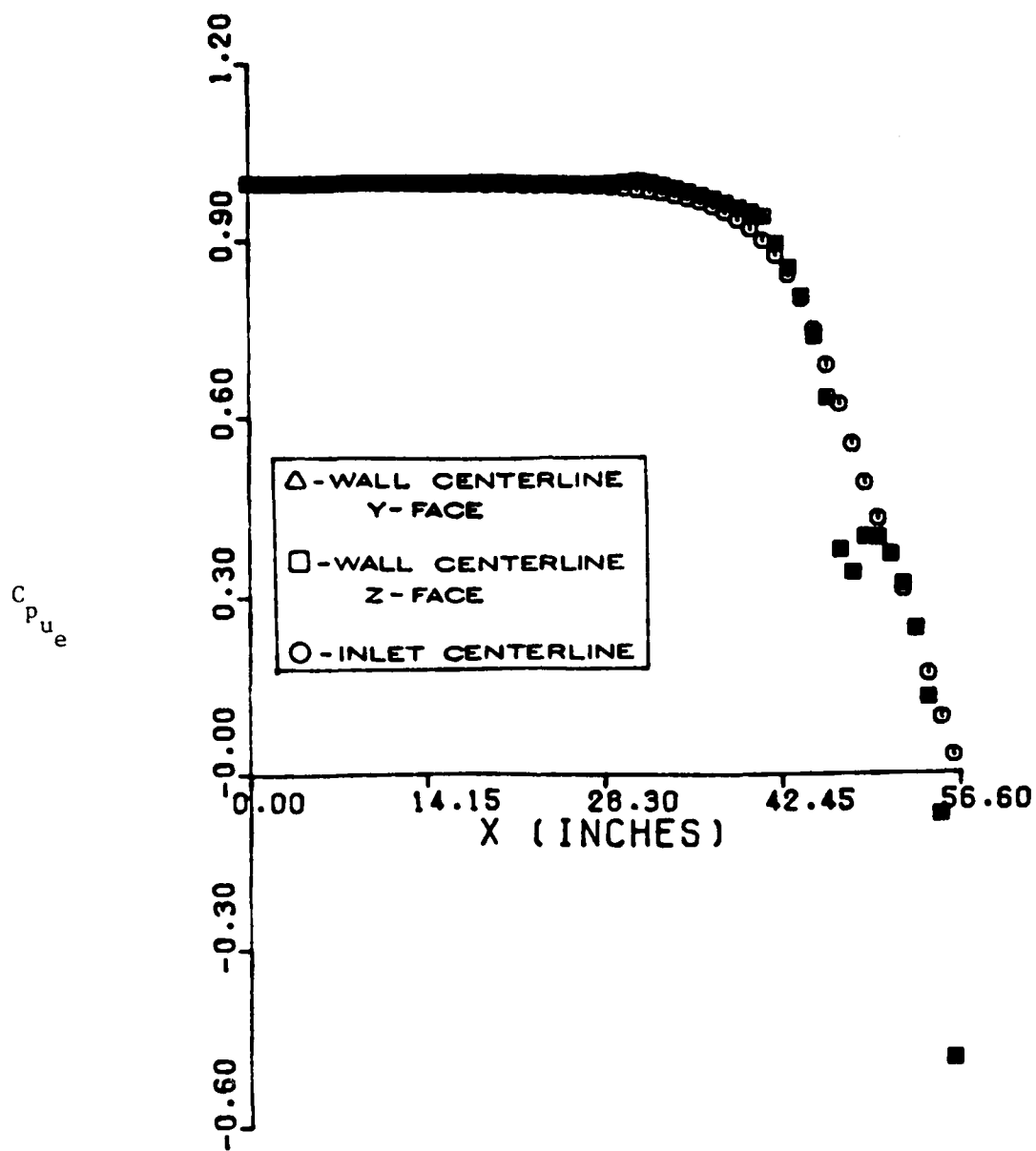


(a) Paneling



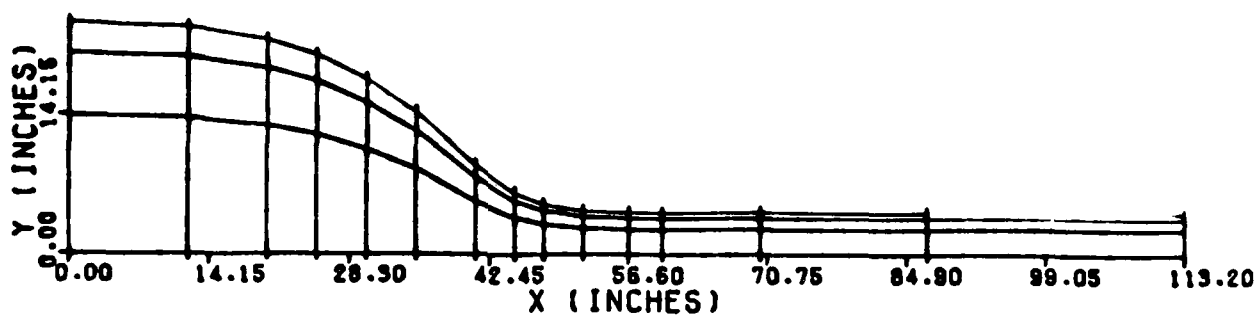
(b) Leakage

Figure 6. Three-Dimensional Paneling Results, Panel Scheme #3

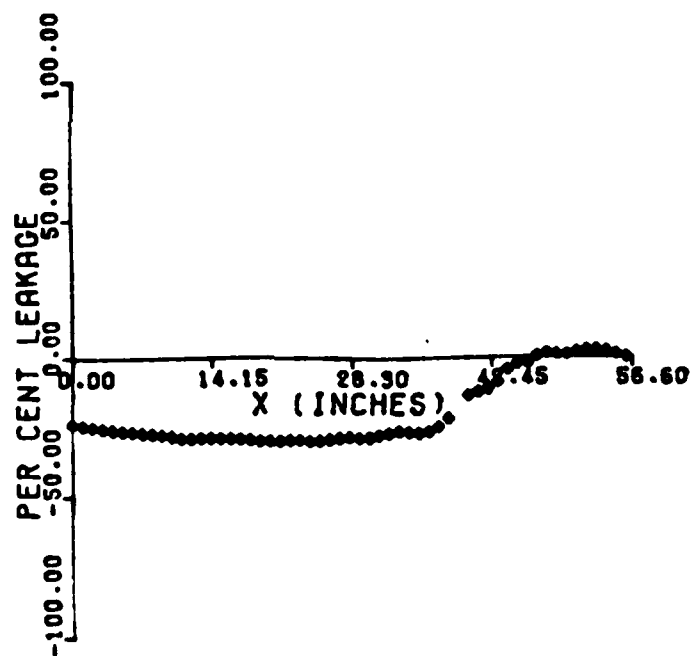


(c) Pressure Coefficients

Figure 6. Three-Dimensional Paneling Results, Panel Scheme #3

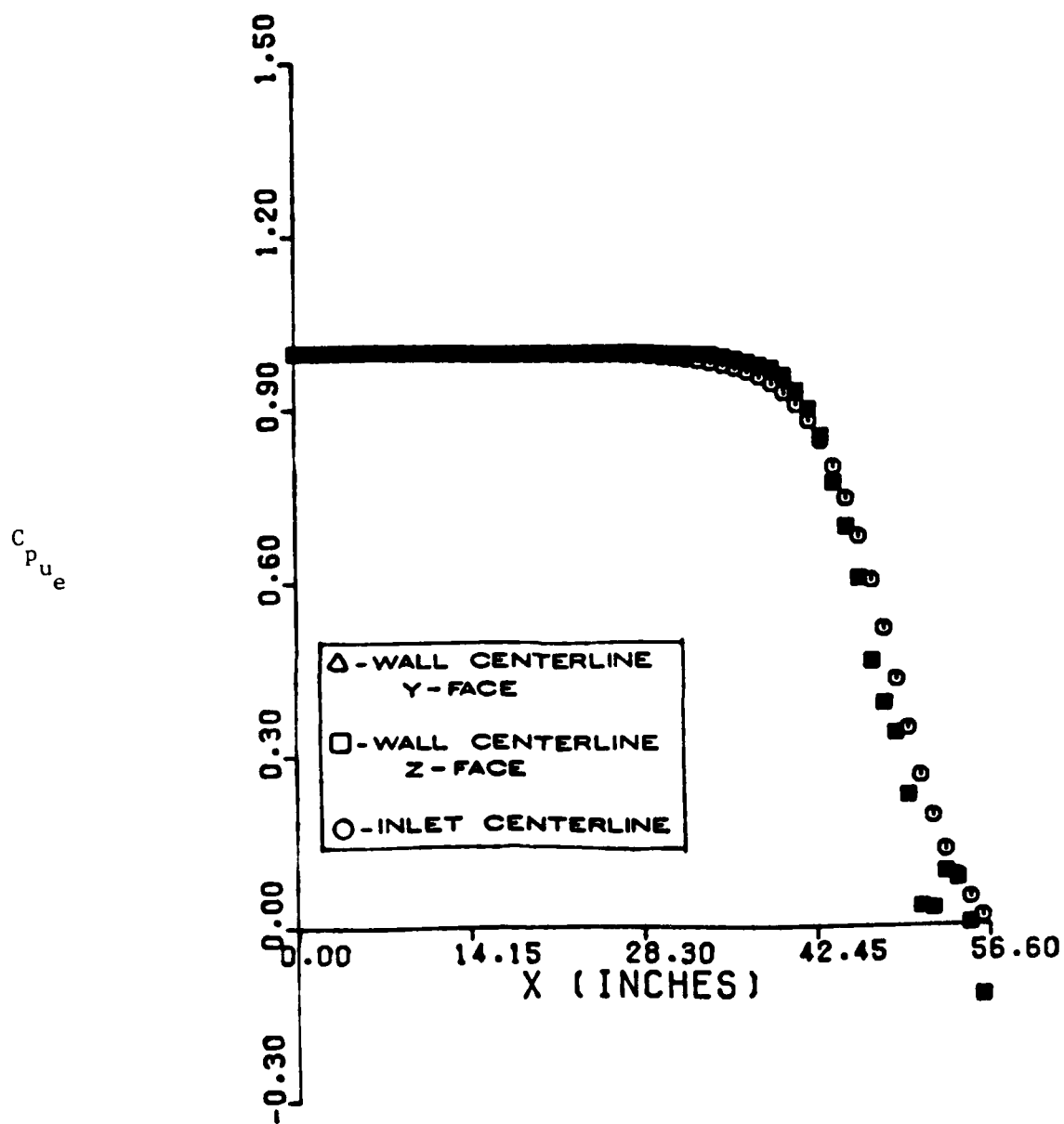


(a) Paneling



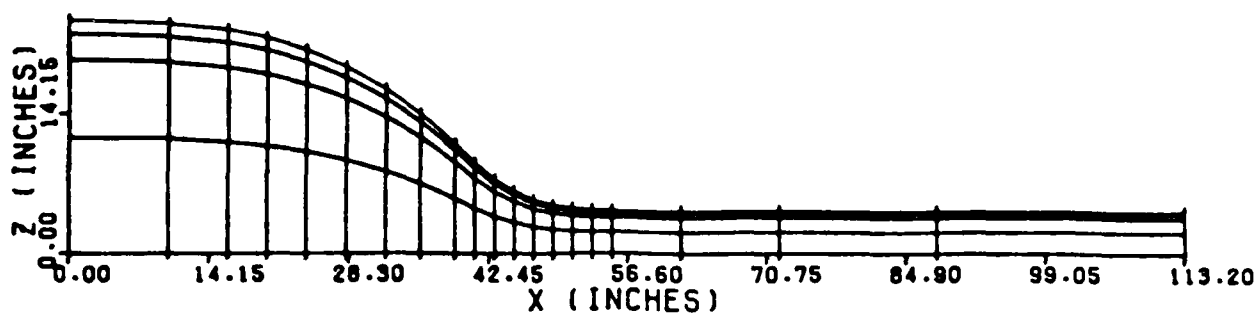
(b) Leakage

Figure 7. Three-Dimensional Paneling Results, Panel Scheme #5

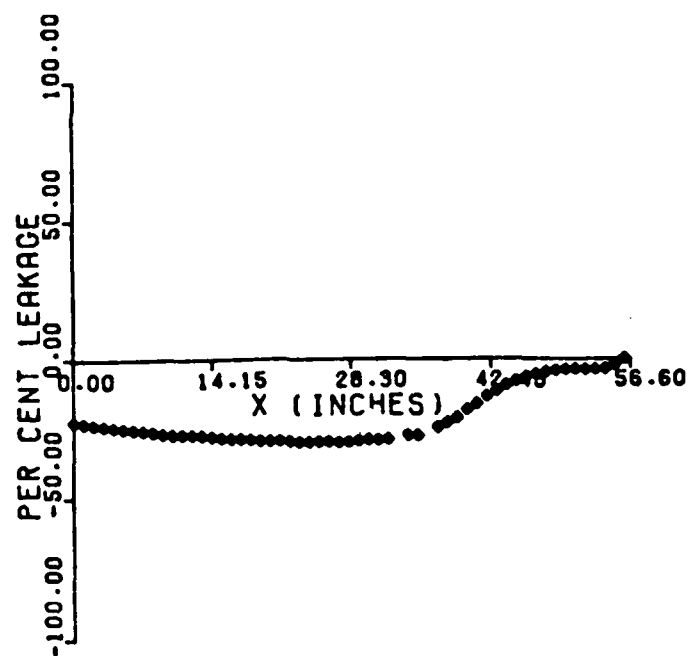


(c) Pressure Coefficients

Figure 7. Three-Dimensional Paneling Results, Panel Scheme #5

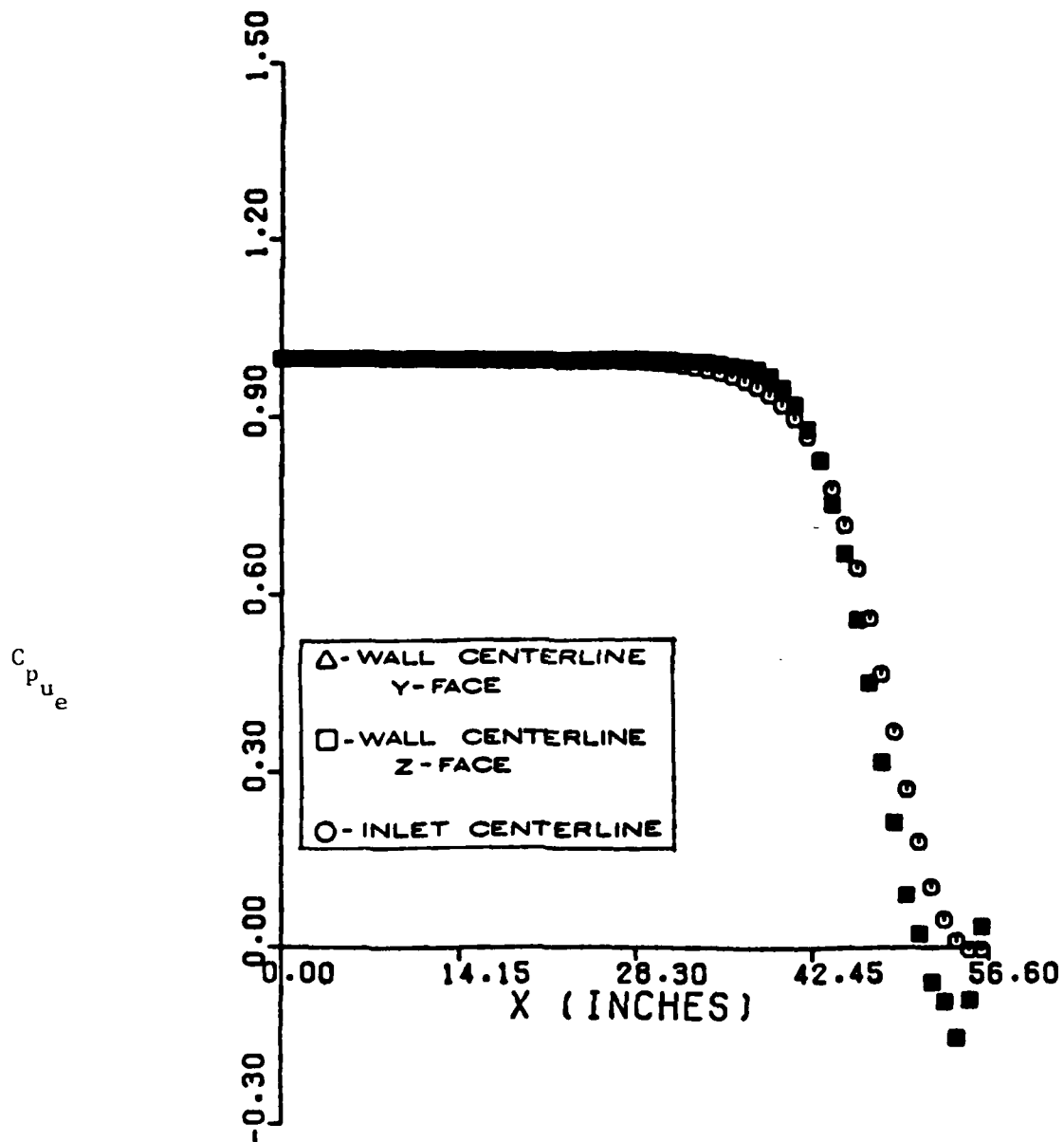


(a) Paneling



(b) Leakage

Figure 8. Three-Dimensional Paneling Results, Panel Scheme #6



(c) Pressure Coefficients

Figure 8. Three-Dimensional Paneling Results, Panel Scheme #6

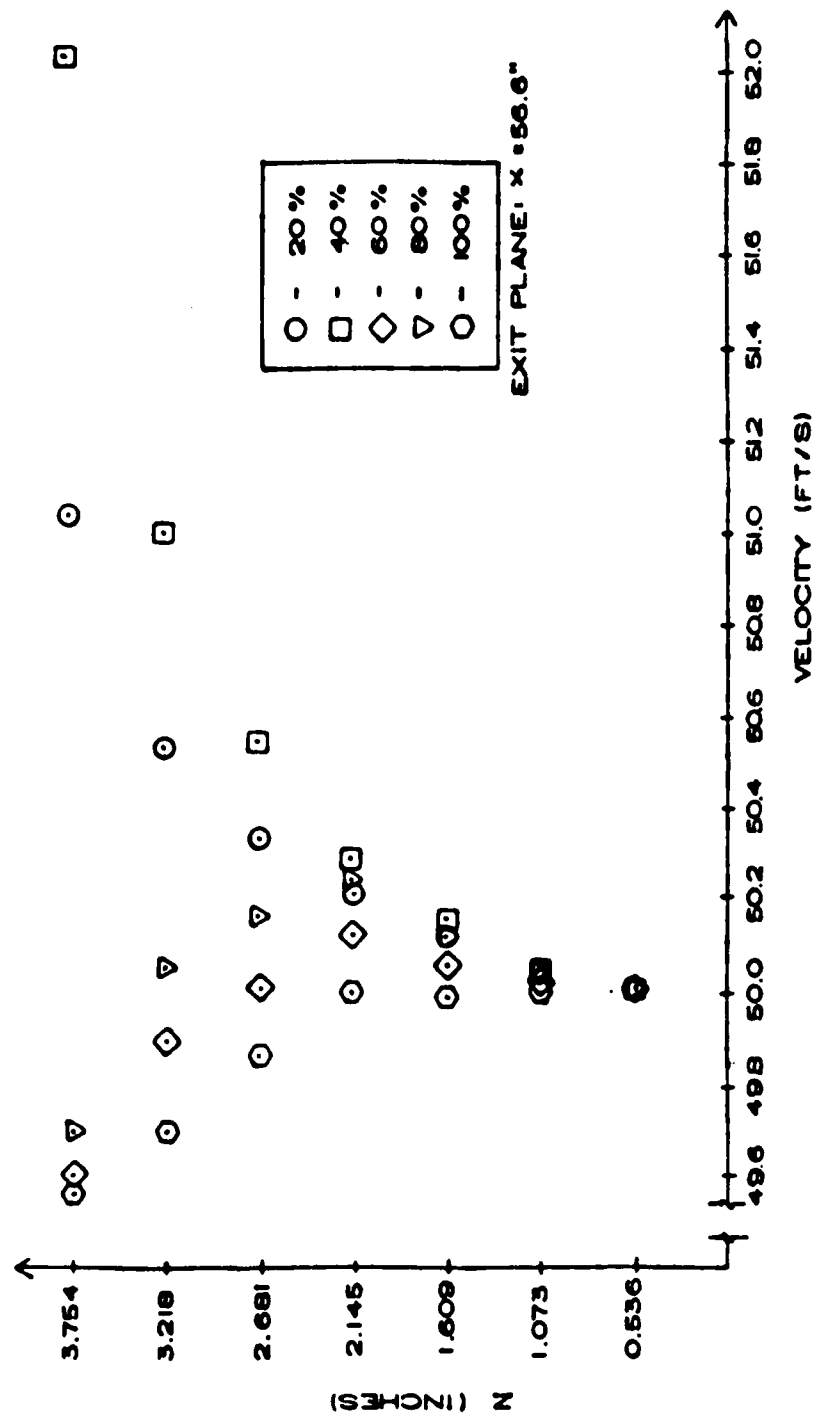


Figure 9. Exit Plane Velocity Profile Dependence on Sink Panel Location

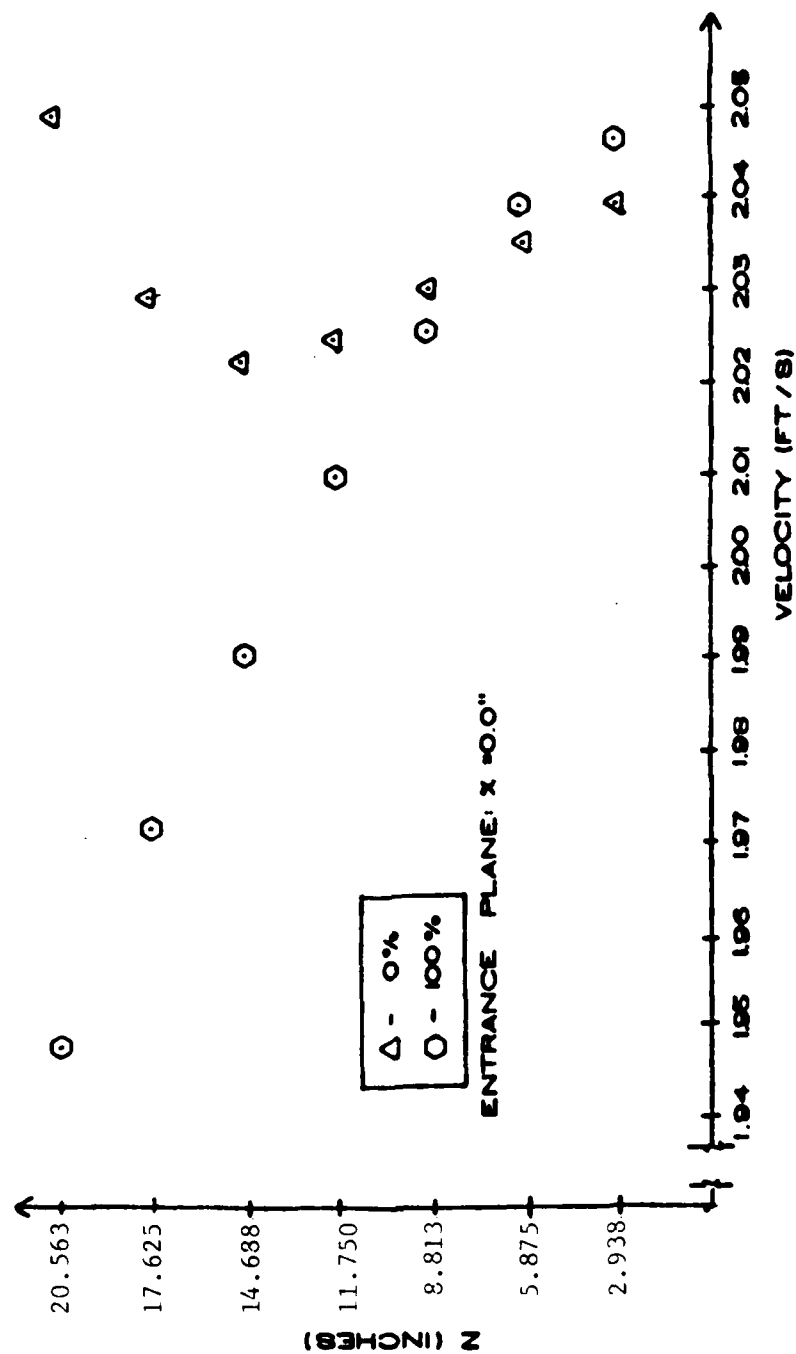


Figure 10. Entrance Plane Velocity Profile Dependence on Upstream Paneling

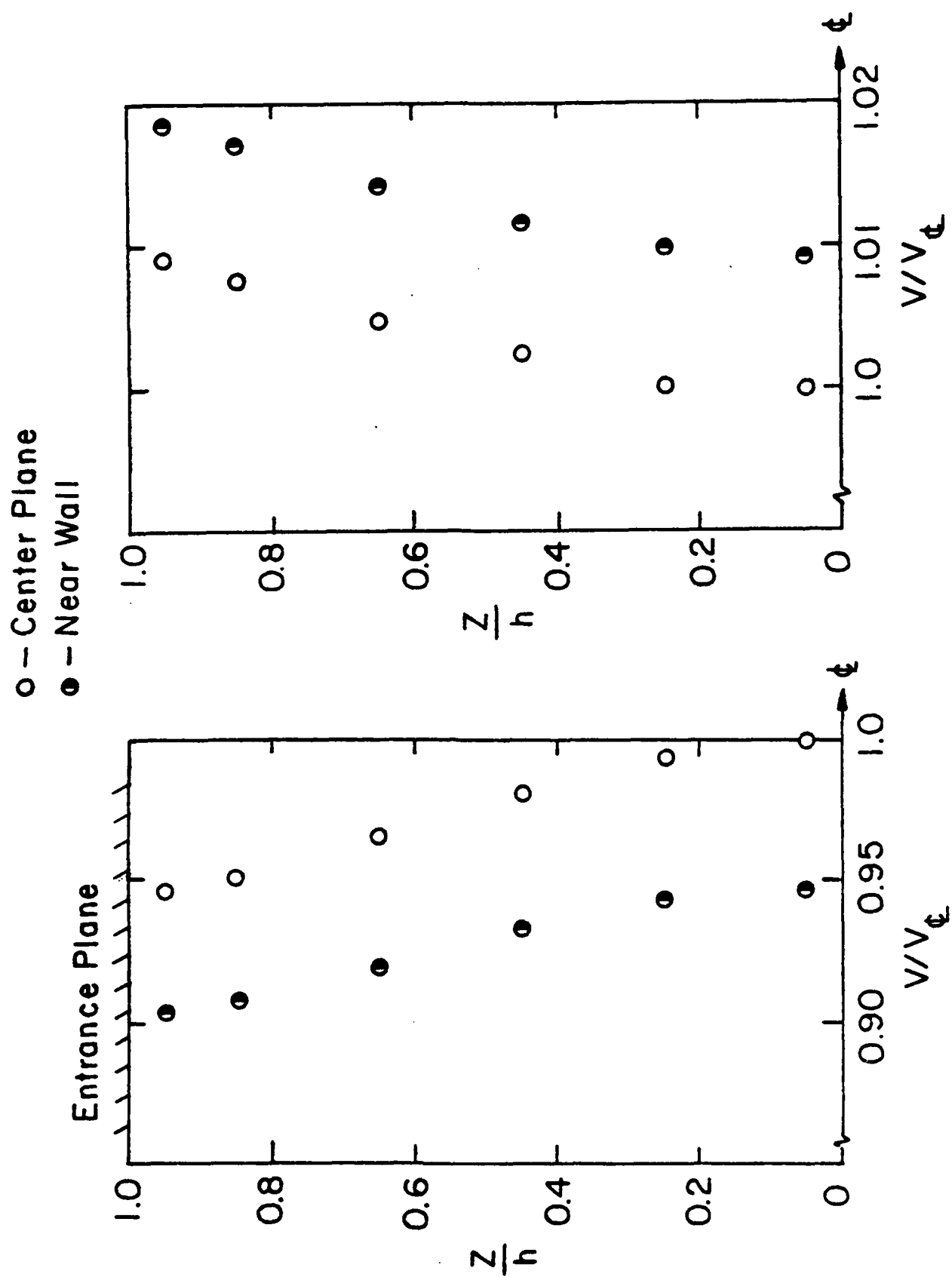


Figure 11. Entrance and Exit Plane Velocity Profiles

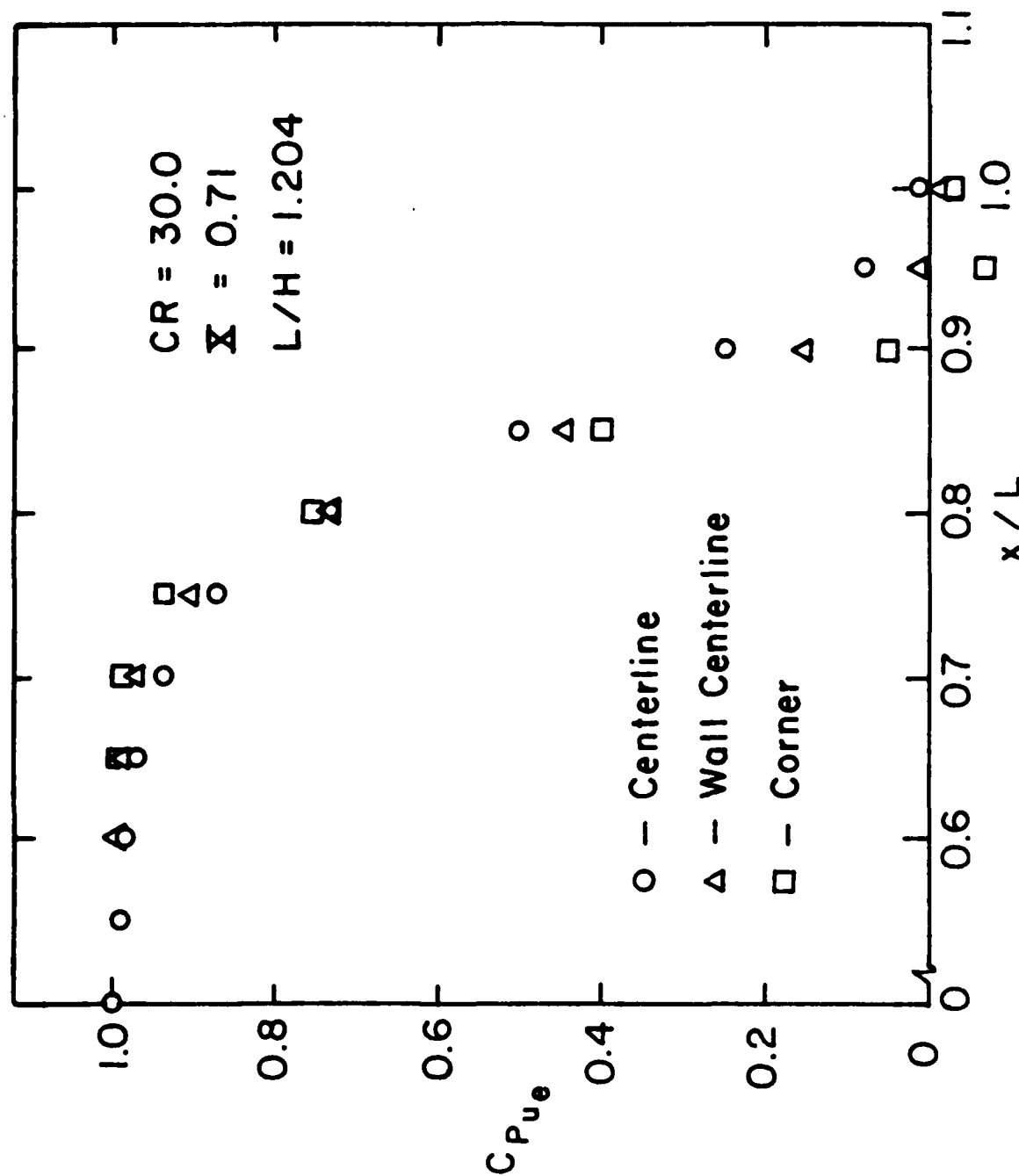


Figure 12. Pressure Coefficients $C_{p_{ue}}$, for Finite Difference

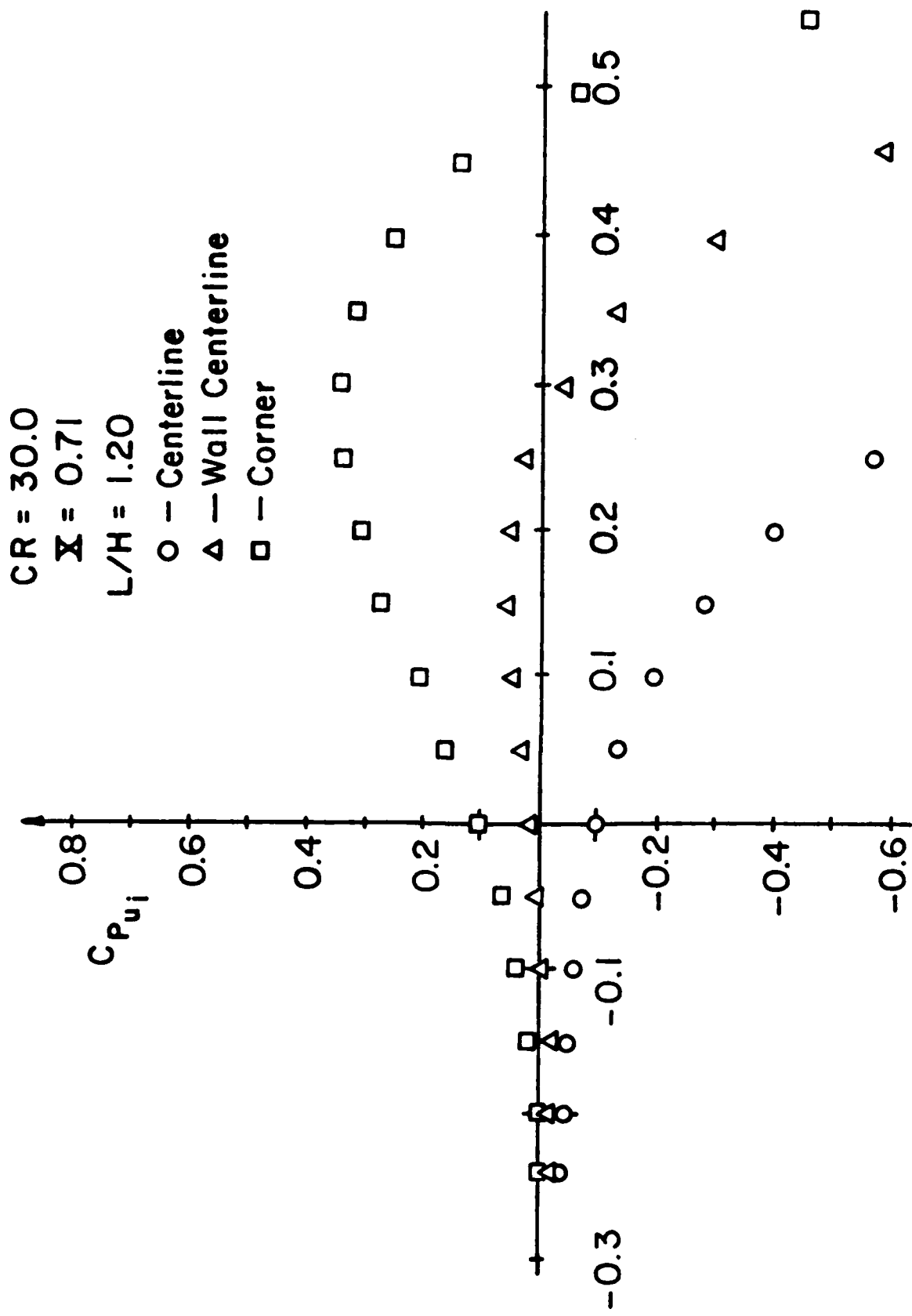


Figure 13. Pressure Coefficient, $C_{p_{u_i}}$, for Finite Difference Solution

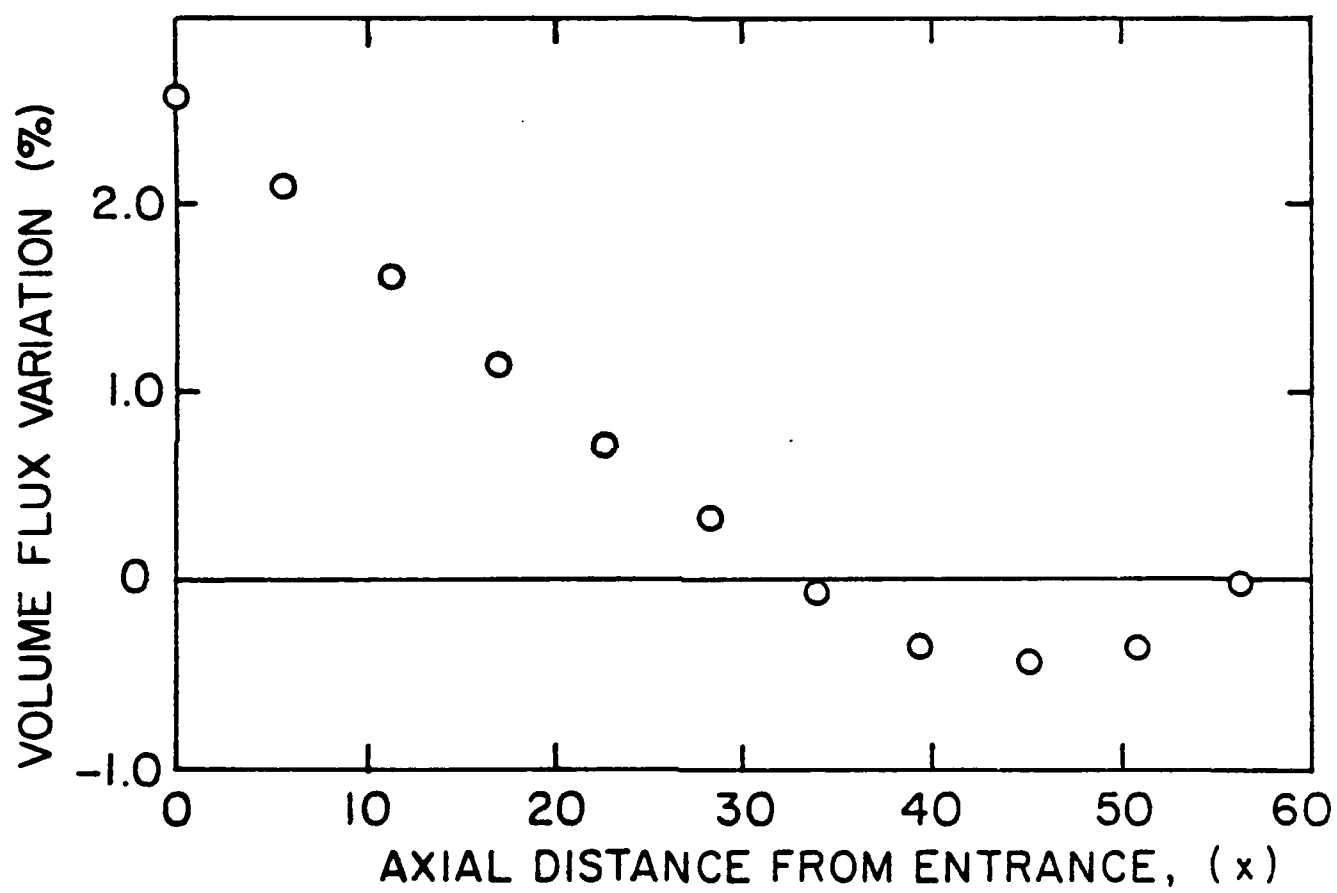


Figure 14. Leakage Calculation Finite Difference Solution.

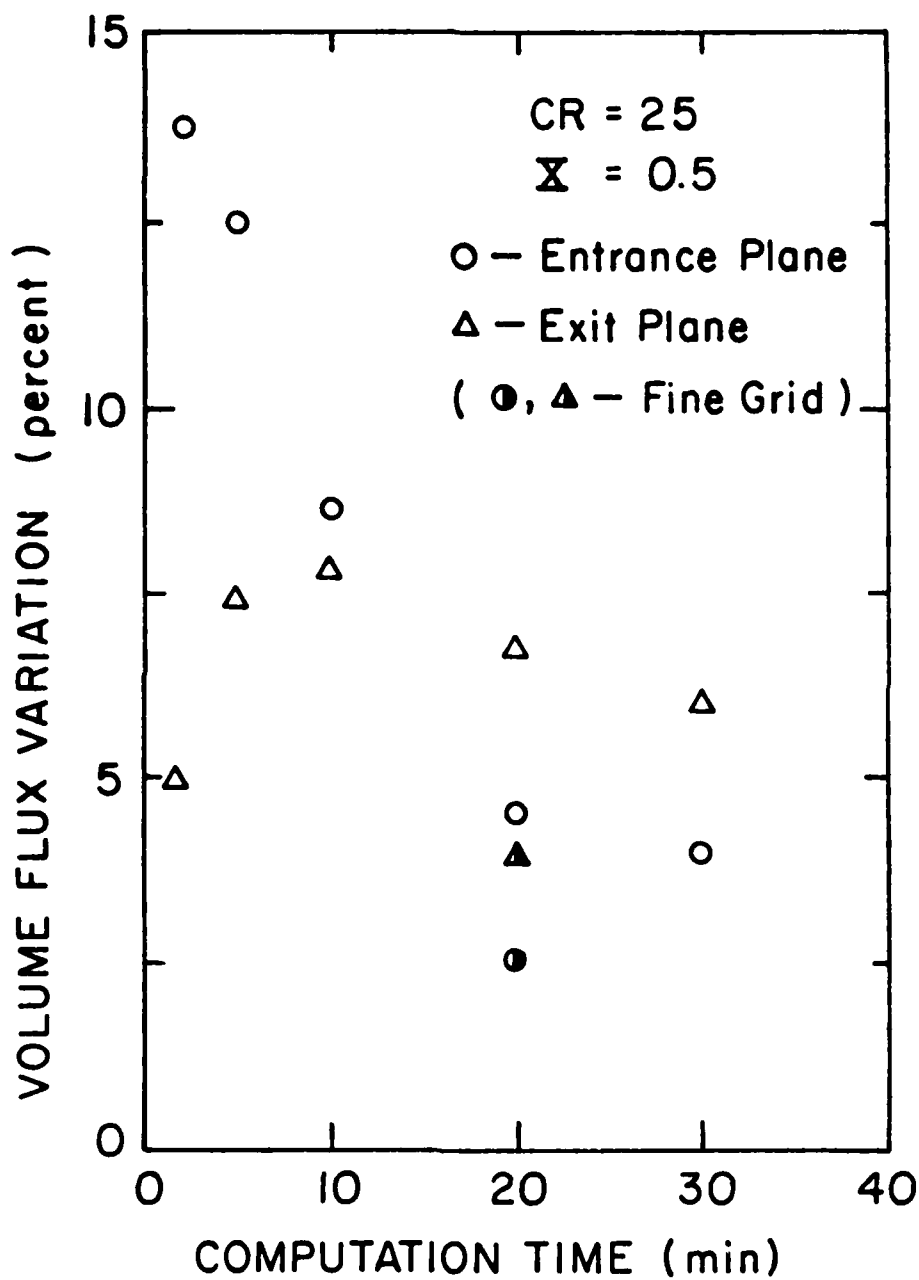


Figure 15. Finite Difference Solution Convergence, Volume Flux Calculation

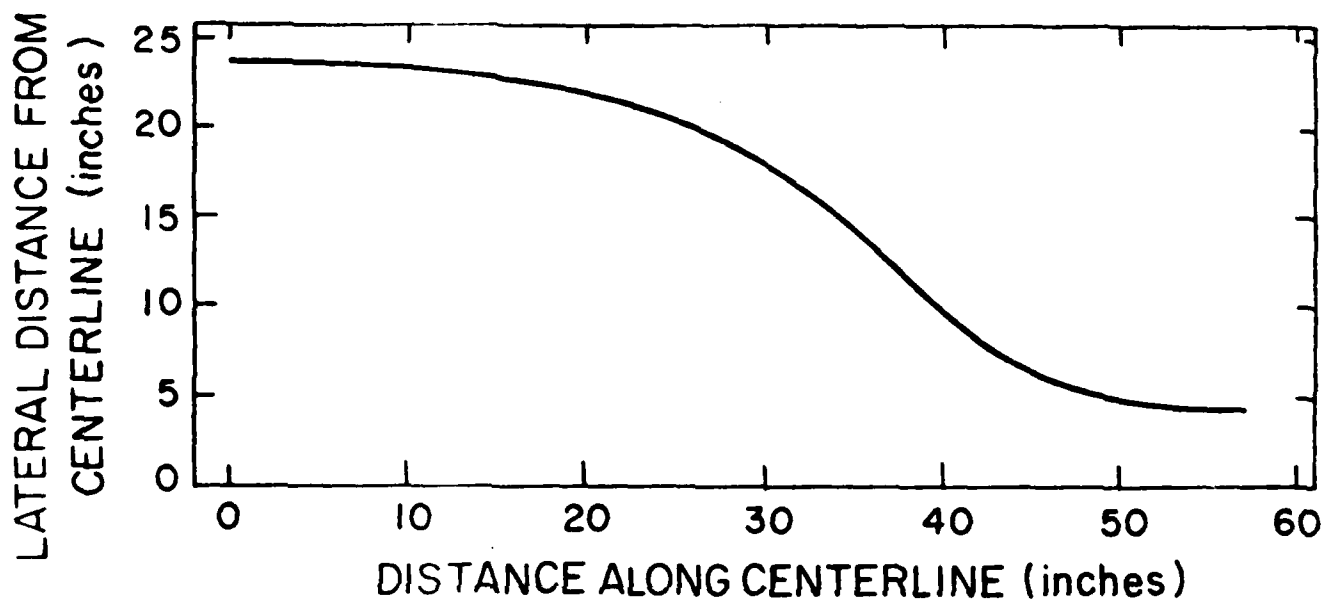


Figure 16. Flow Visualization Inlet Wall Contour

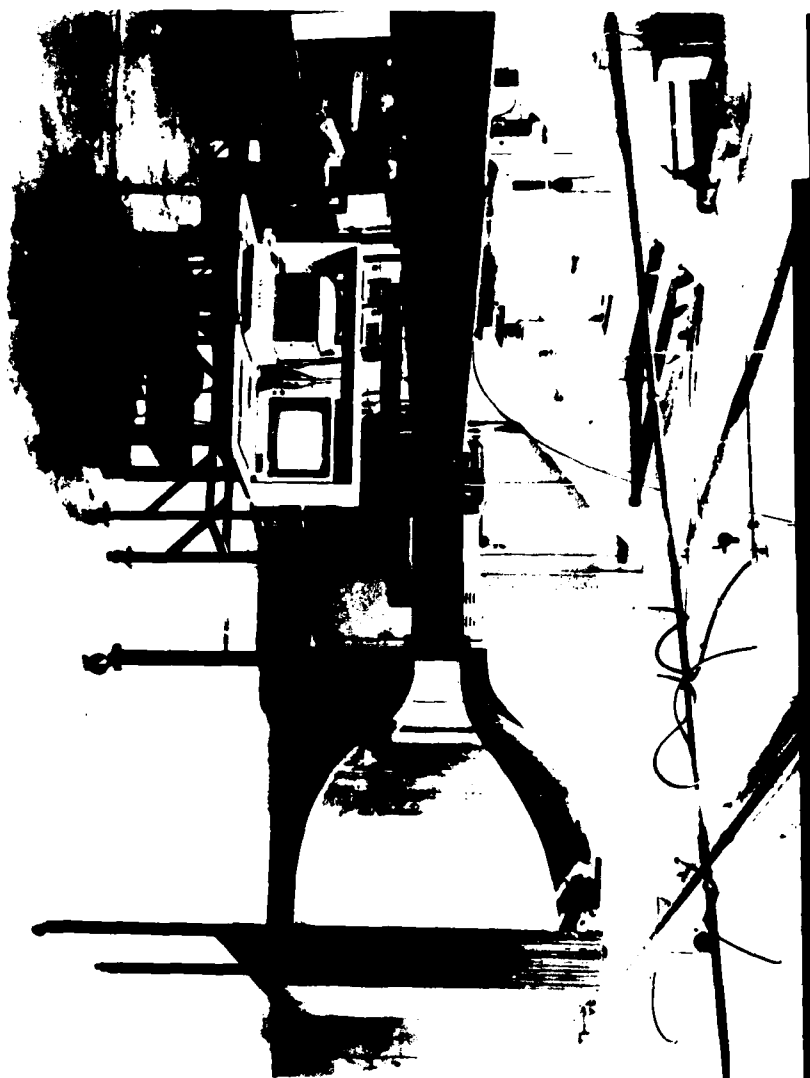


Figure 17. Photograph of Experimental Facility

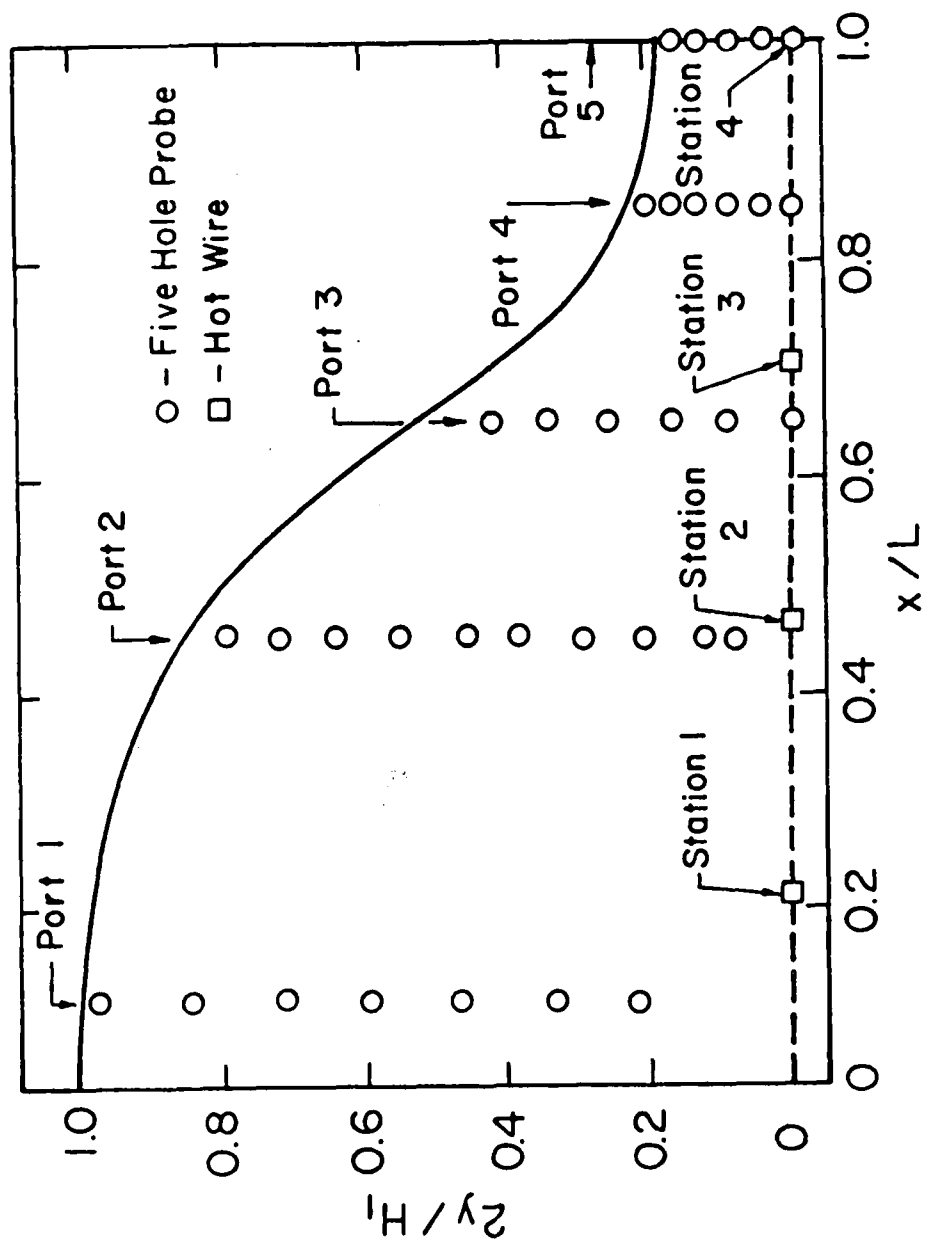


Figure 18. Five-hole probe and Hot-wire Data Locations

O Screens ($V_{TS} = 212 \text{ fps}$)
 II Screens ($V_{TS} = 203 \text{ fps}$)

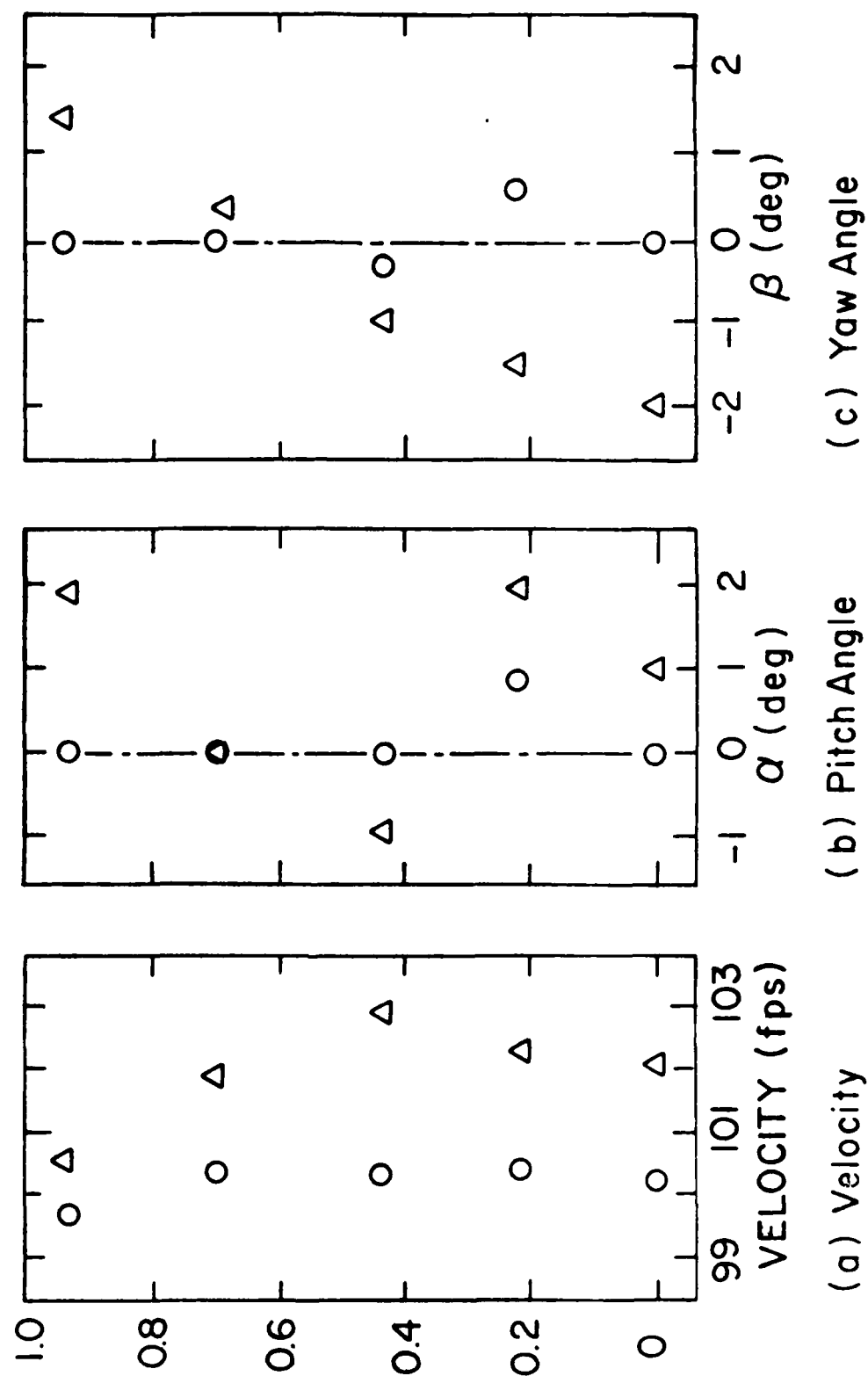


Figure 19. Five-hole Probe Data, Port 5

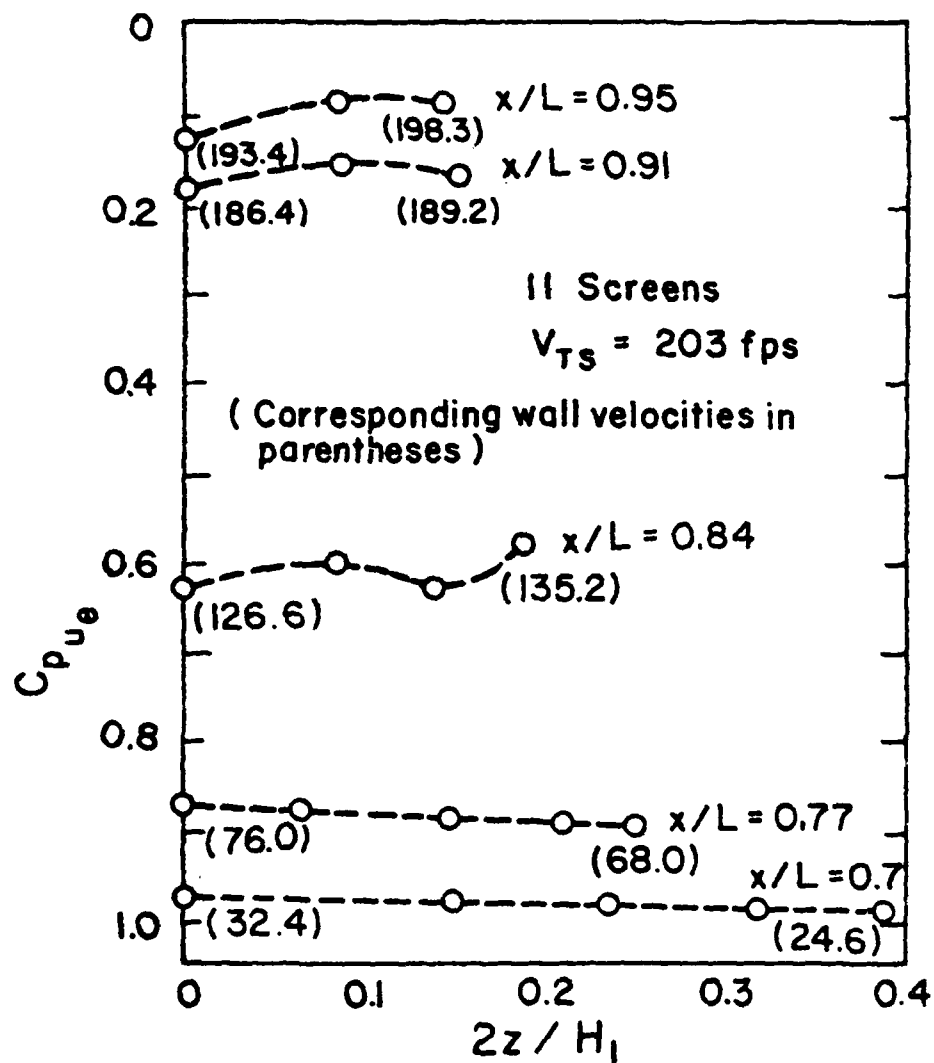


Figure 20. Lateral Wall Pressure Coefficients

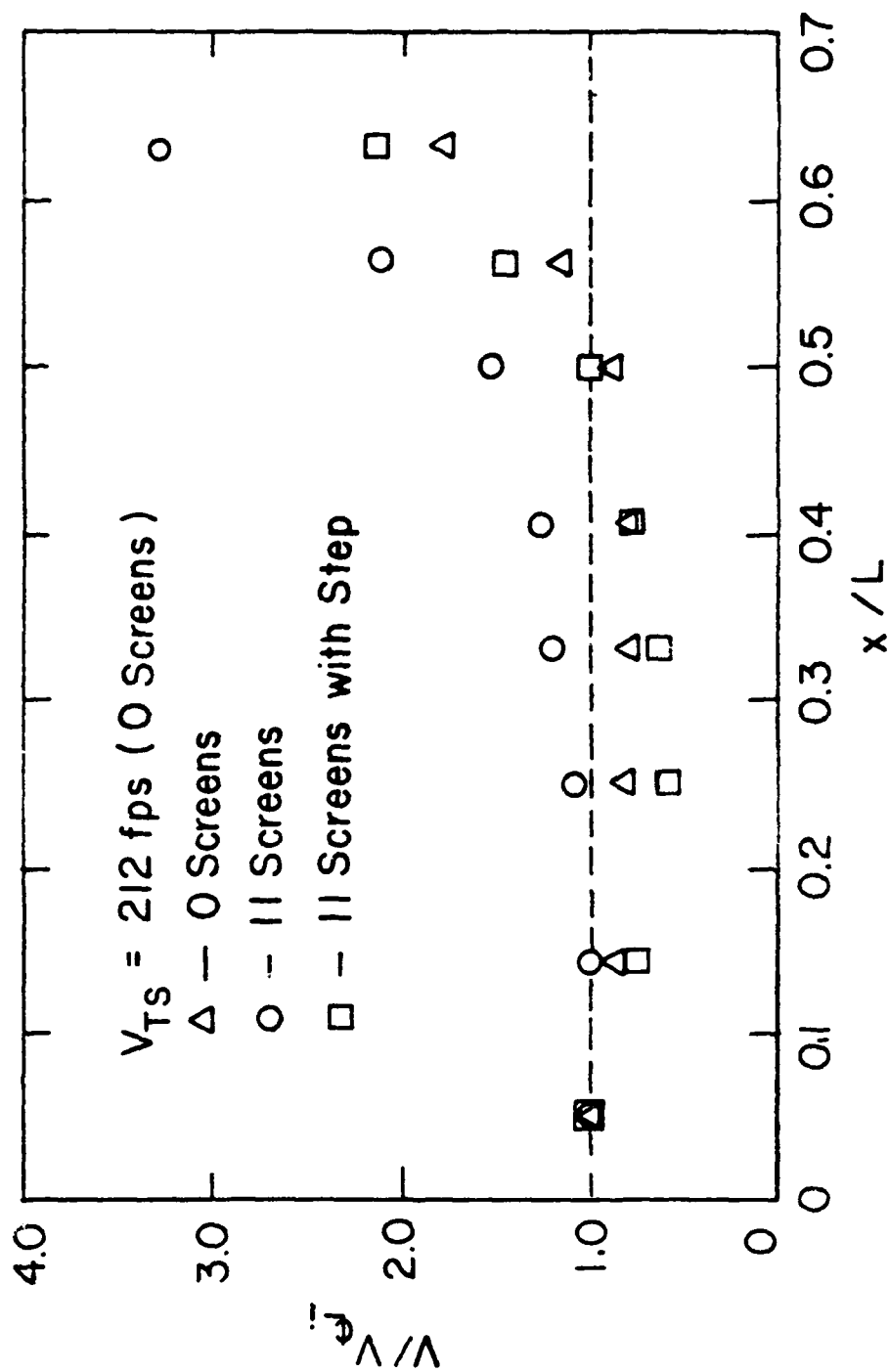


Figure 21. Experimental Wall Centerline Velocity Ratios

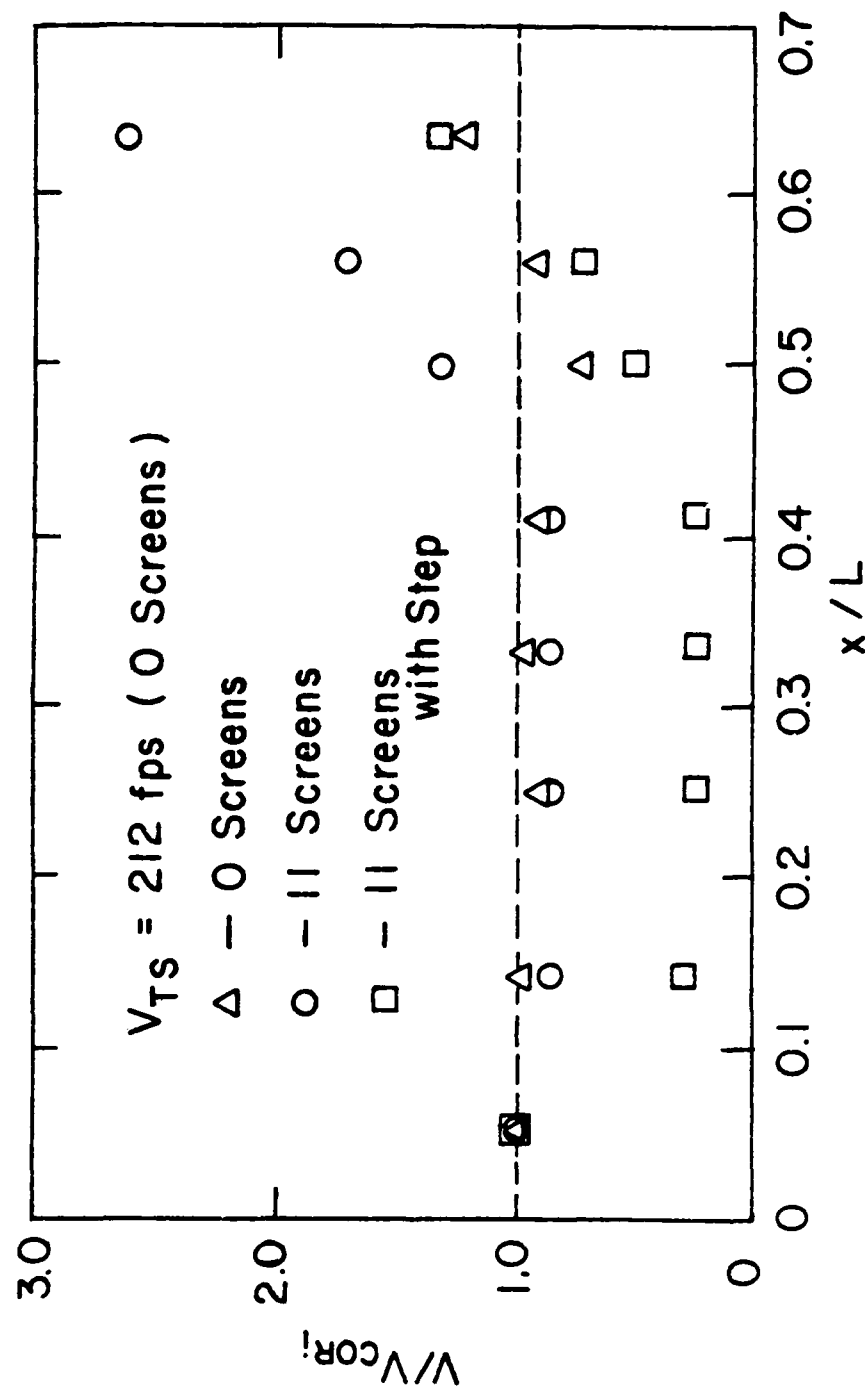
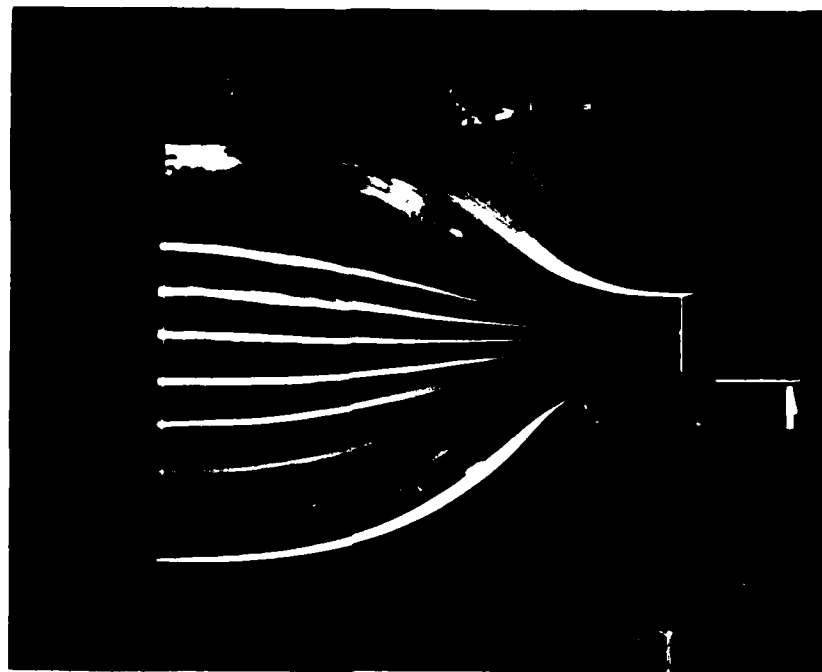
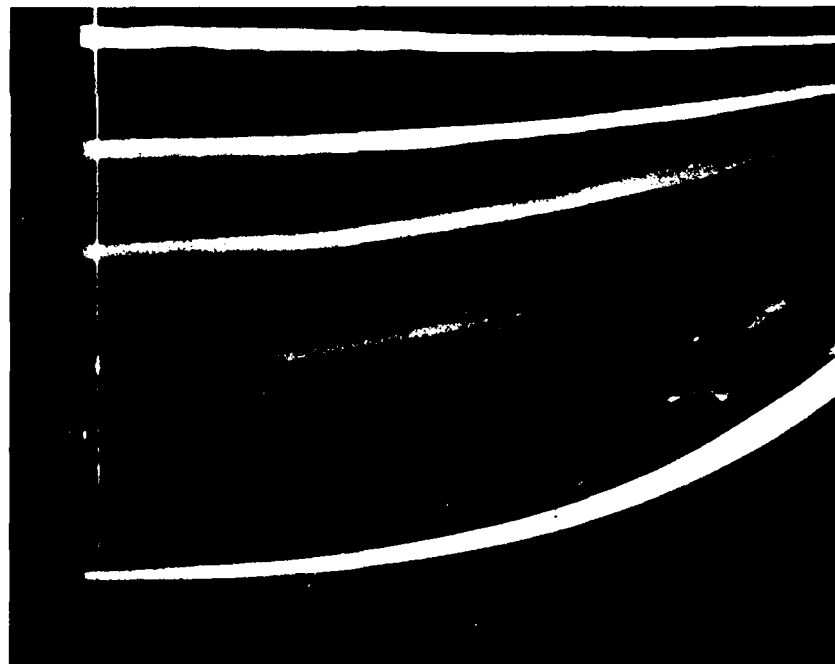


Figure 22. Experimental Corner Region Velocity Ratios



a. Entire Inlet



b. Close-up

Figure 23. Flow Visualization of Entrance Plane Wall Discontinuity ("Step")

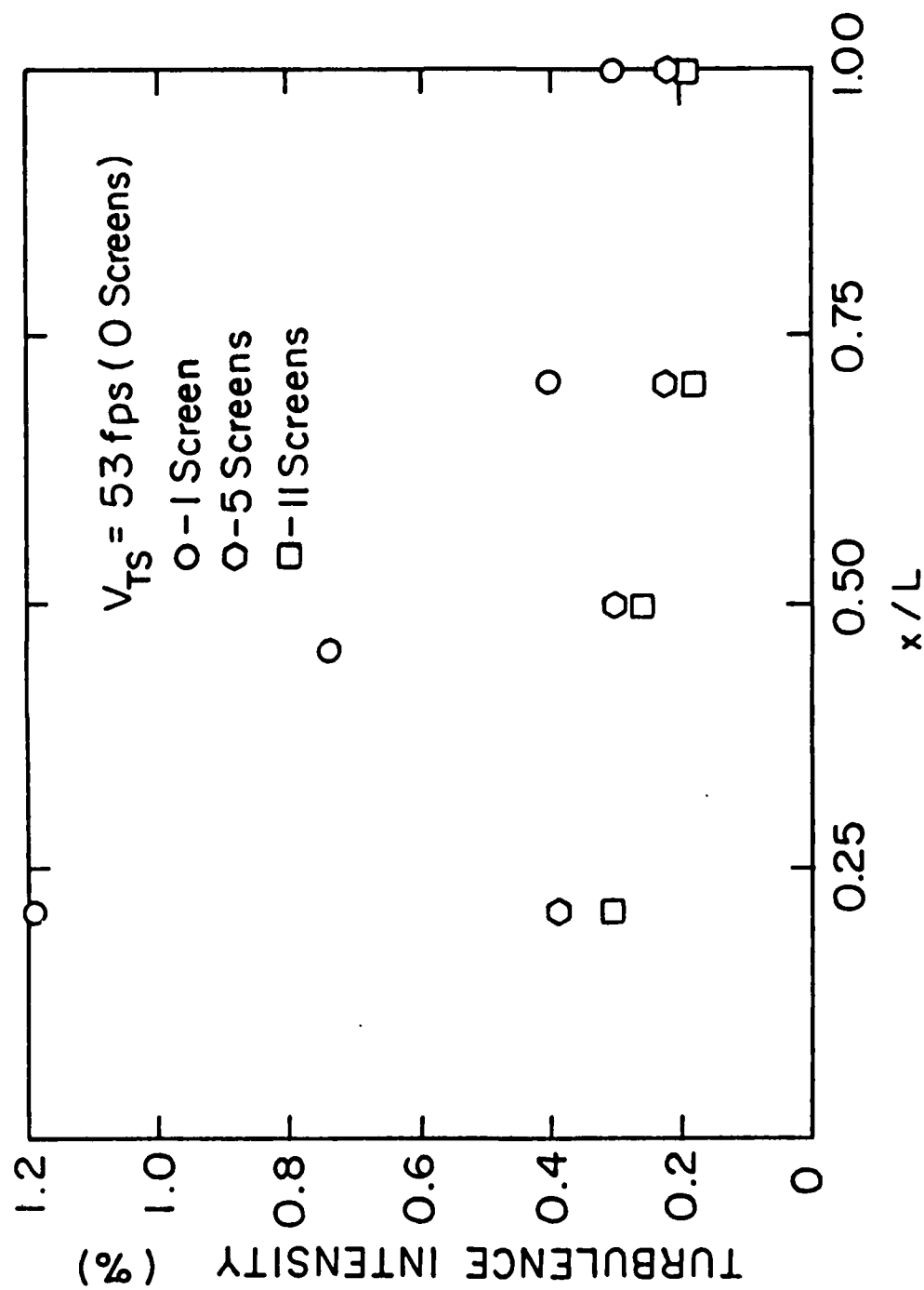


Figure 24. Experimental Axial Turbulence Intensities

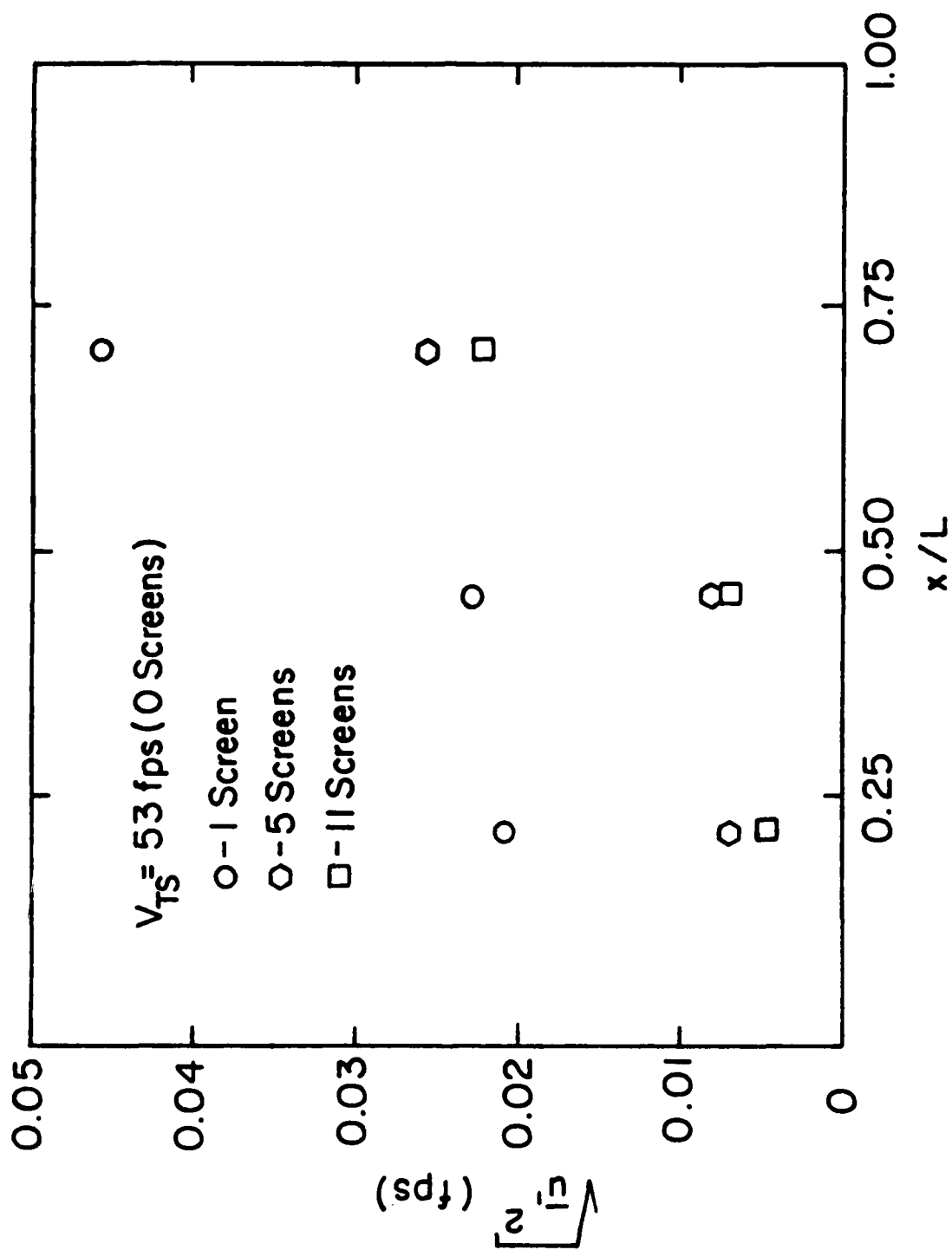
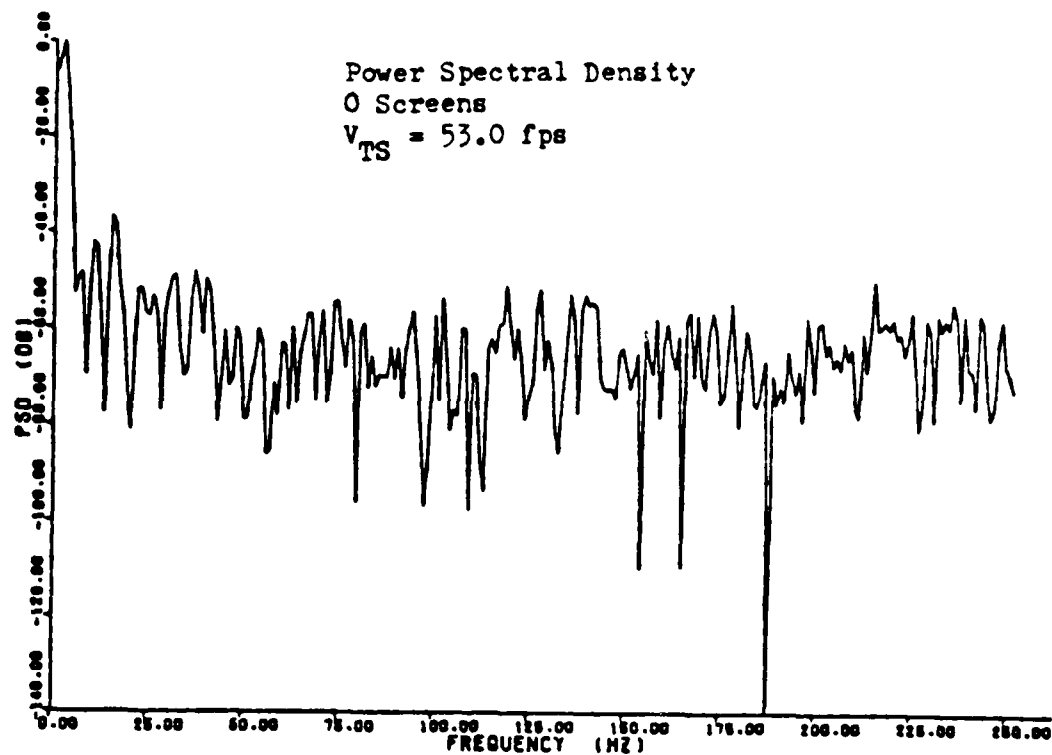
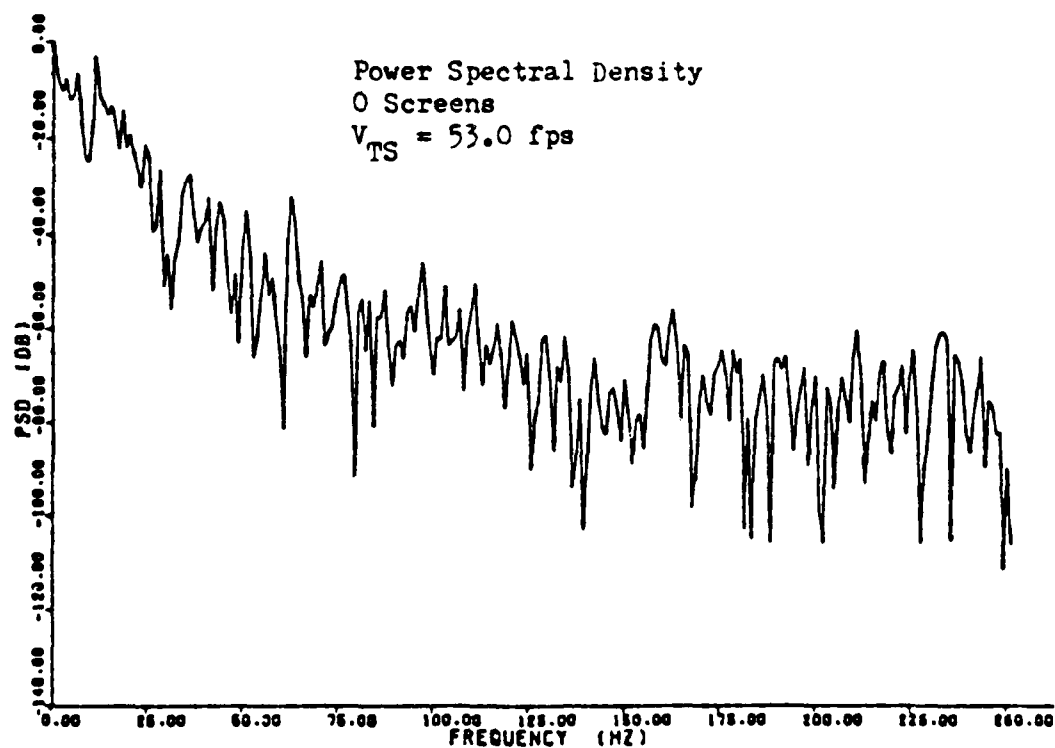


Figure 25. Experimental RMS Velocities

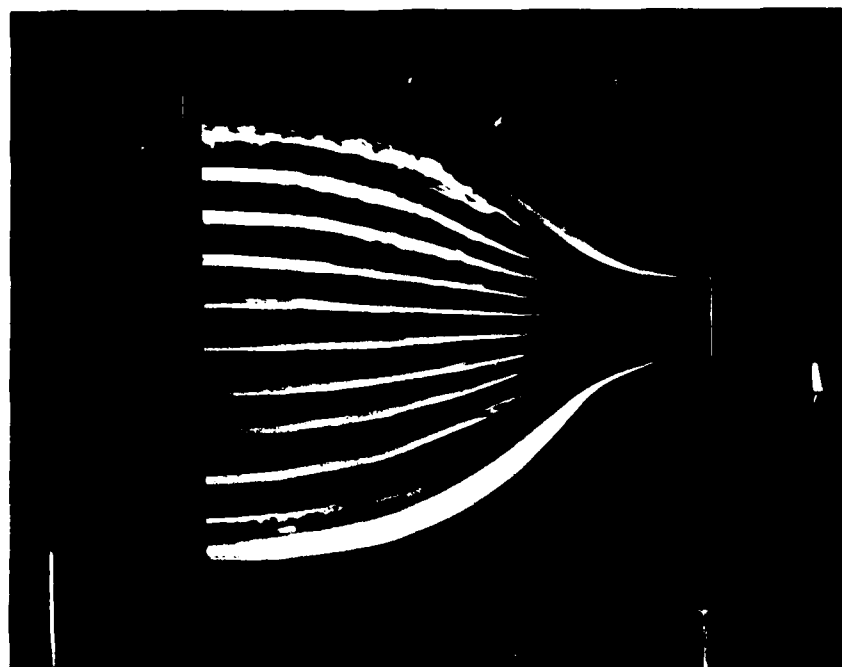


a. Station 1

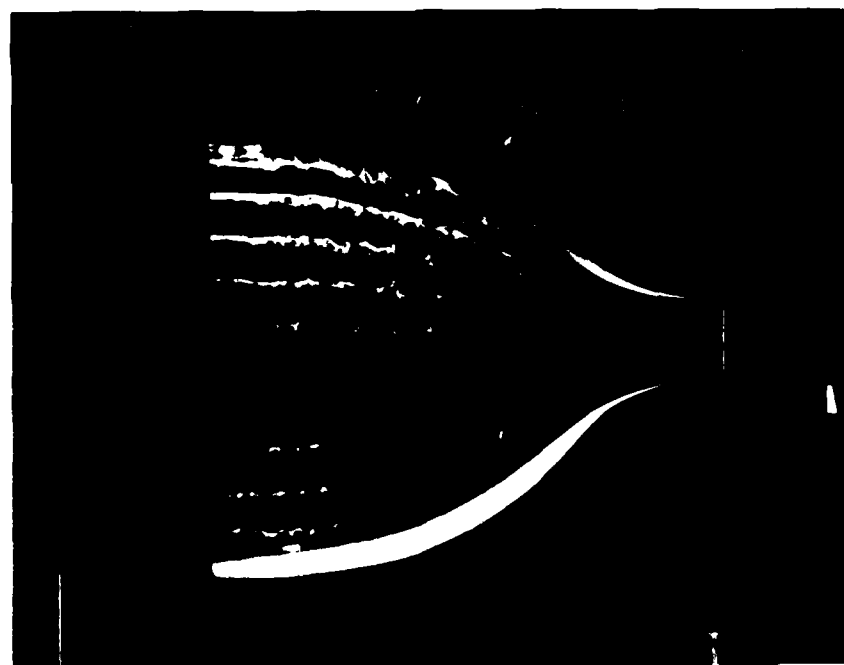


b. Station 4

Figure 26. Turbulence Frequency Spectra



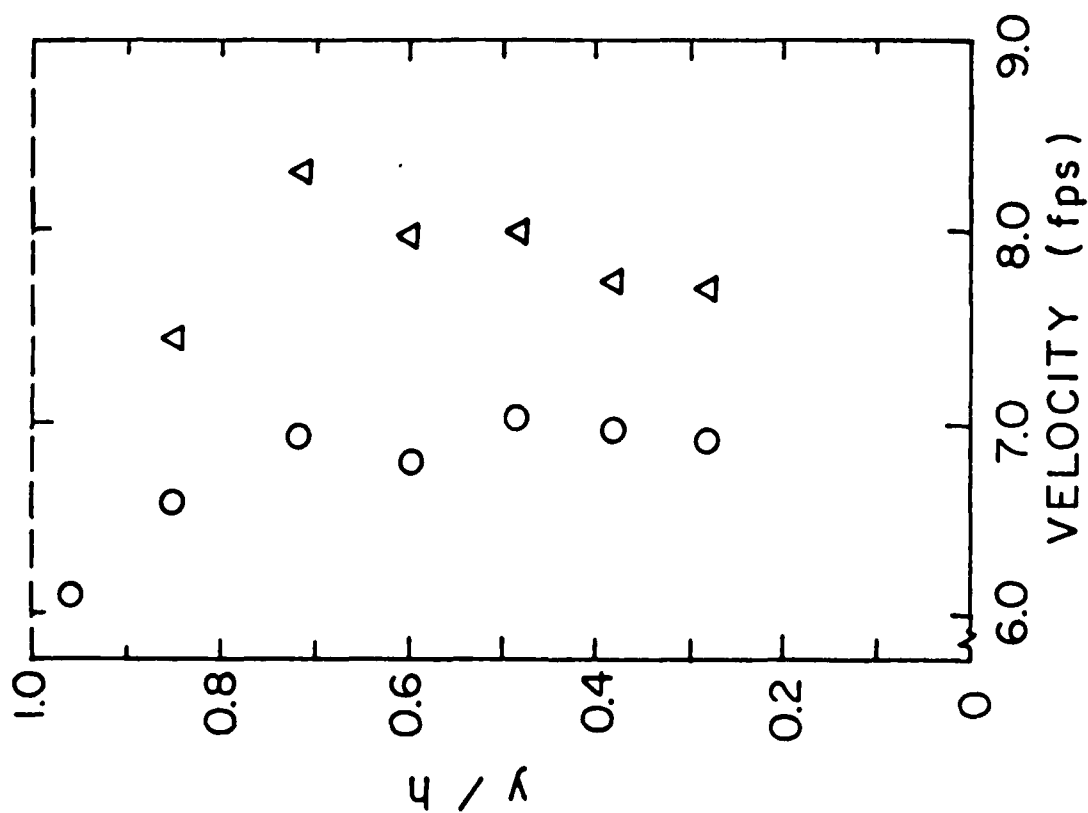
a. Screens Flush



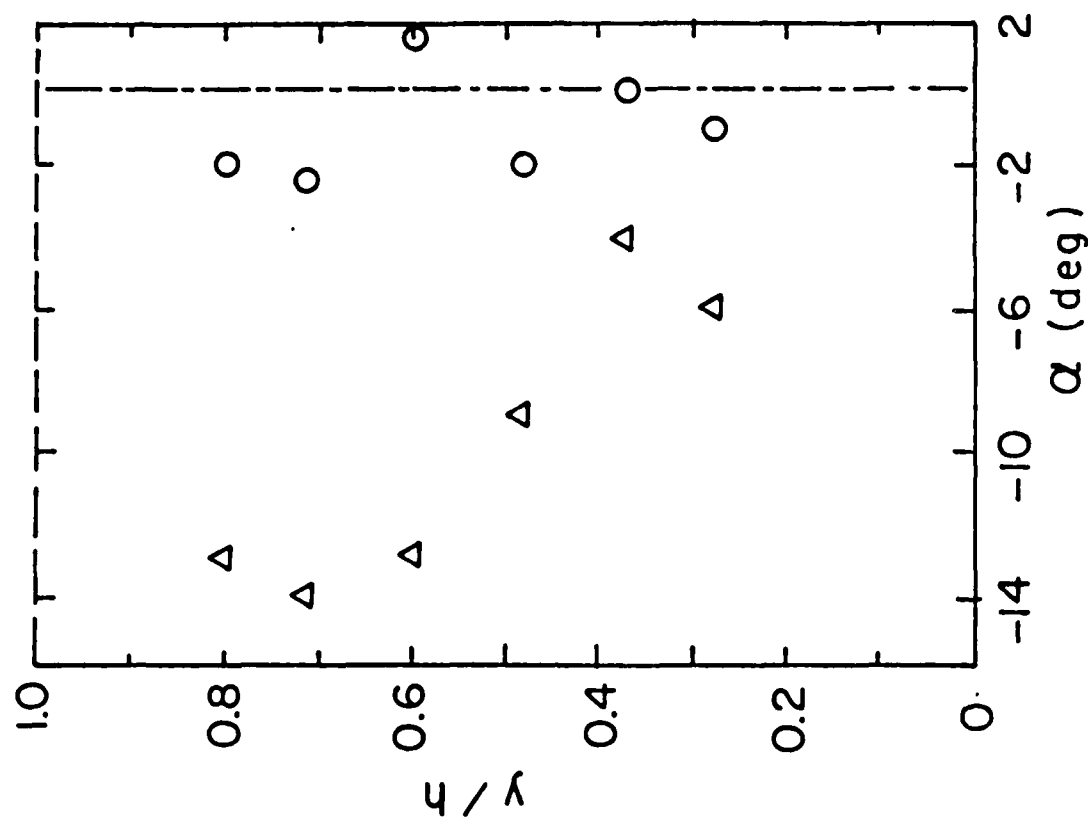
b. Screen Step

Figure 27. Smoke Flow Visualization Along Inlet Wall

Δ - 0 Screens ($V_{TS} = 212$ fps)
 \circ - 11 Screens ($V_{TS} = 203$ fps)



(a) Flow Velocities



(b) Pitch Angles

Figure 28. Five-Hole Probe Data, Port 1

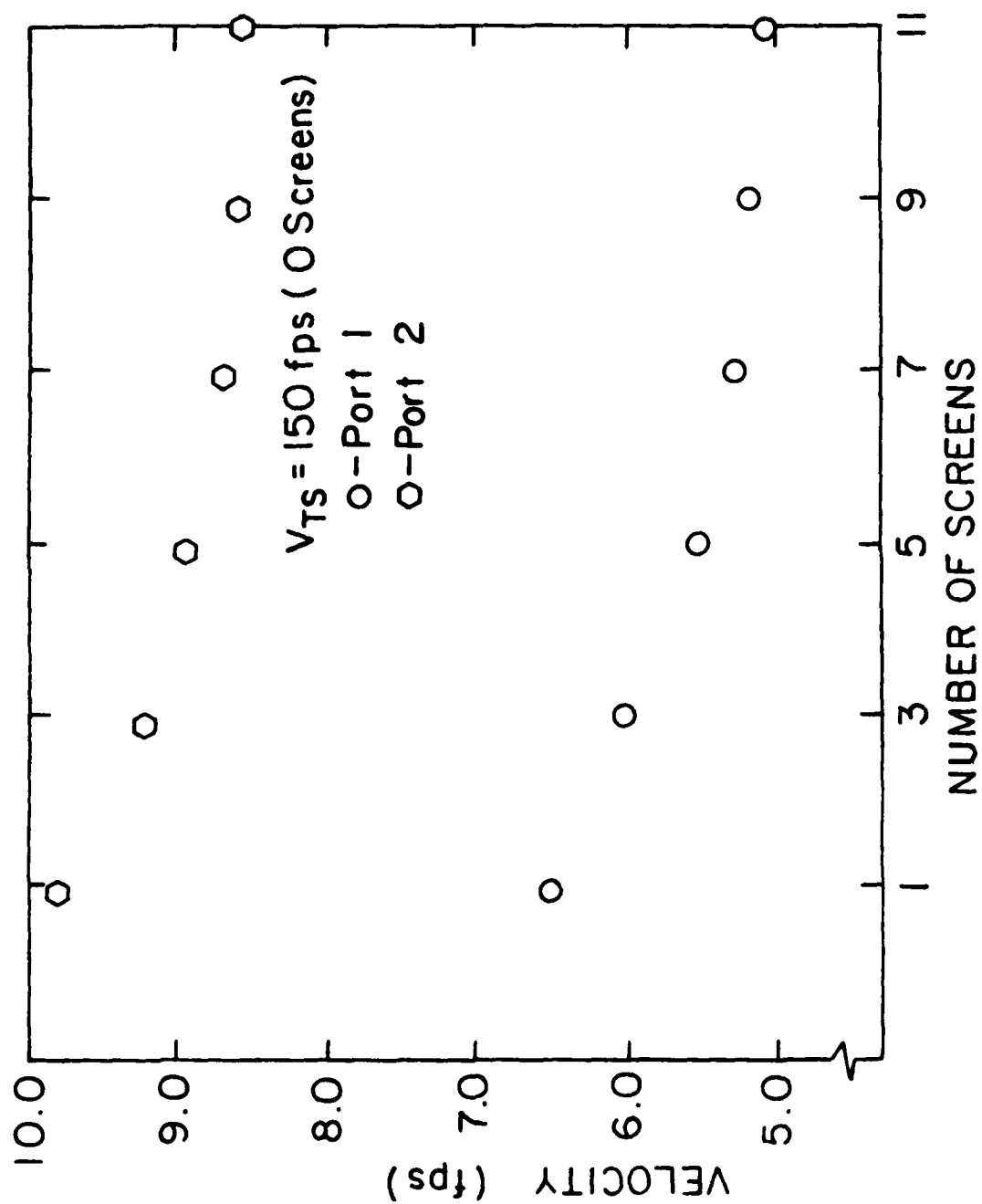


Figure 29. Effect of Screens on Centerline Velocities

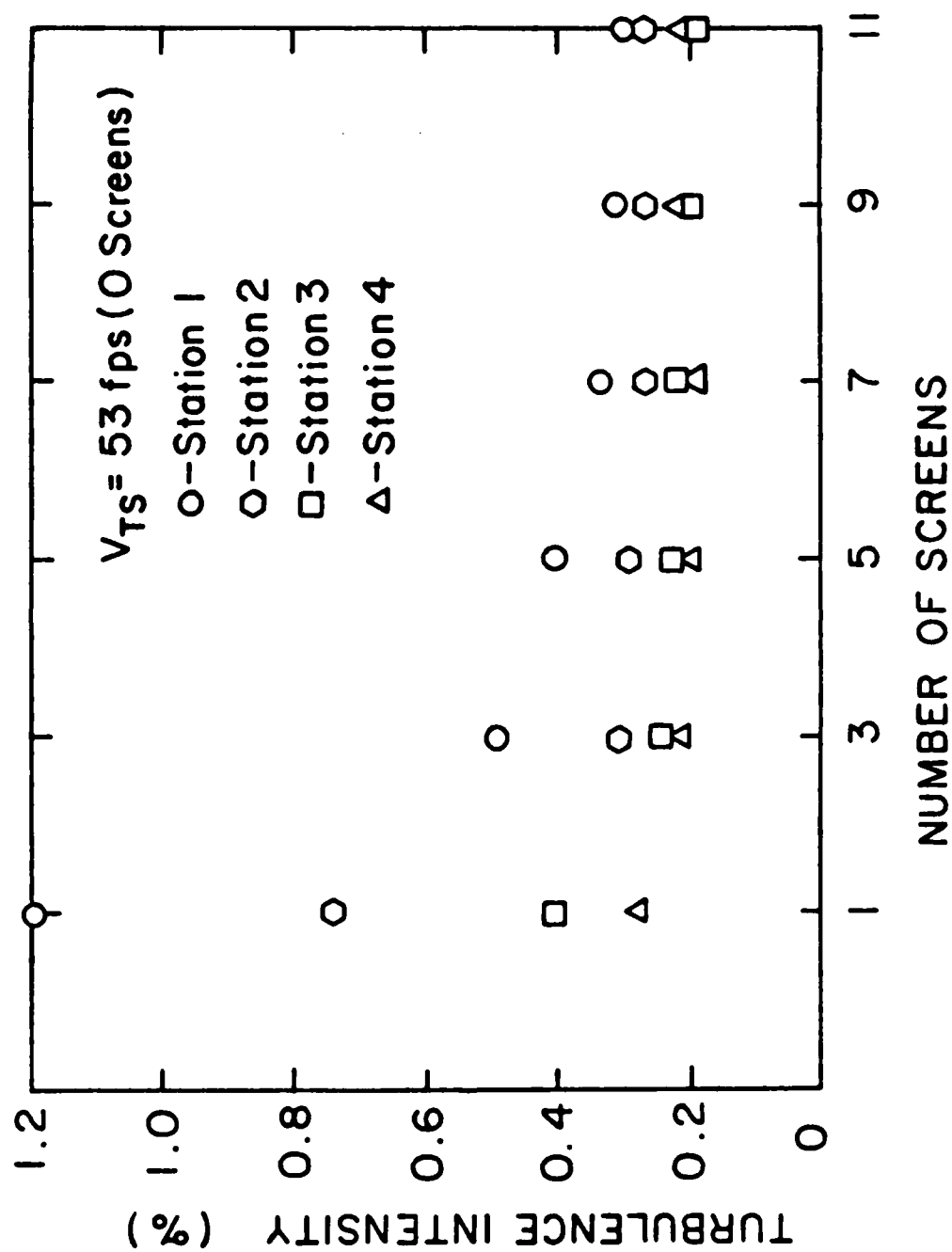


Figure 30. Axial Turbulence Intensities, Variation with Additional Screens

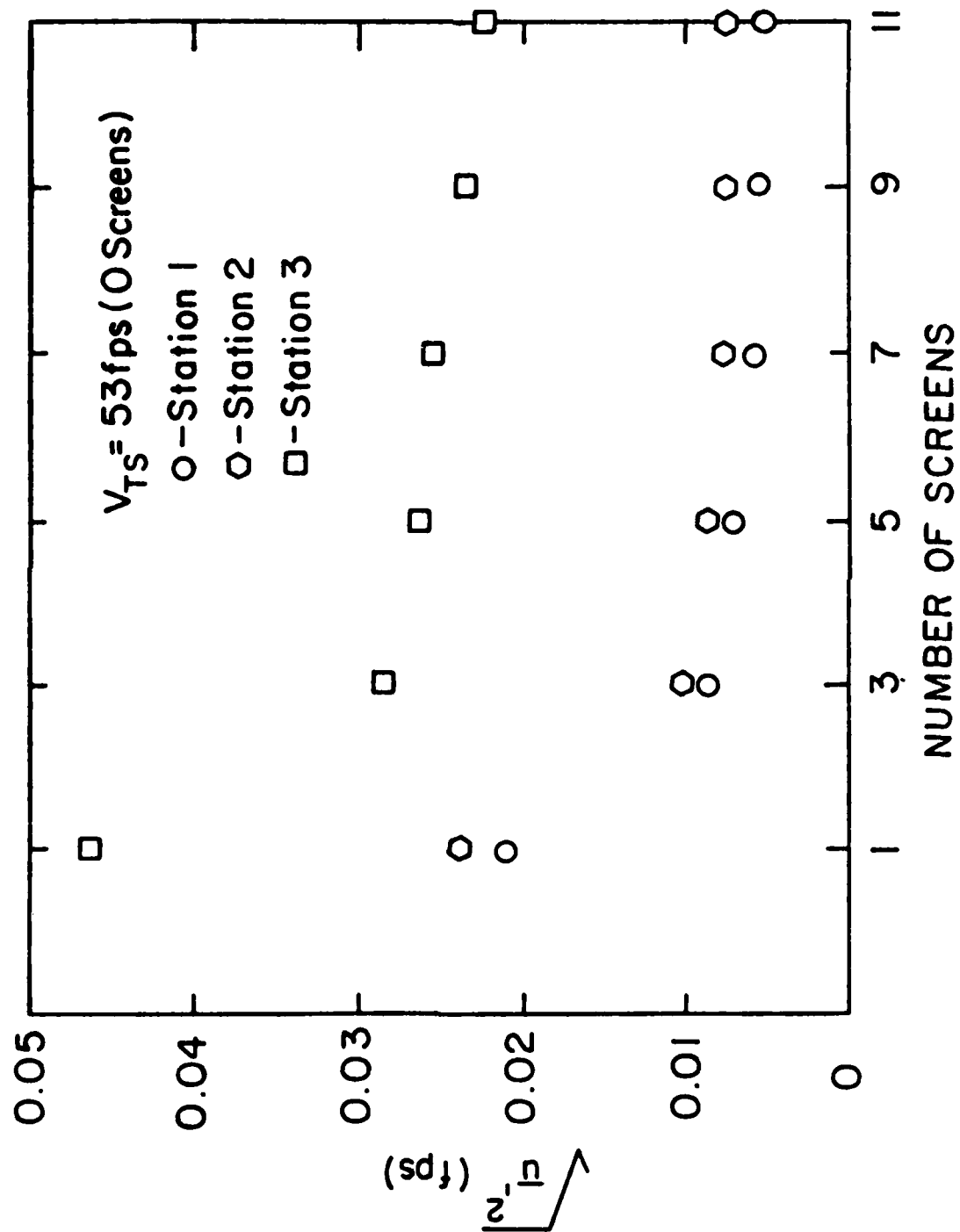
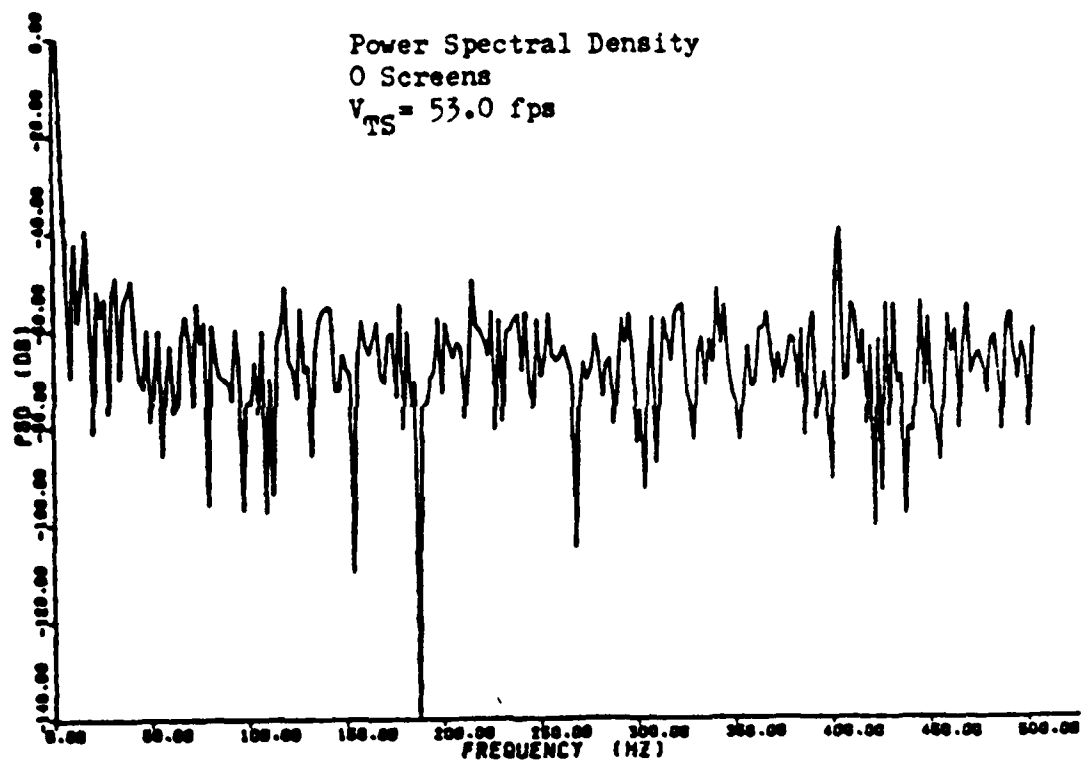
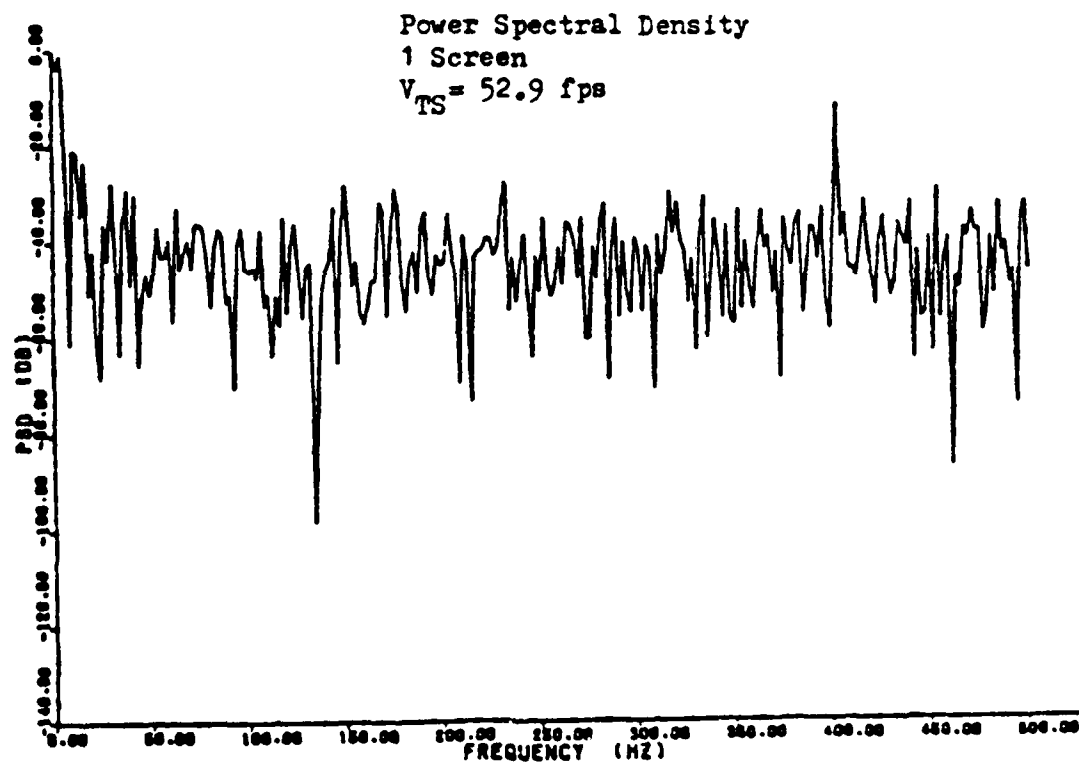


Figure 31. RMS Velocities, Variation with Additional Screens



a. 0 Screens, Station 11



b. 1 Screen, Station 1

Figure 32. Turbulence Frequency Spectra



a. 2 Screens



b. 4 Screens



c. 11 Screens

Figure 33. Flow Visualization of Turbulence Screen Influence

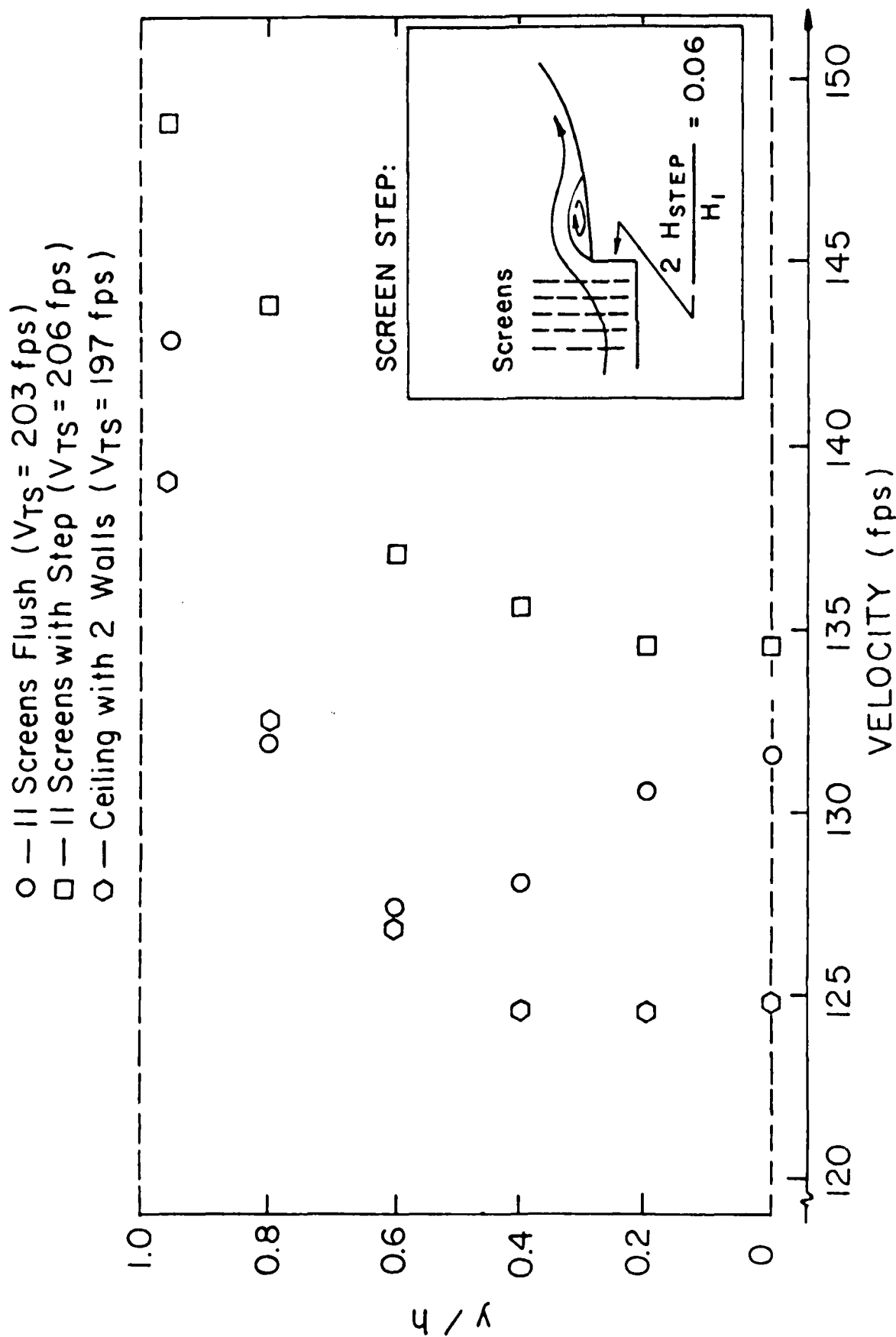


Figure 34. Five-Hole Probe Velocity Measurements, Port 4

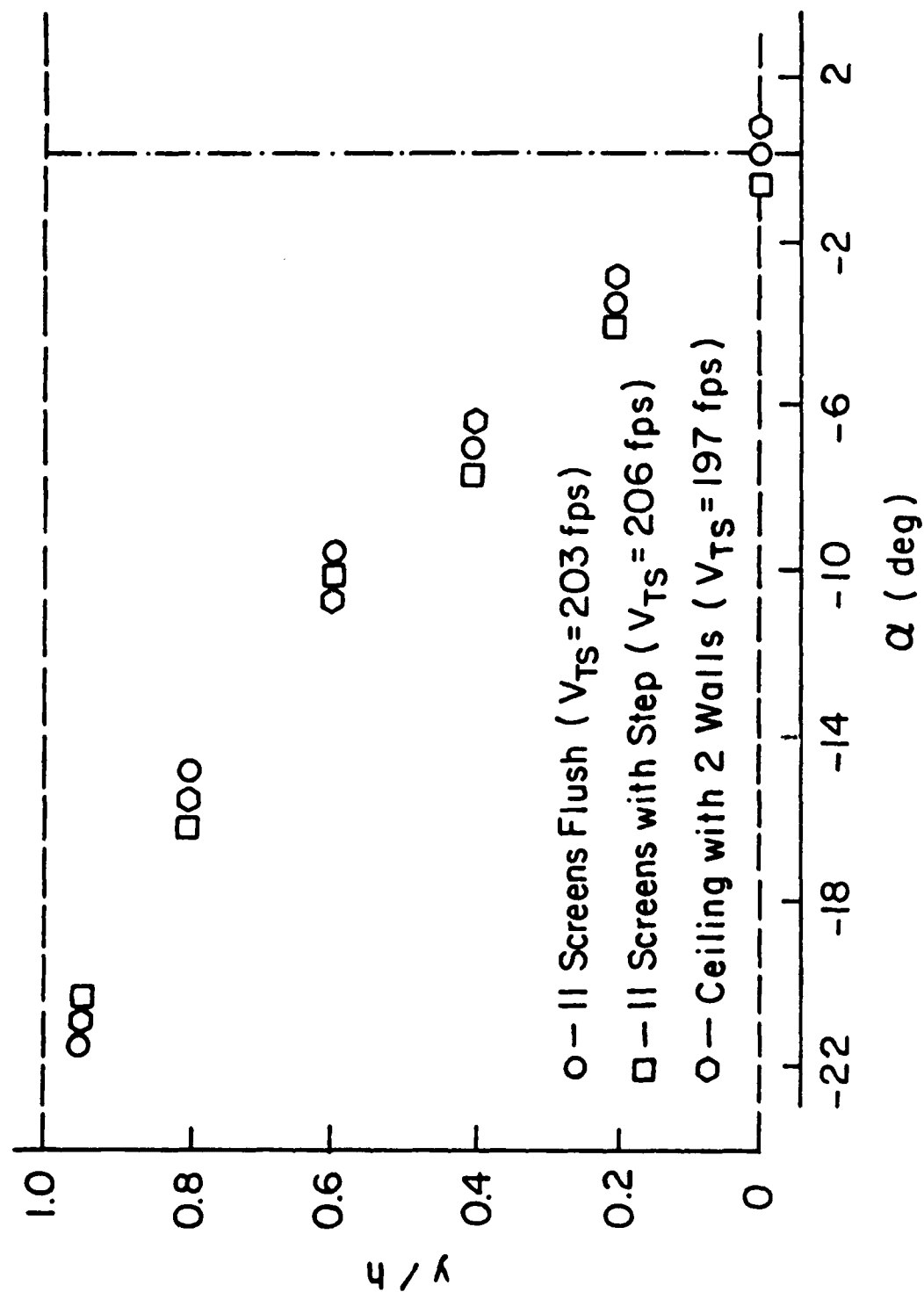


Figure 35. Five-Hole Probe, Pitch Angles, Port 4

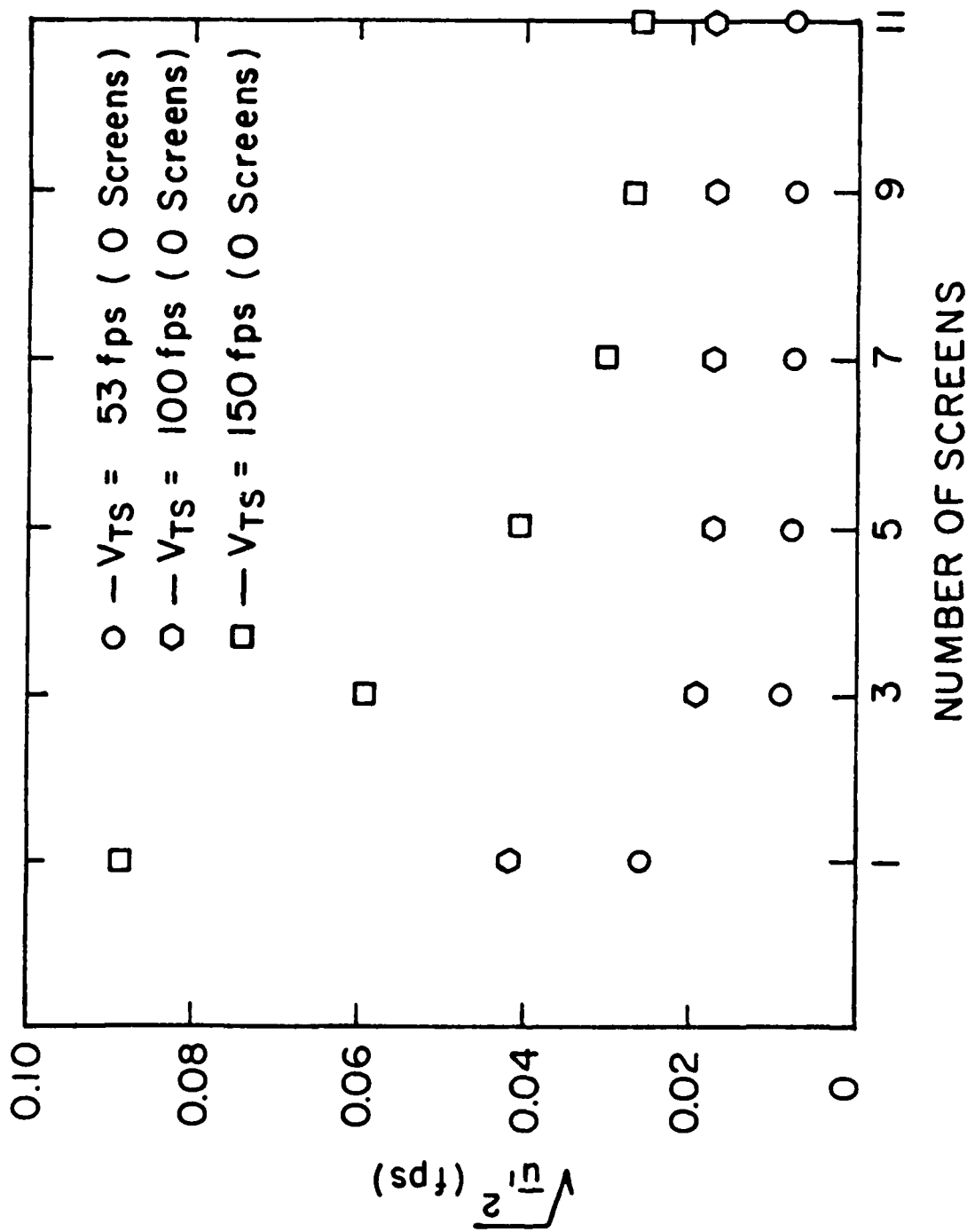


Figure 36. RMS Velocities at Station 1

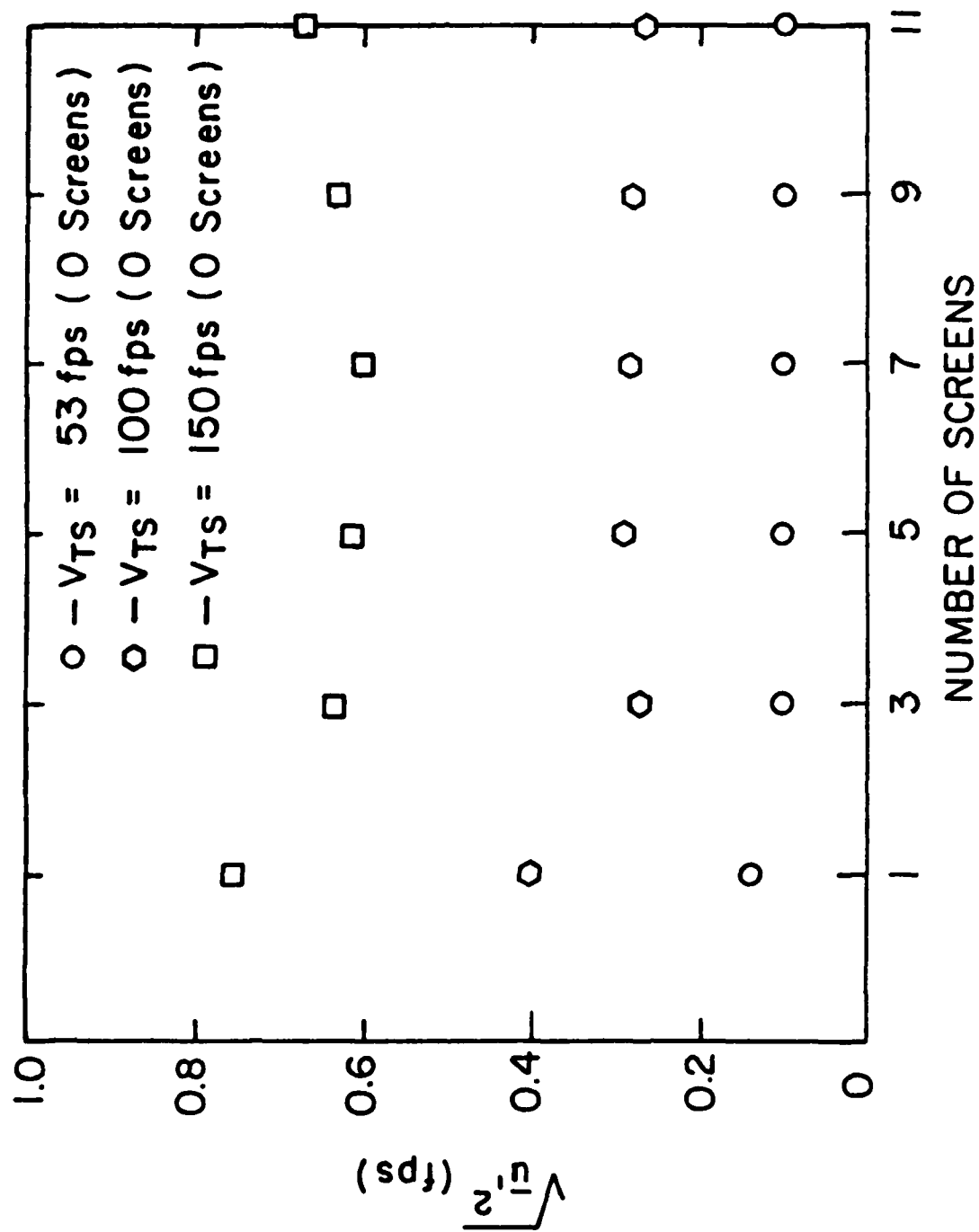
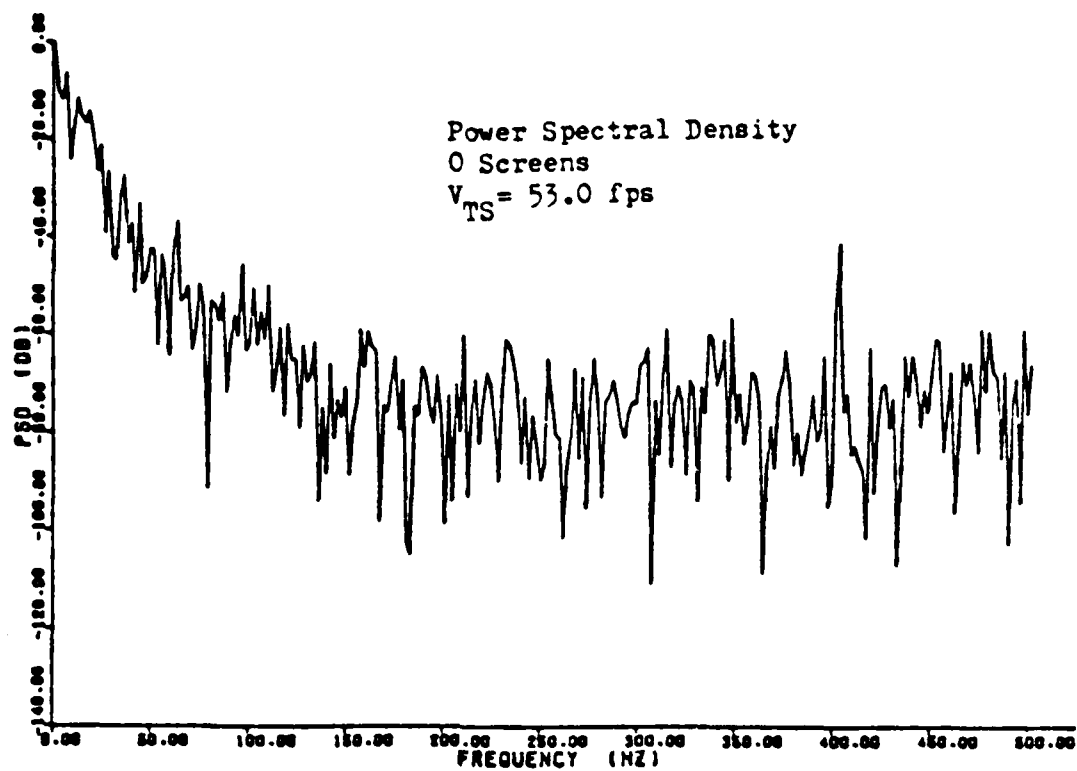
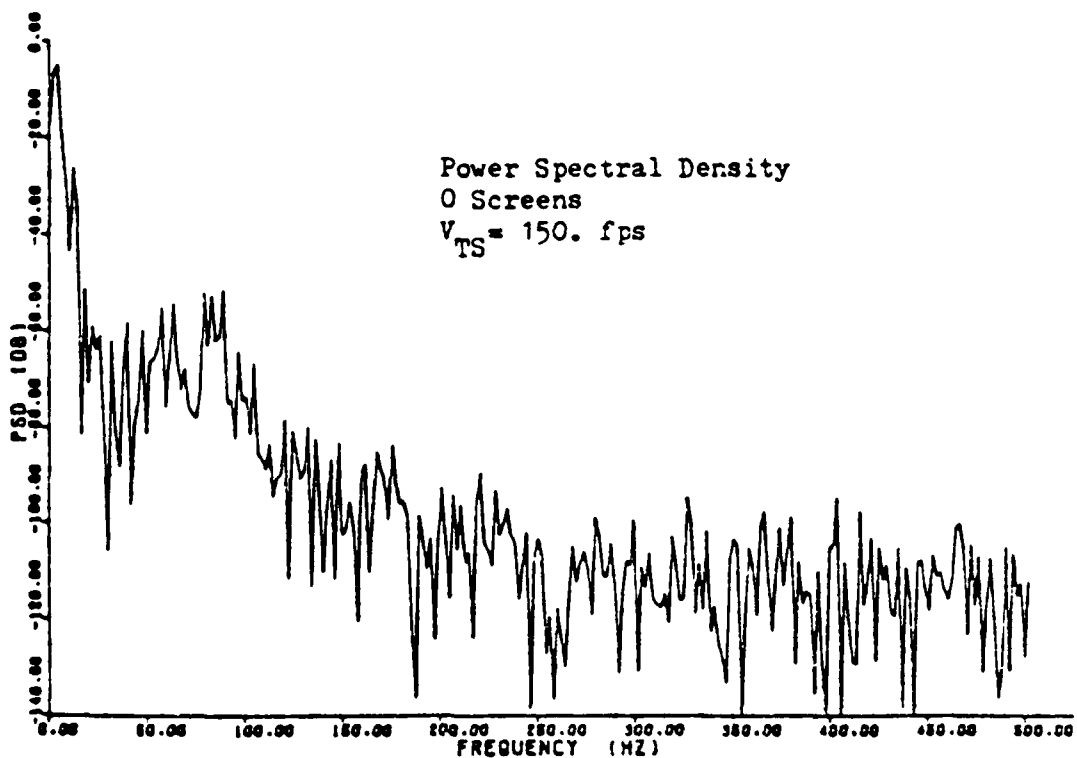


Figure 37. RMS Velocities at Station 4

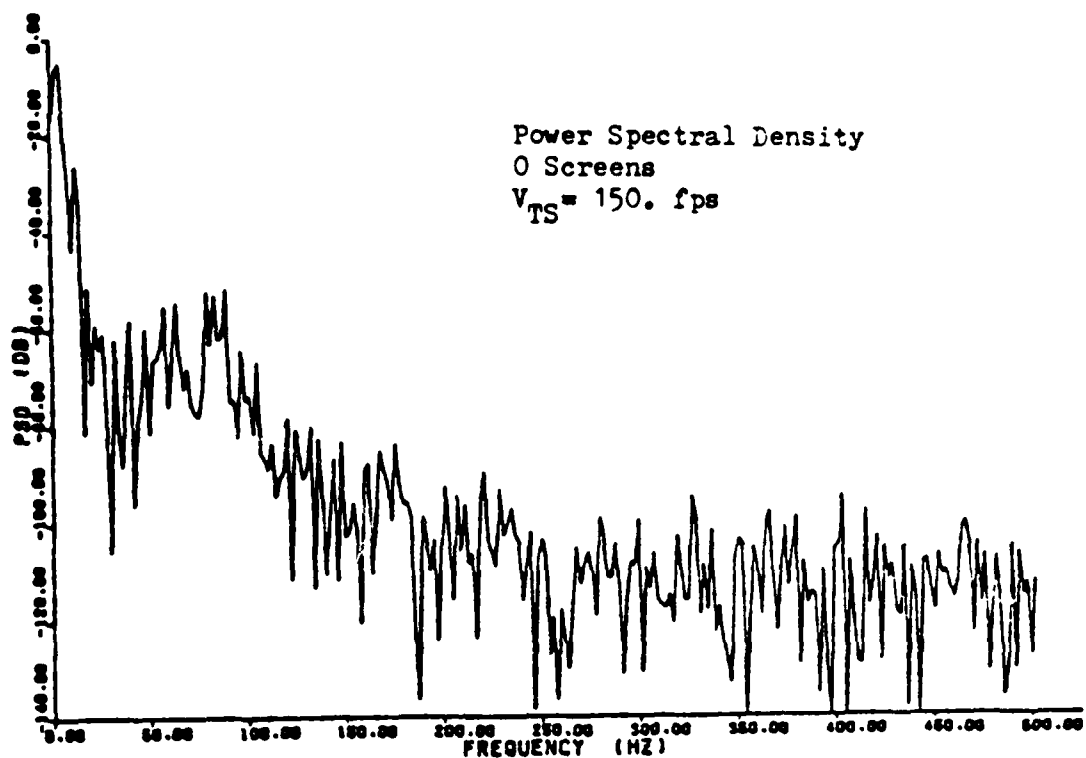


a. $V_{TS} = 53.0$ fps

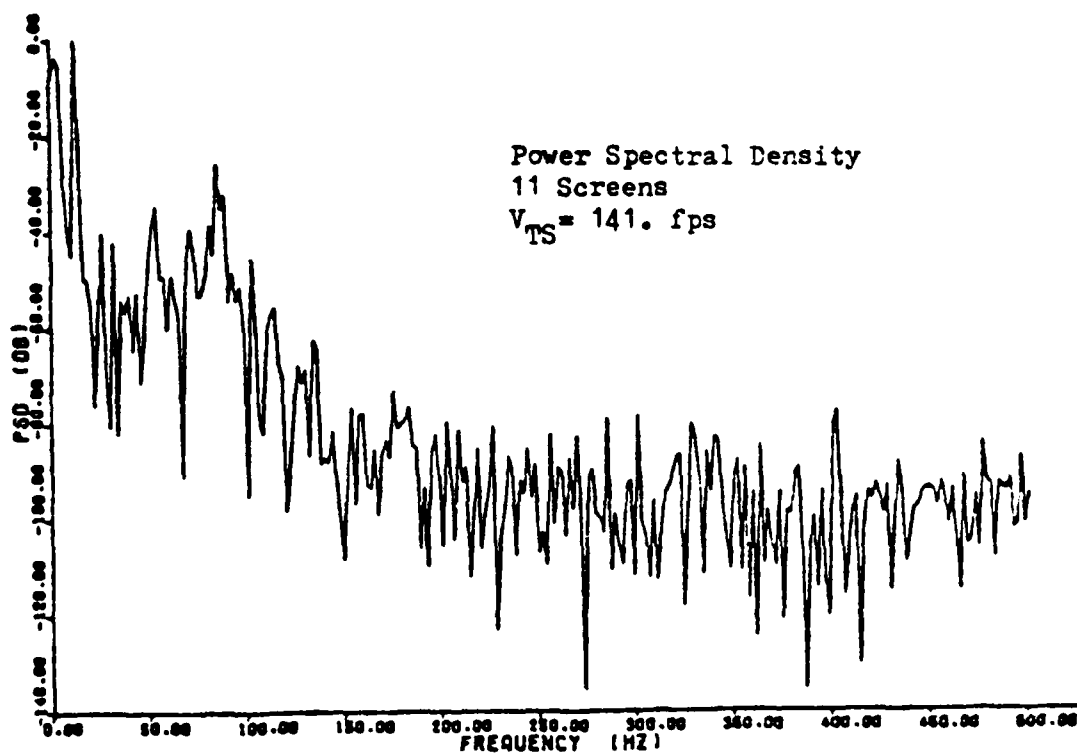


b. $V_{TS} = 150$ fps

Figure 38. Turbulence Frequency Spectra, Station 4



a. 0 Screens, $V_{TS} = 150 \text{ fps}$



b. 11 Screens, $V_{TS} = 141 \text{ fps}$

Figure 39. Turbulence Frequency Spectra, Station 4

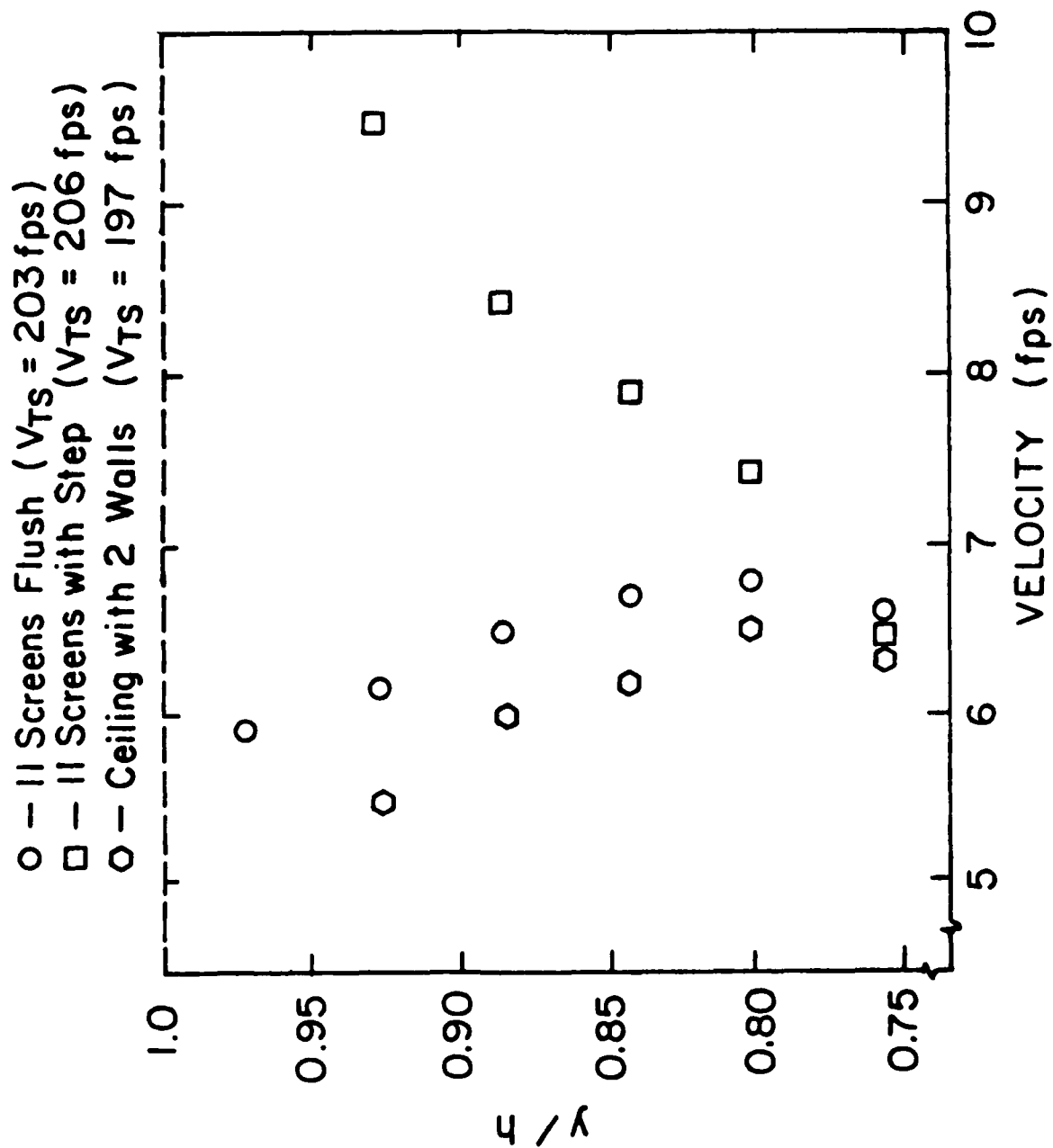


Figure 40. Velocities Near Inlet Wall

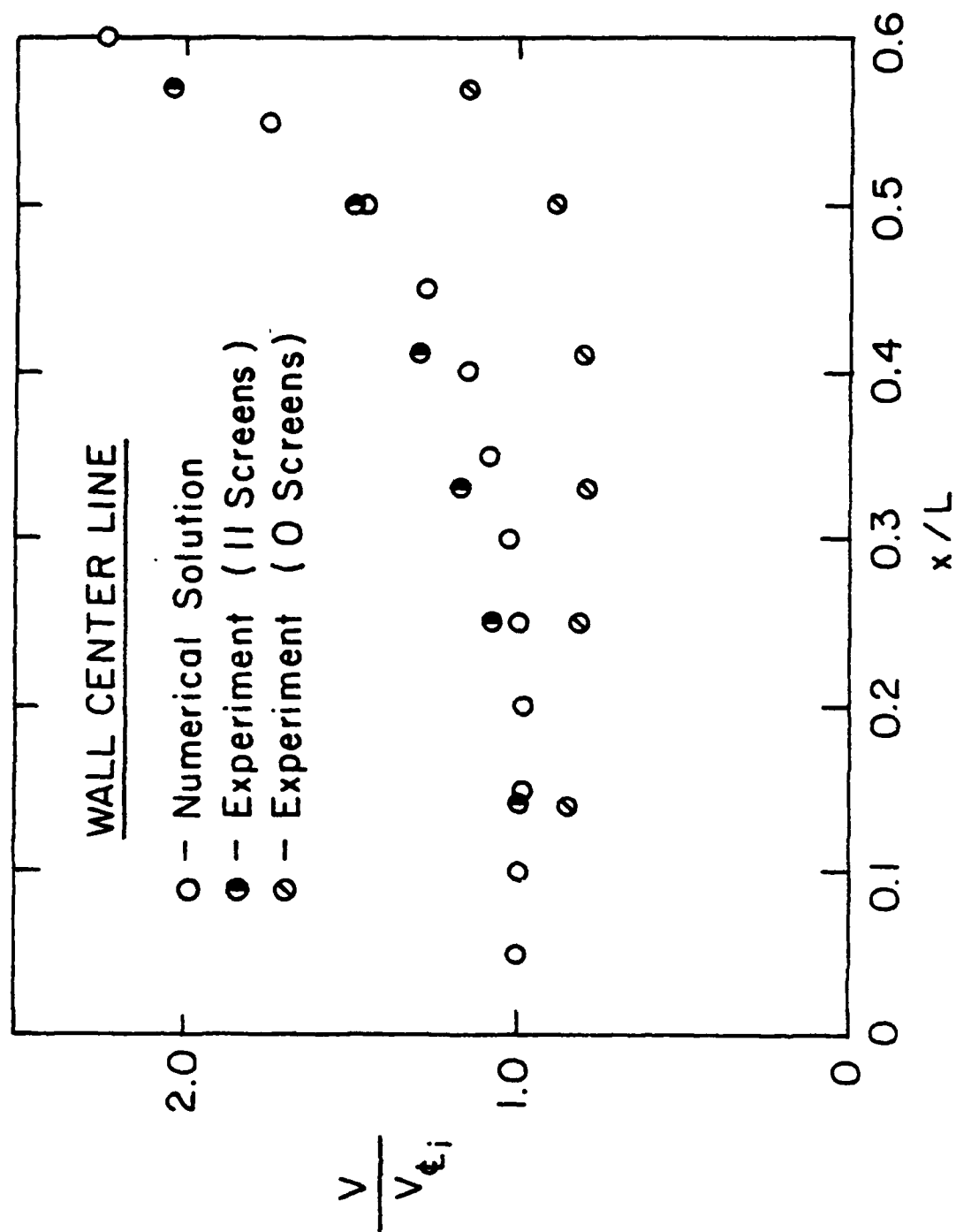


Figure 41. Comparison of Experimental and Numerical Results, Wall Centerline

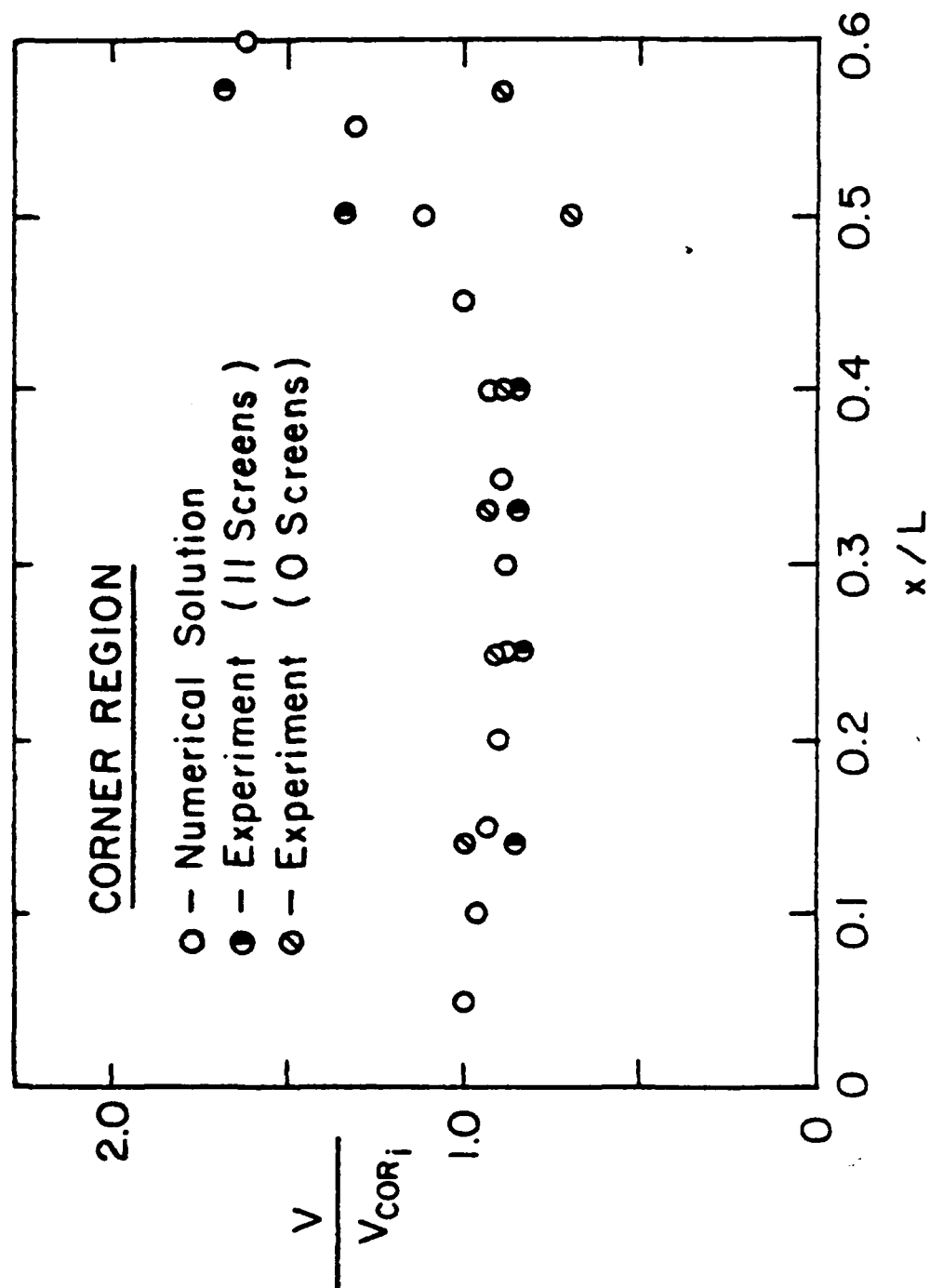


Figure 42. Comparison of Experimental and Numerical Results, Corner Region

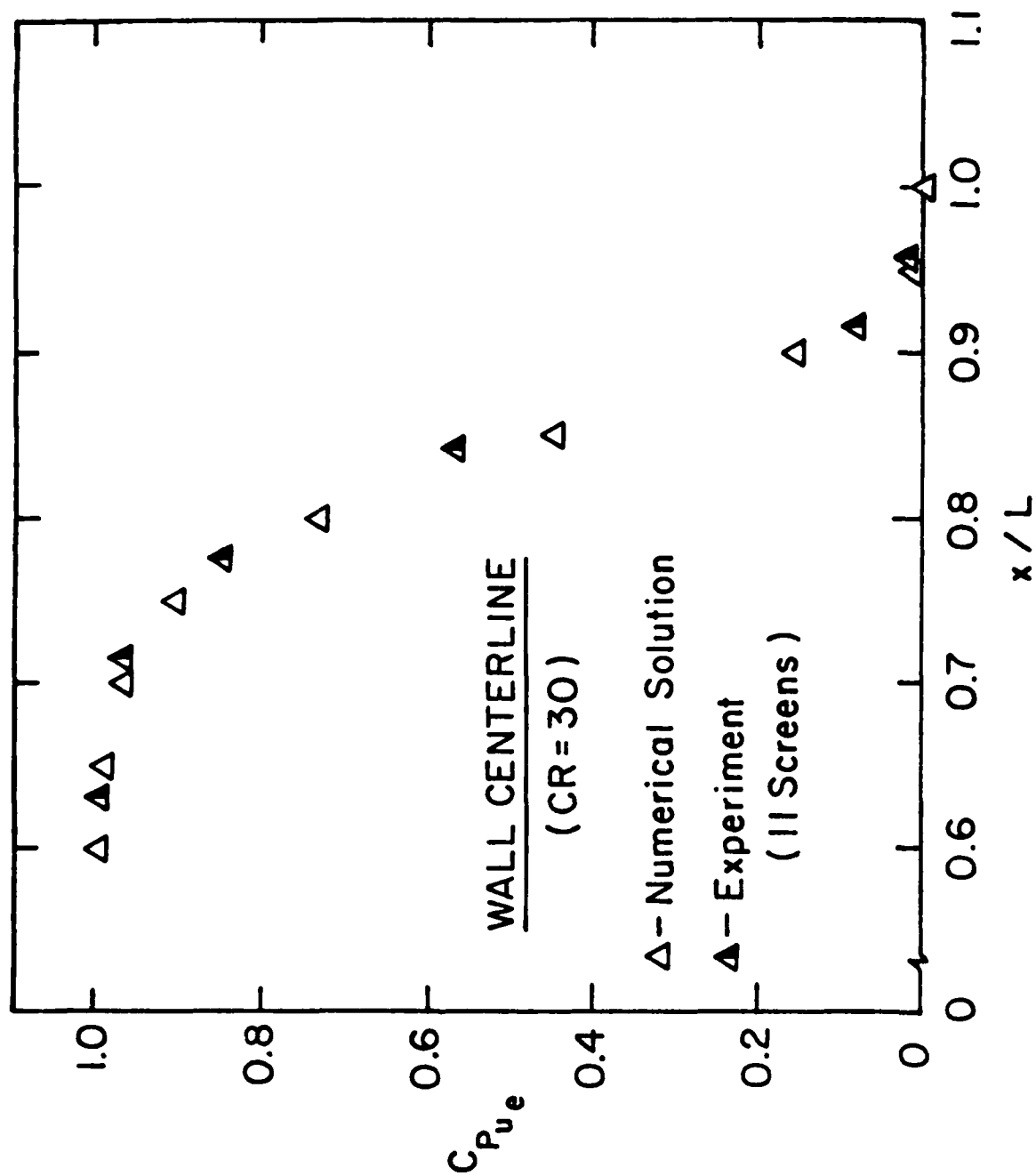


Figure 43. Comparisons of Experimental and Numerical Results

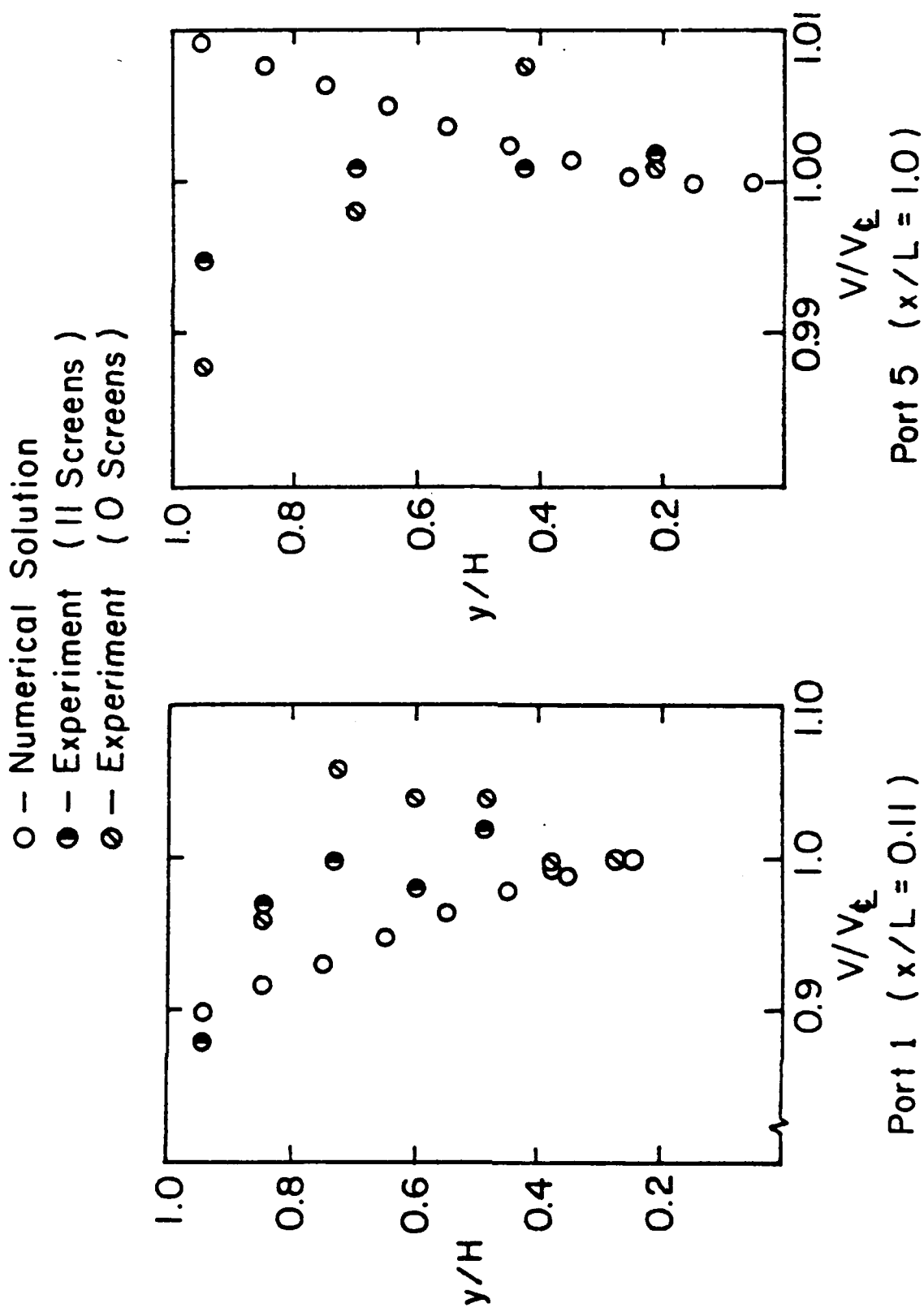
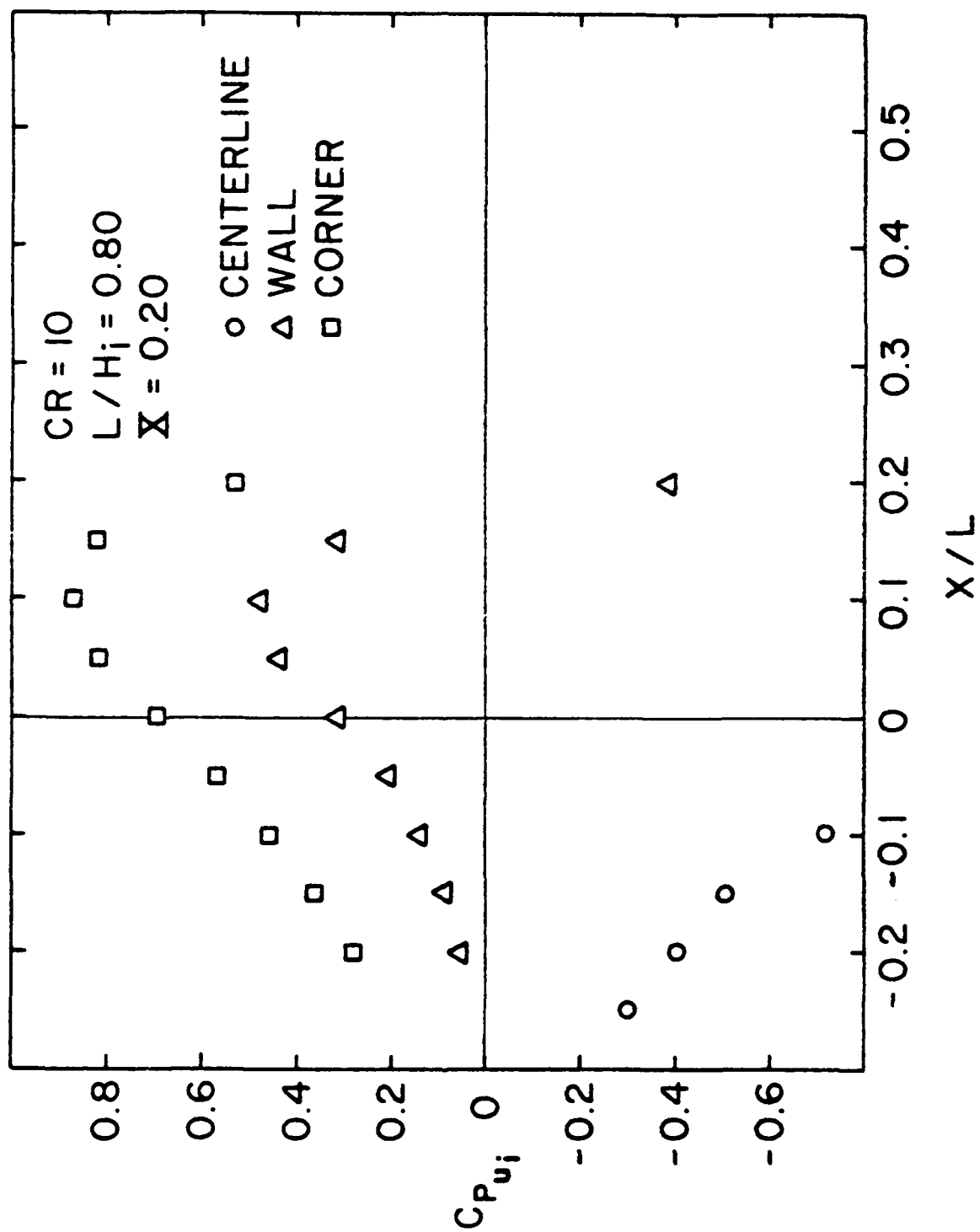
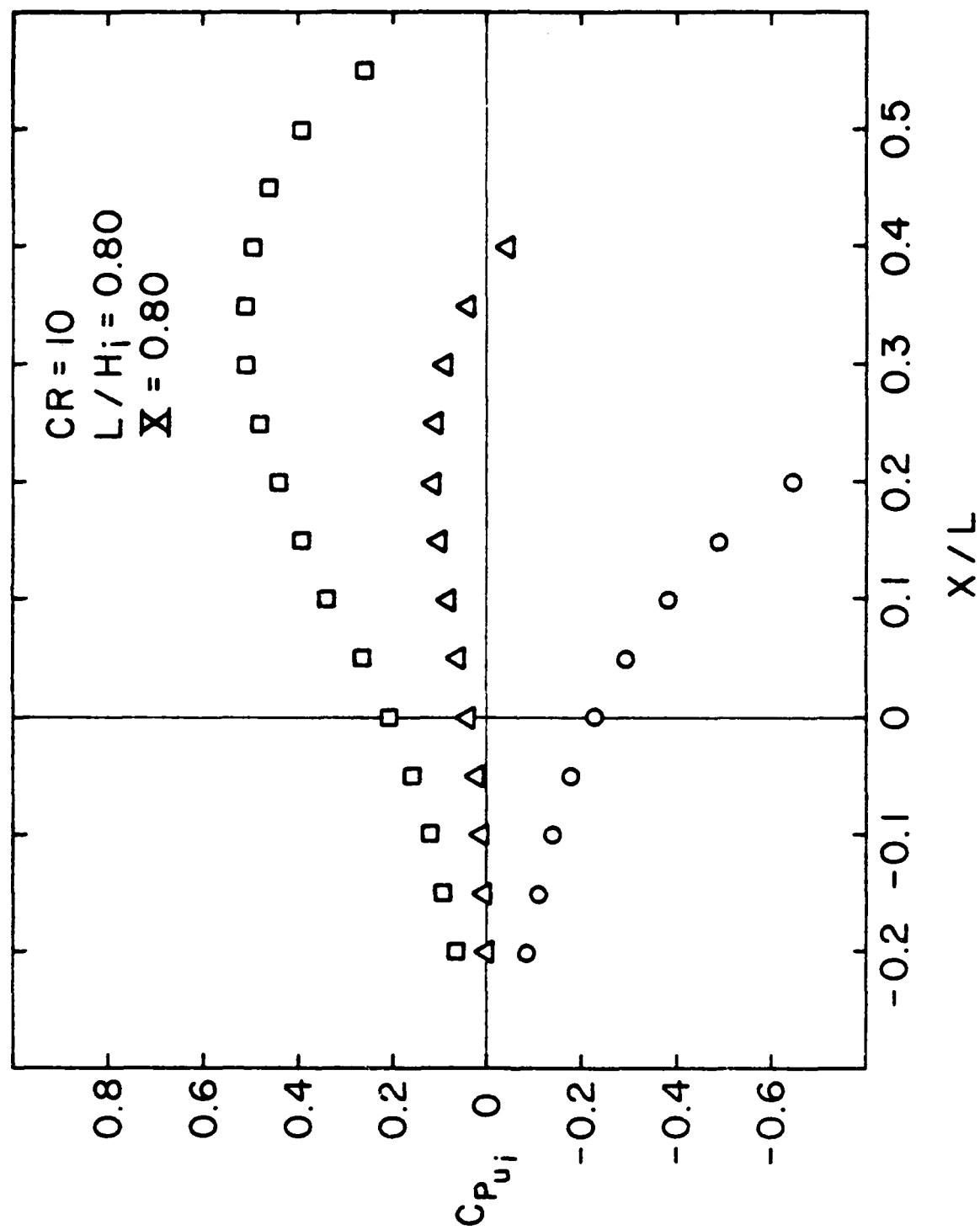


Figure 44. Comparison of Experimental and Numerical Velocity Profile



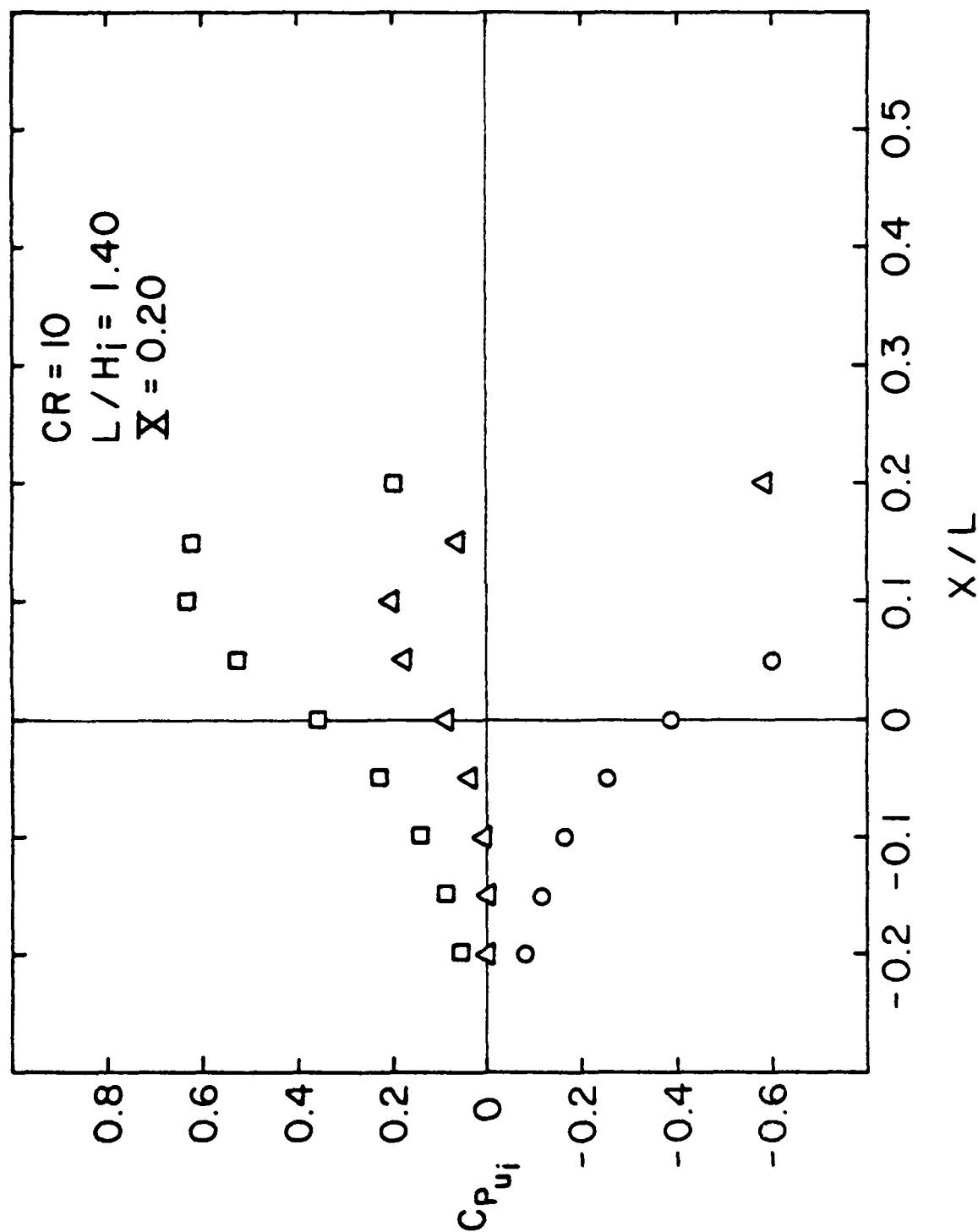
a. $L/H_i = 0.80$, $X = 0.20$

Figure 45. Pressure Distribution, CR = 10



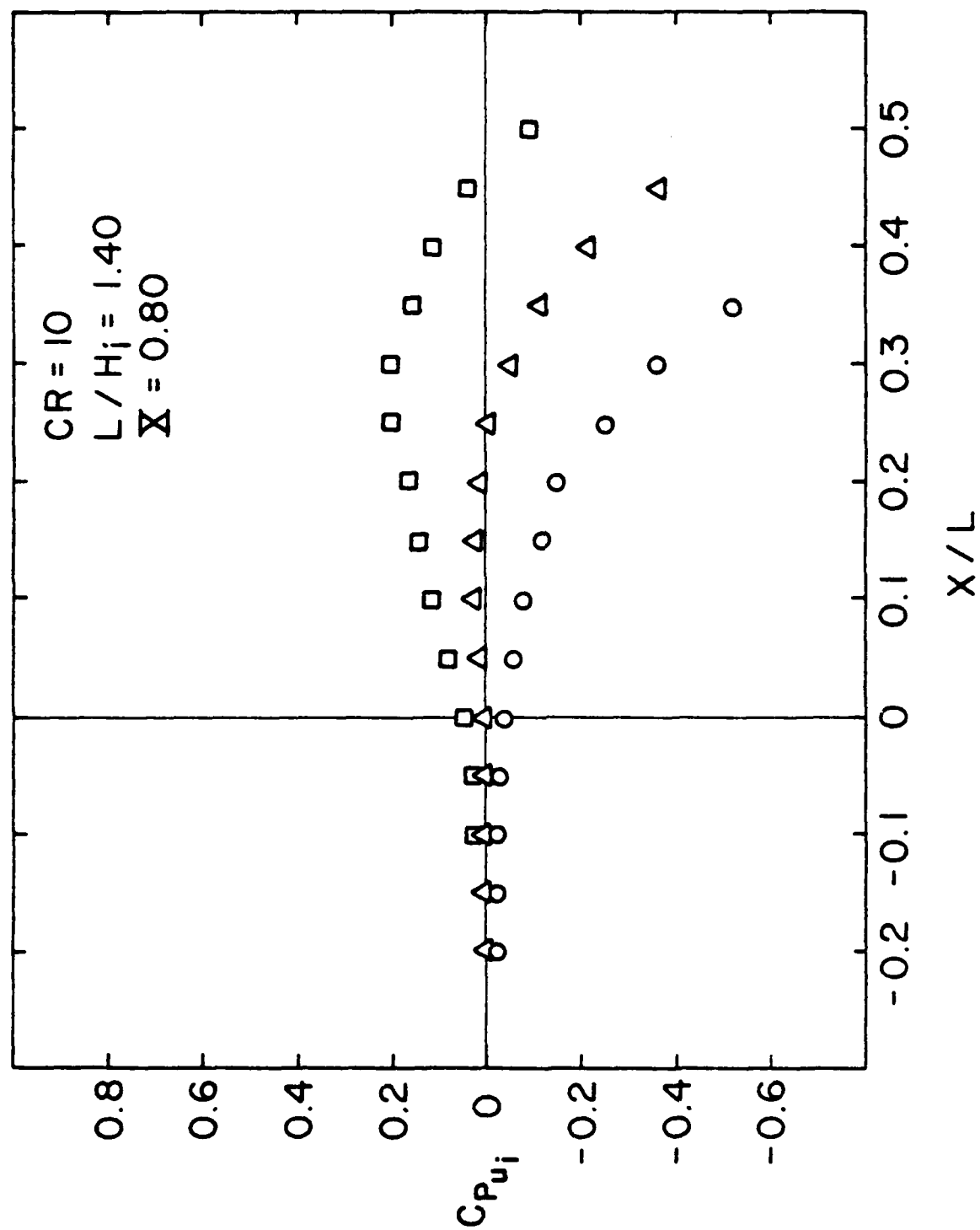
b. $L/H_i = 0.80$, $X = 0.80$

Figure 45. Pressure Distribution, $CR = 10$



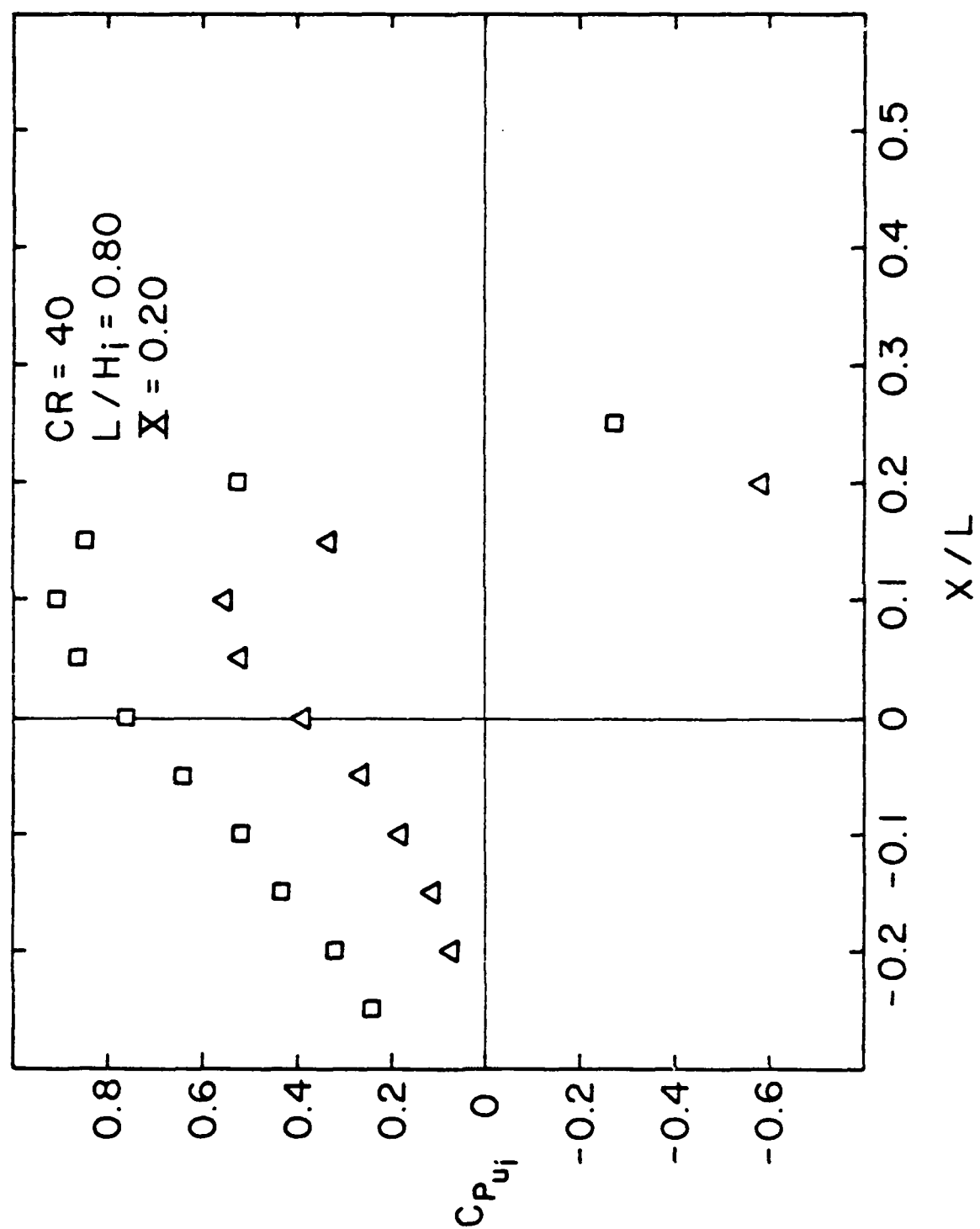
c. $L/H_i = 1.40$, $X = 0.20$

Figure 45. Pressure Distribution, $CR = 10$



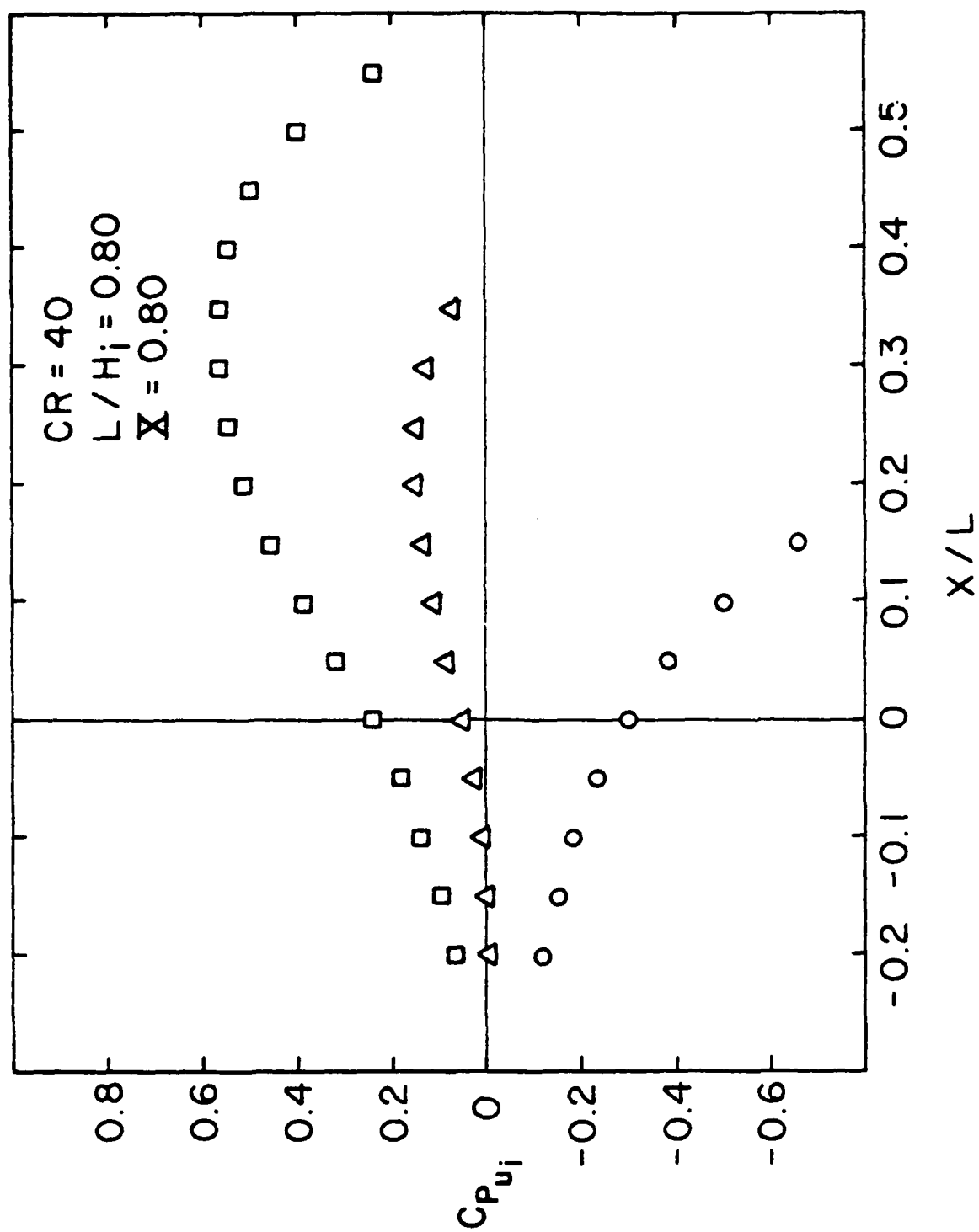
d. $L/H_i = 1.40$, $X = 0.80$

Figure 45. Pressure Distribution, CR = 10



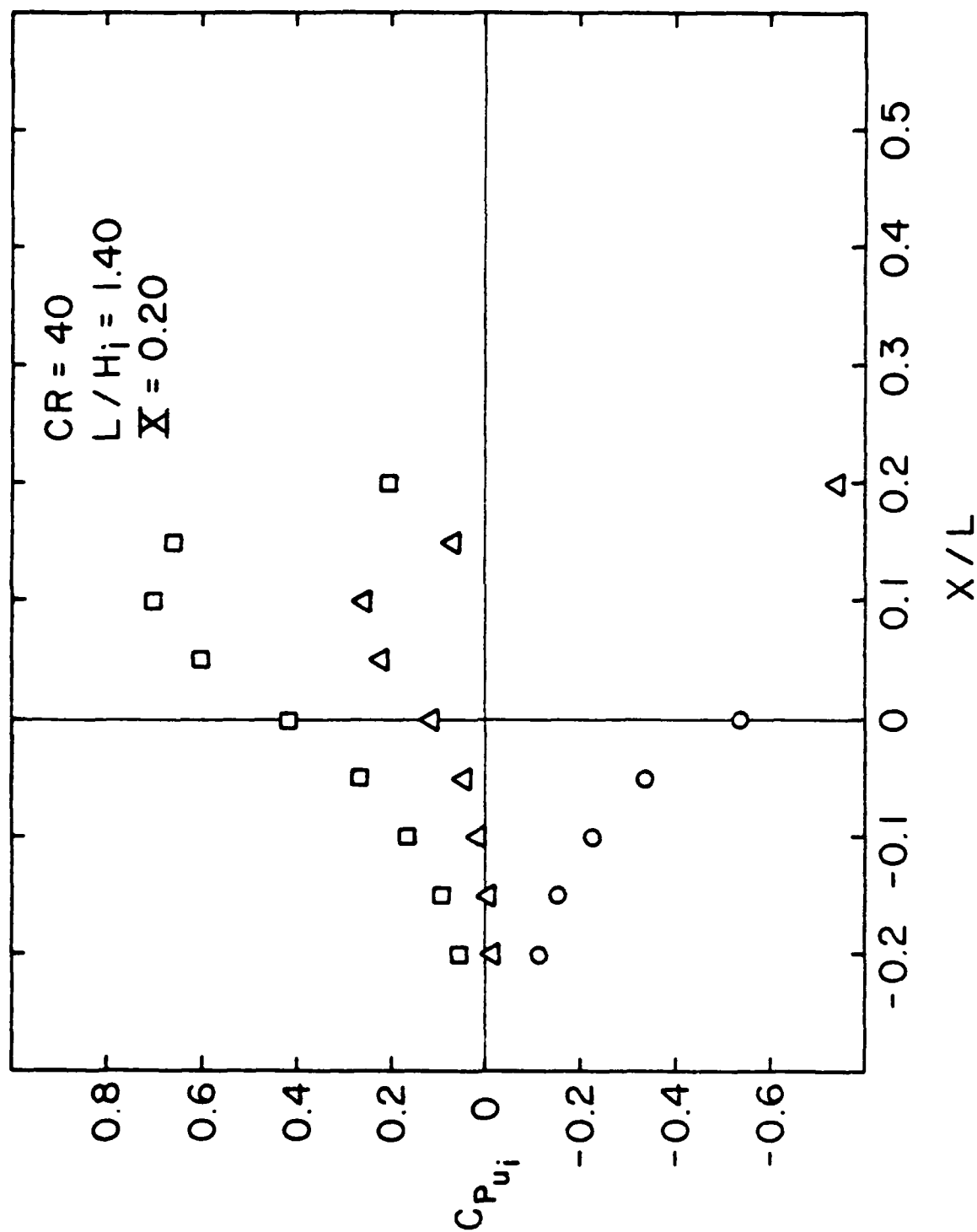
a. $L/H_i = 0.80$, $X = 0.20$

Figure 46. Pressure Distributions, CR = 40



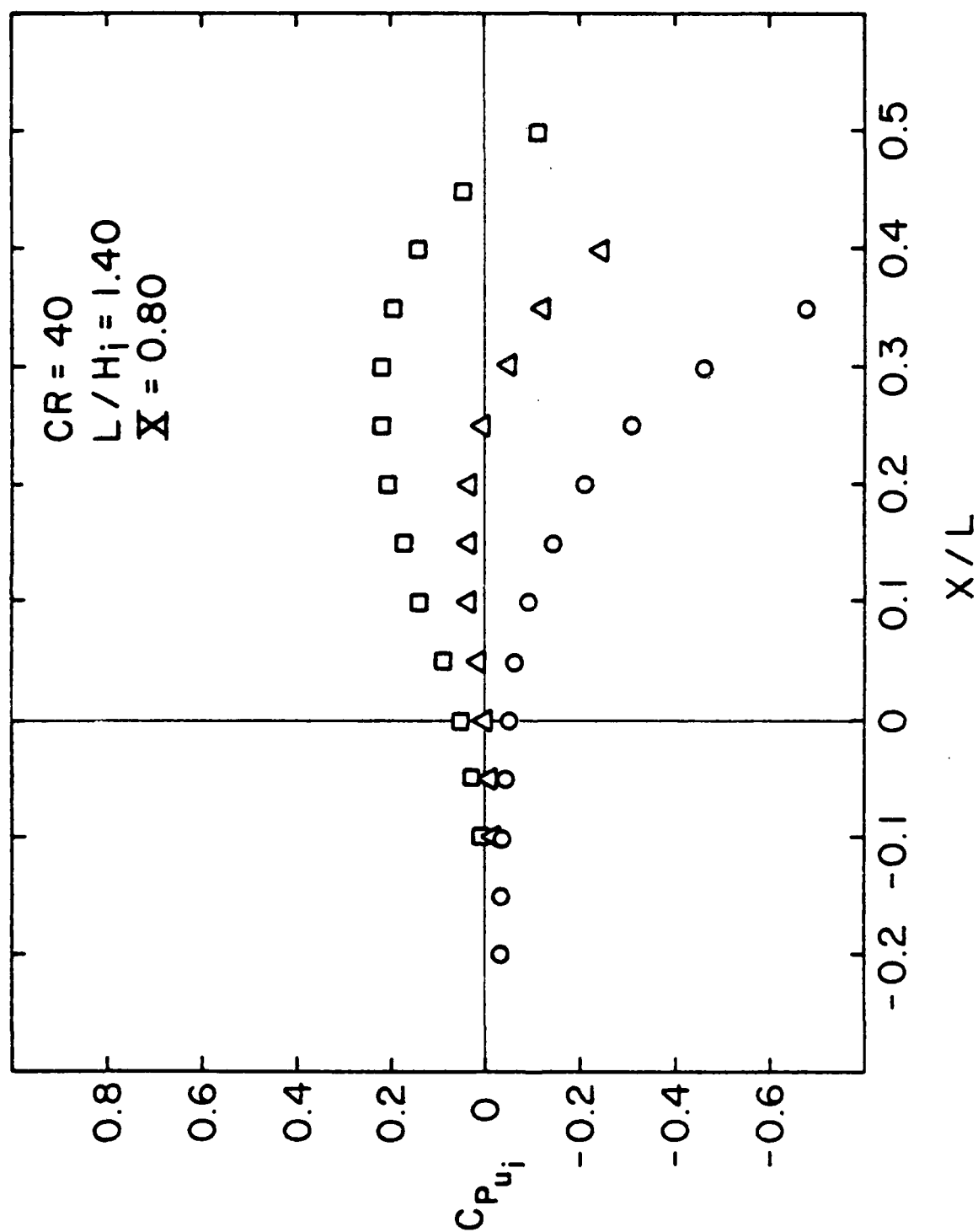
b. $L/H_i = 0.80$, $X = 0.80$

Figure 46. Pressure Distributions, CR = 40



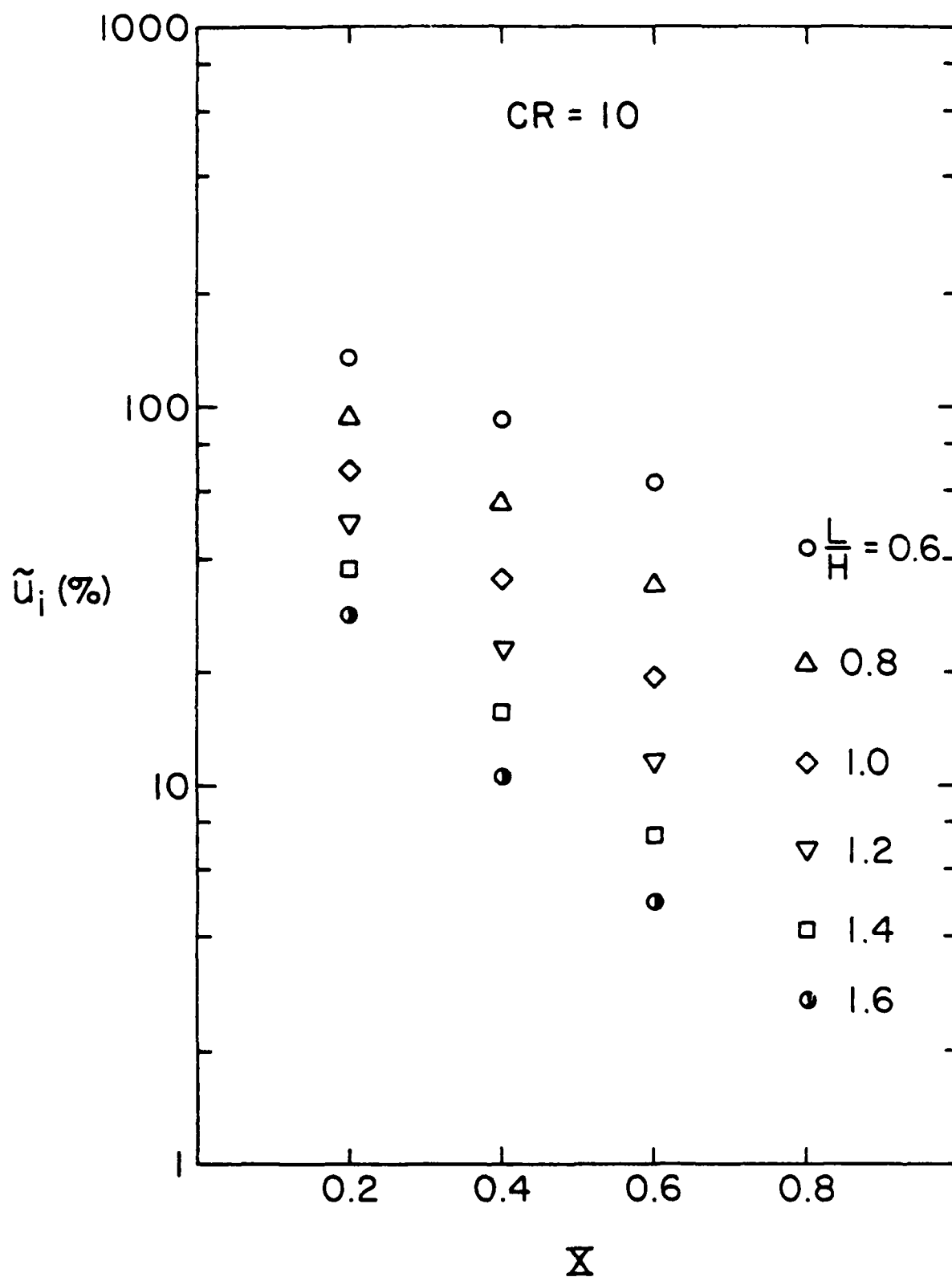
c. $L/H_i = 1.40$, $X = 0.20$

Figure 46. Pressure Distributions, CR = 40



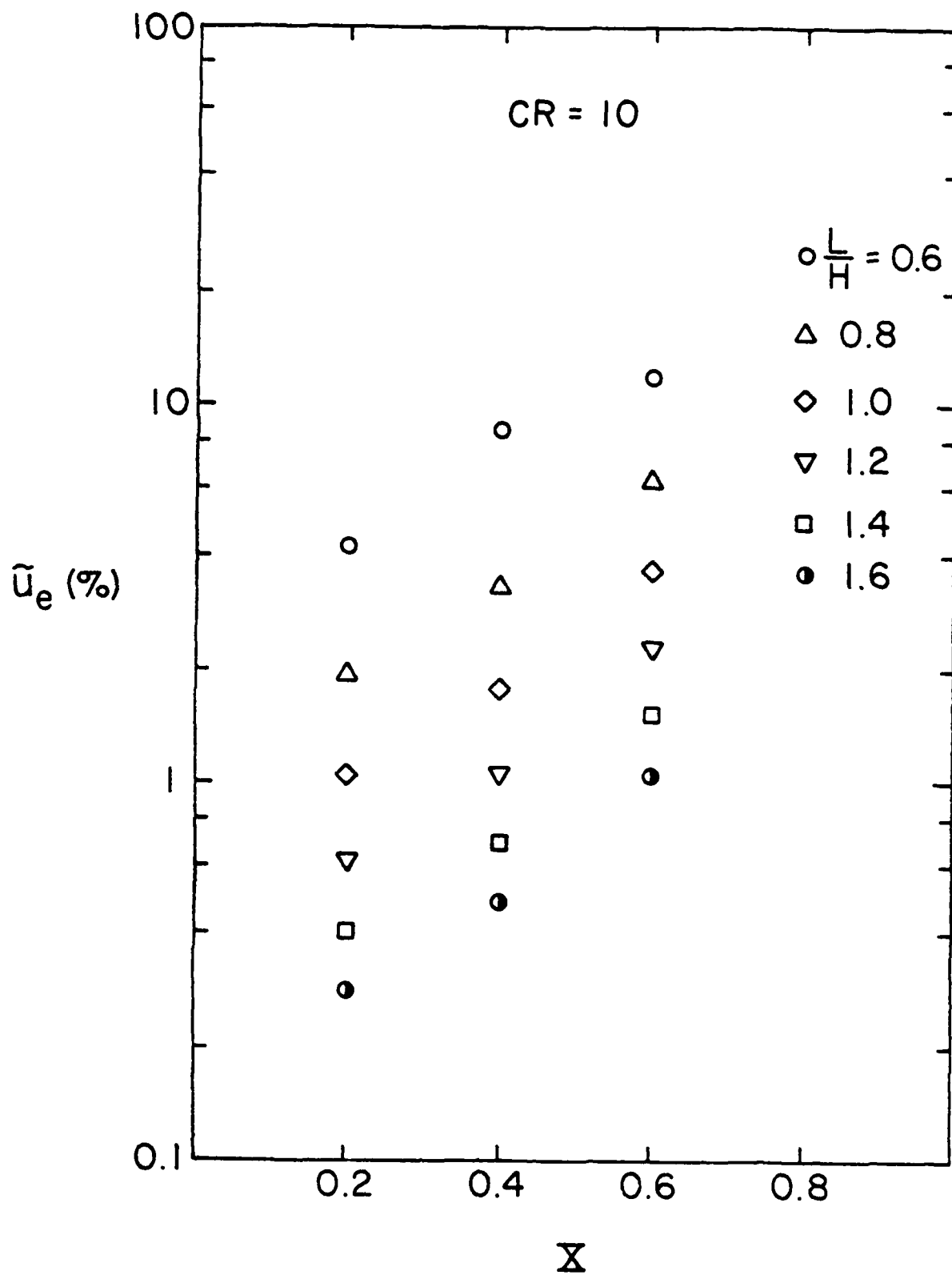
d. $L/H_i = 1.40$, $X = 0.80$

Figure 46. Pressure Distributions, $CR = 40$



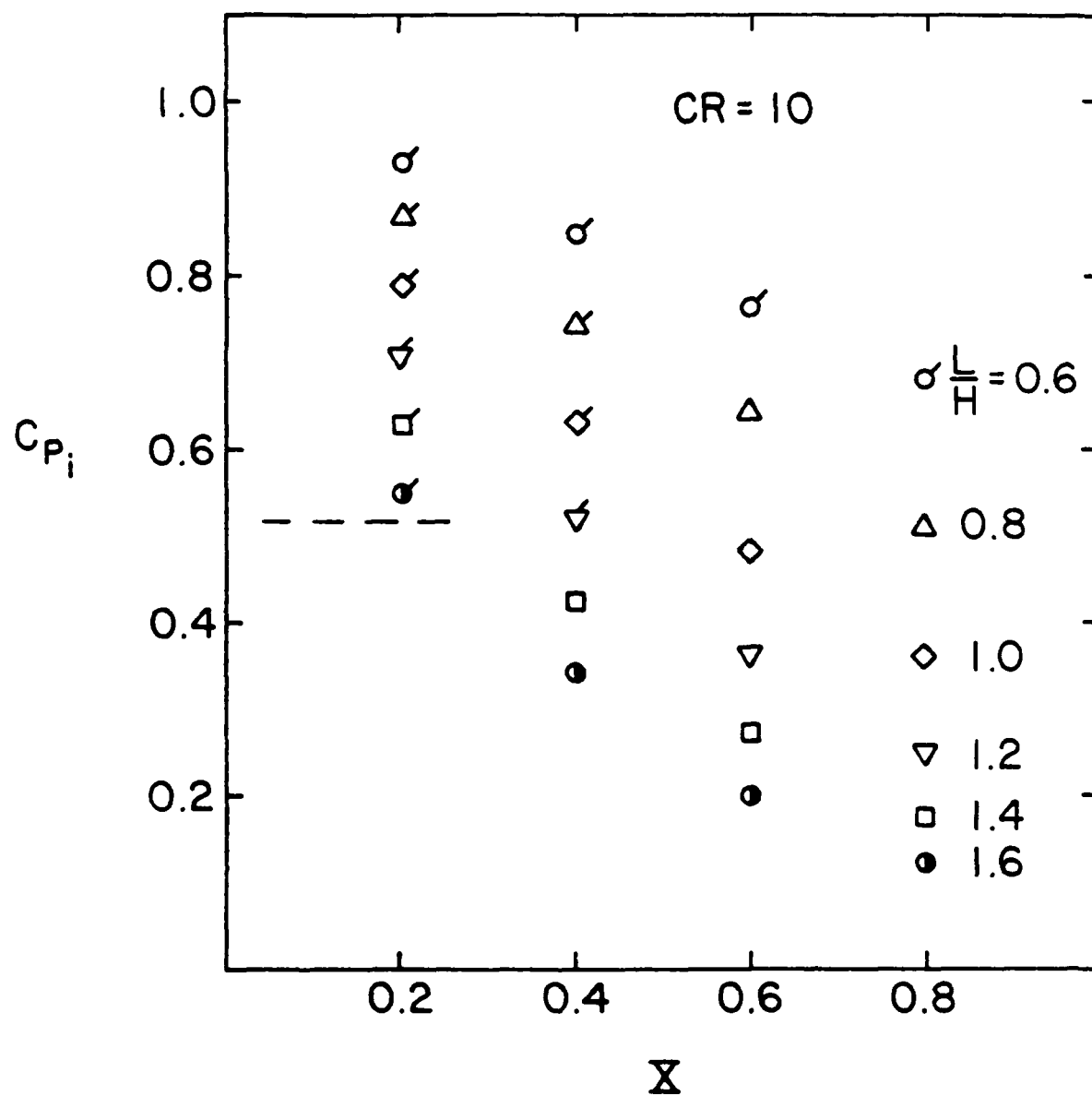
a. \tilde{u}_i vs X

Figure 47. Inlet Design Charts, CR = 10, H/W = 1.0



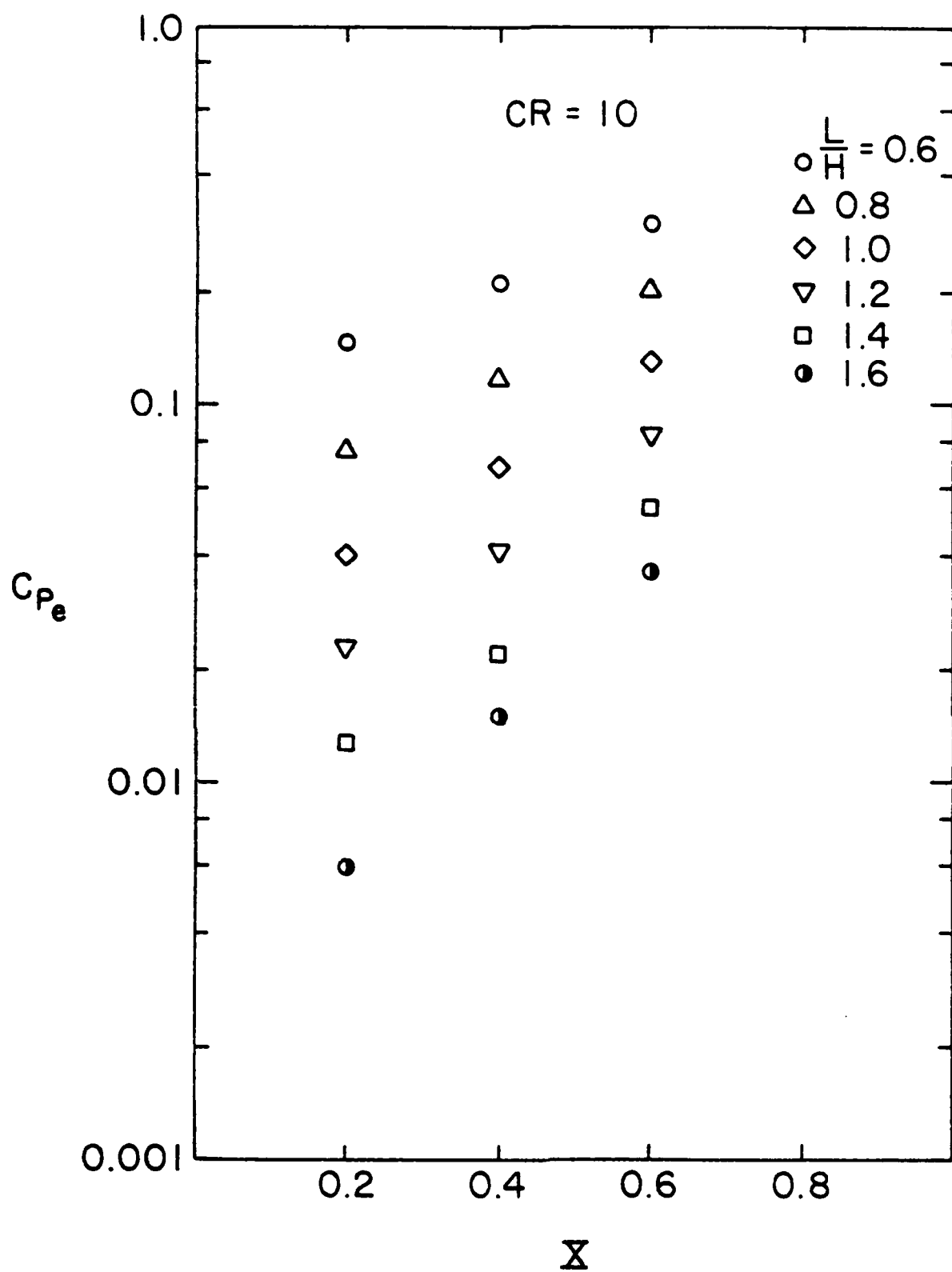
b. \tilde{u}_e vs X

Figure 47. Inlet Design Charts, CR = 10, H/W = 1.0



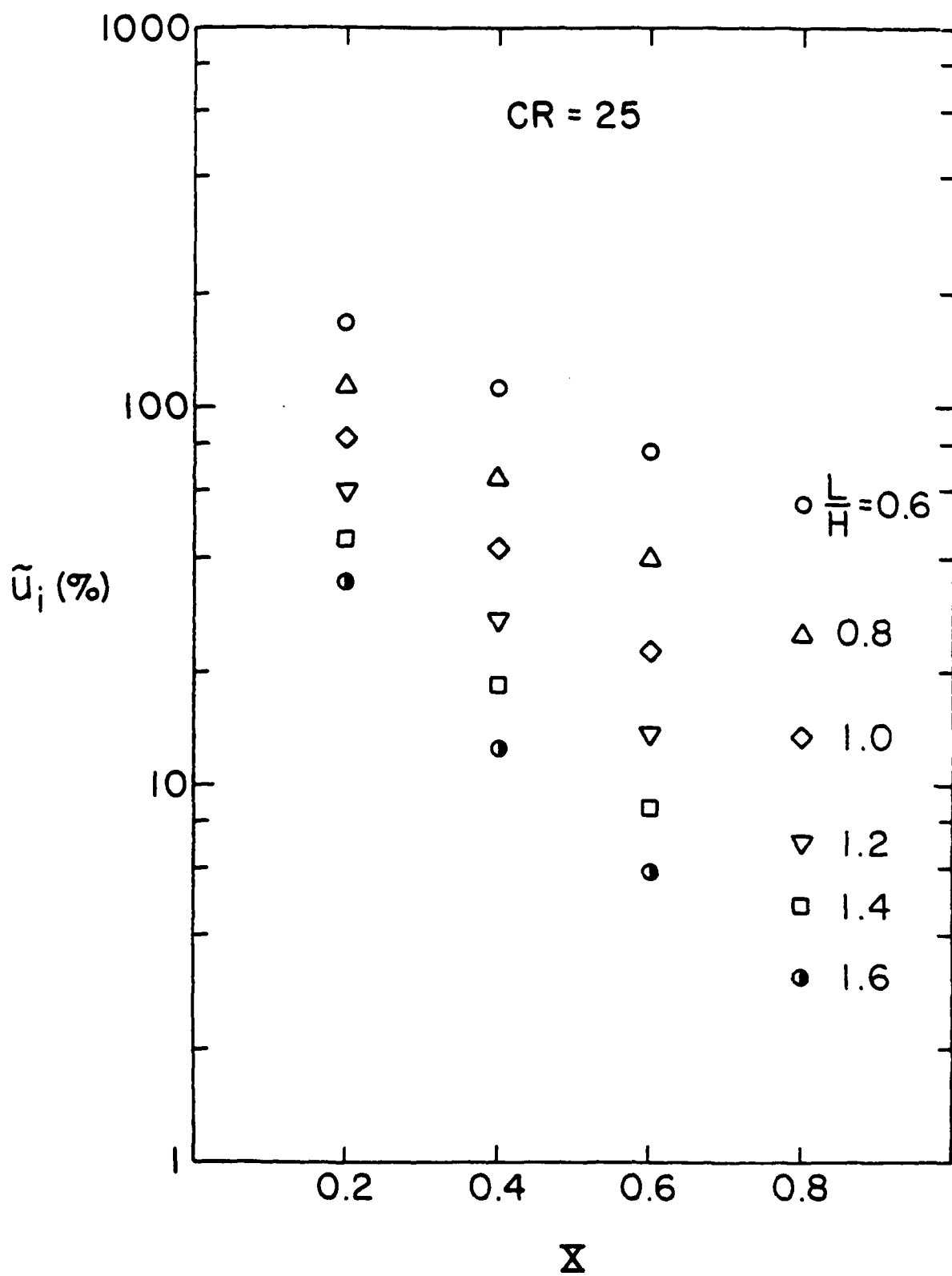
c. C_{P_i} vs X

Figure 47. Inlet Design Charts, CR = 10, H/W = 1.0



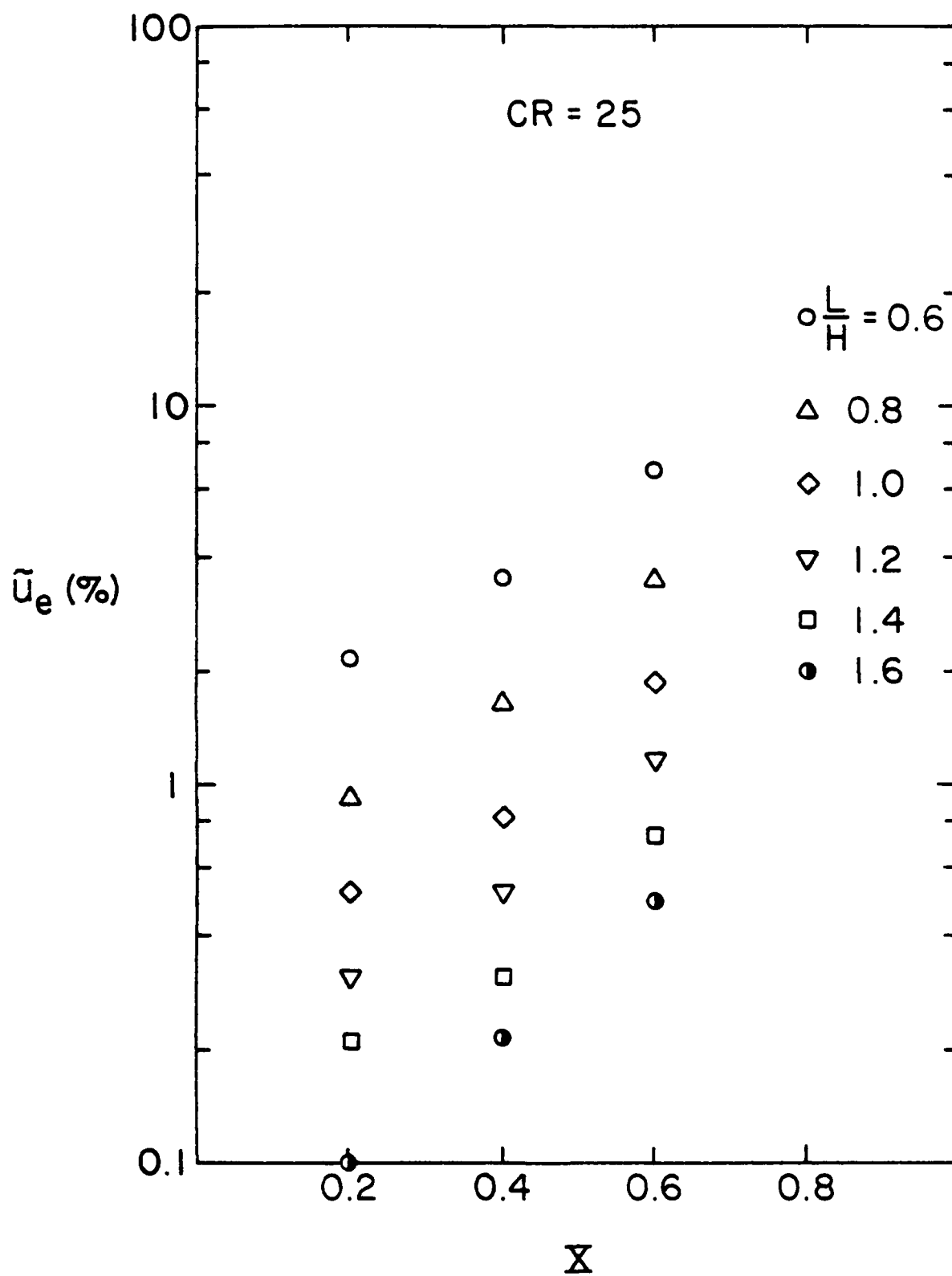
d. C_{Pe} vs X

Figure 47. Inlet Design Charts, CR = 10, H/W = 1.0



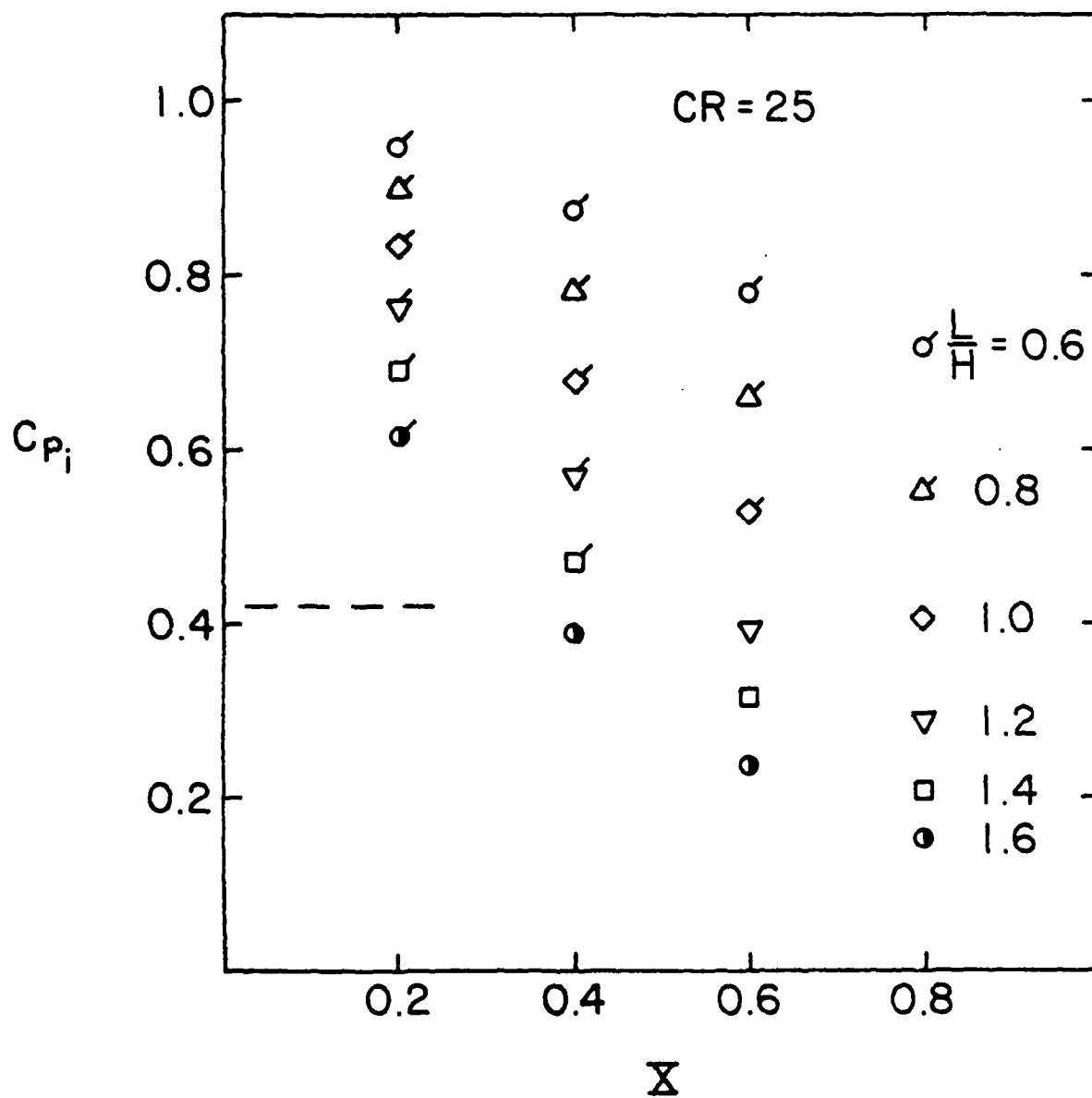
a. \tilde{u}_i vs X

Figure 48. Inlet Design Charts, CR = 25, H/W = 1.0



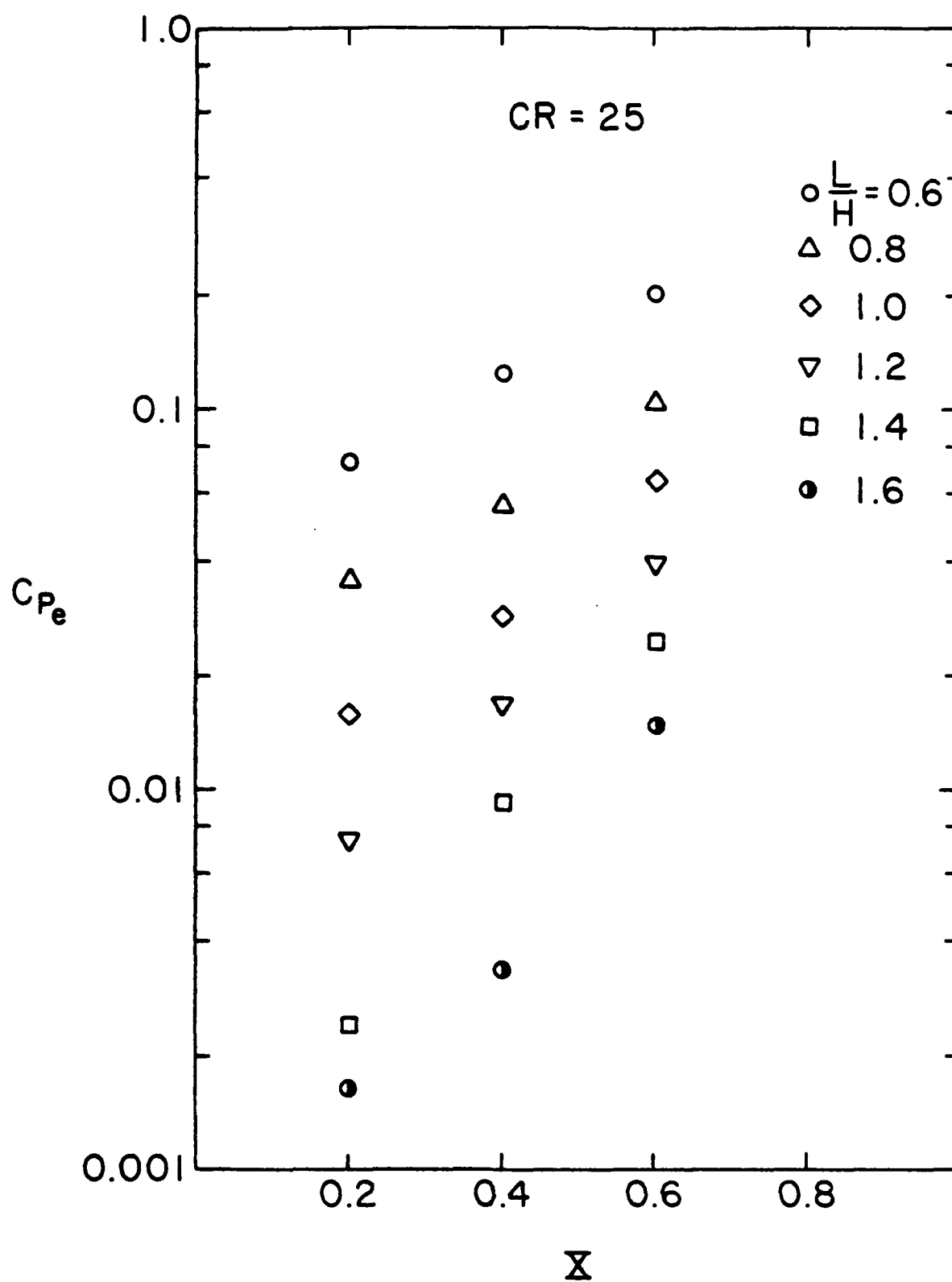
b. \tilde{U}_e vs X

Figure 48. Inlet Design Charts, CR = 25, H/W = 1.0



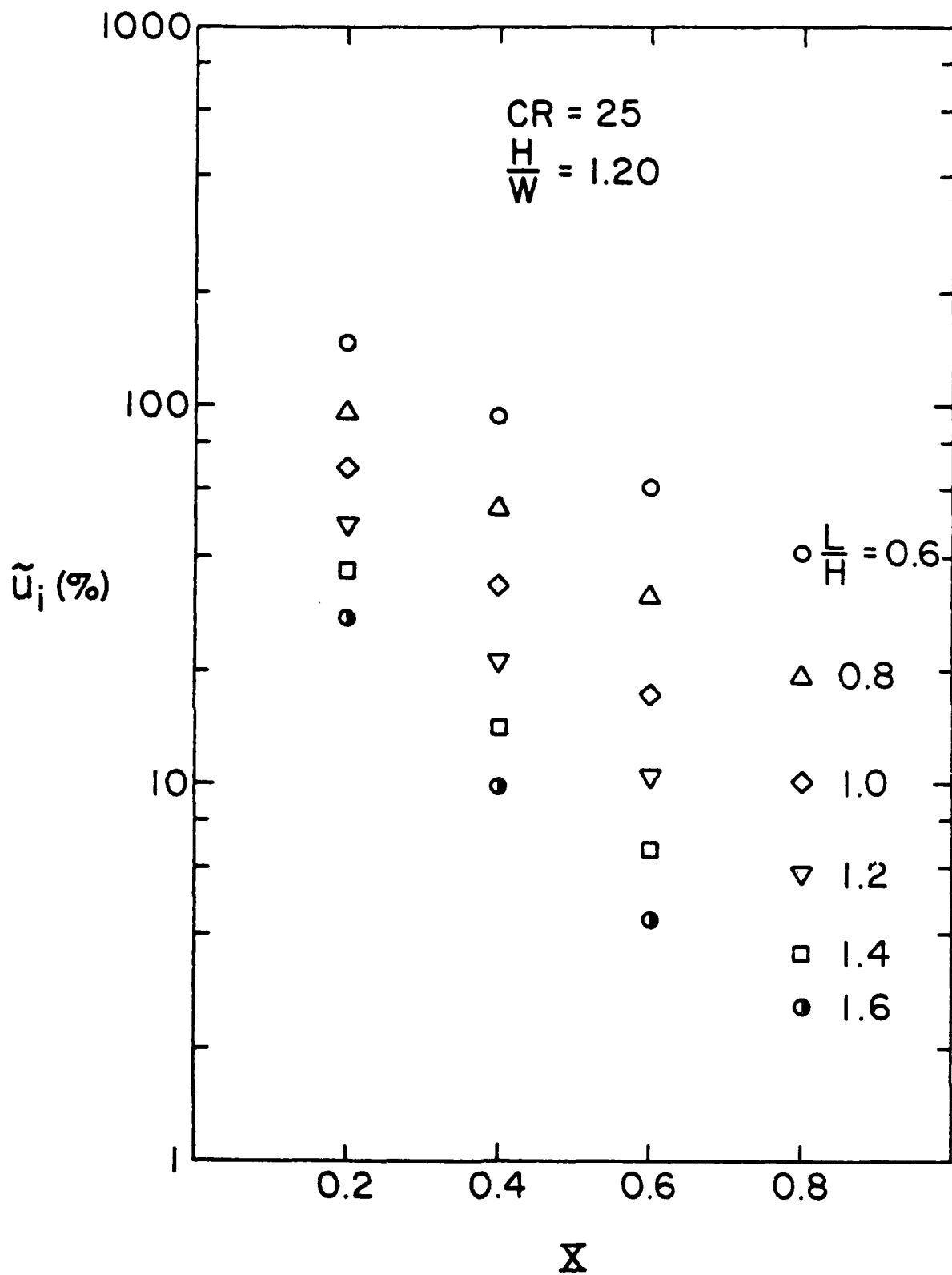
c. C_{p_i} vs X

Figure 48. Inlet Design Charts, CR = 25, H/W = 1.0



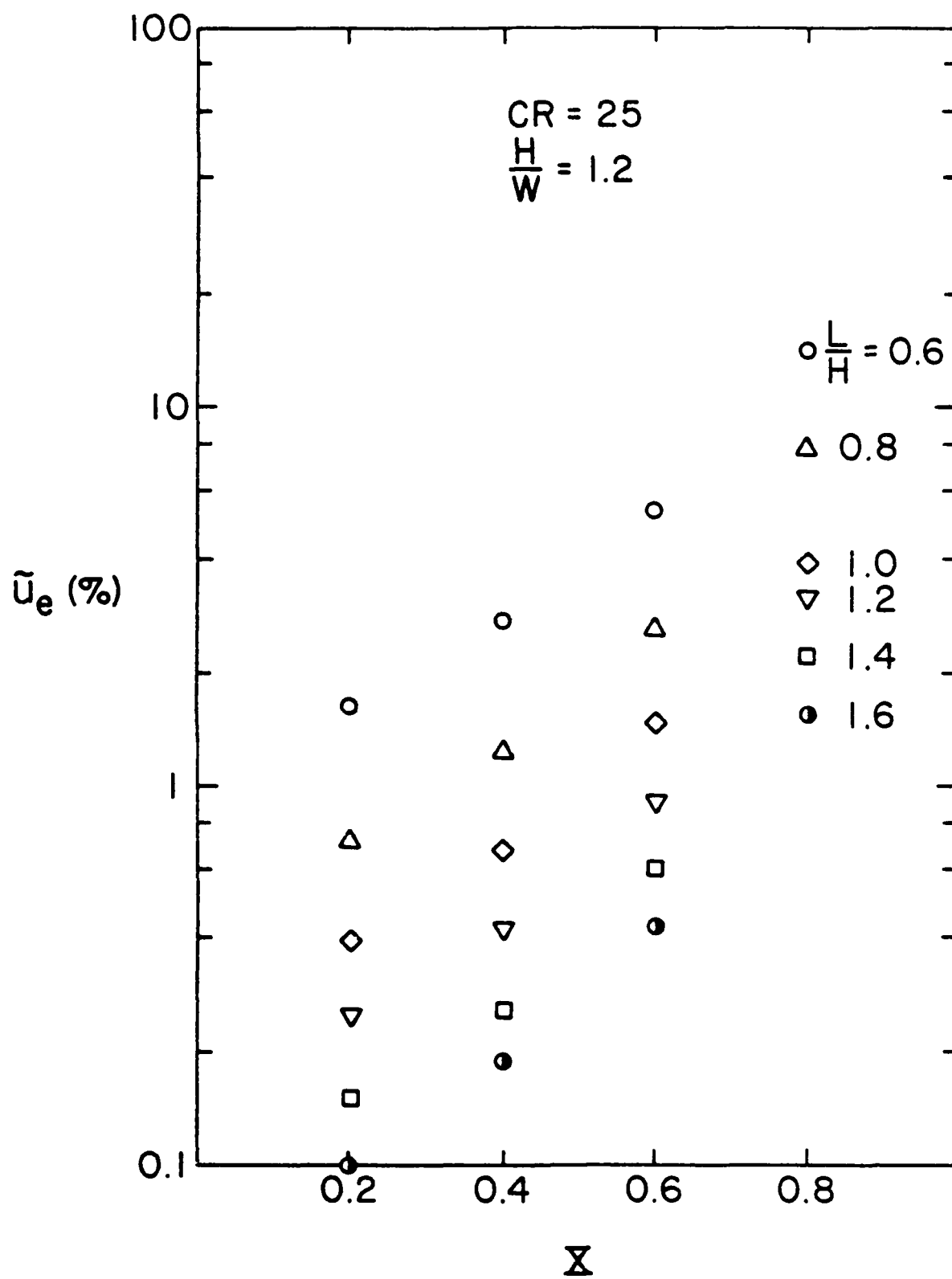
d. C_{Pe} vs X

Figure 48. Inlet Design Charts, CR = 25, H/W = 1.0



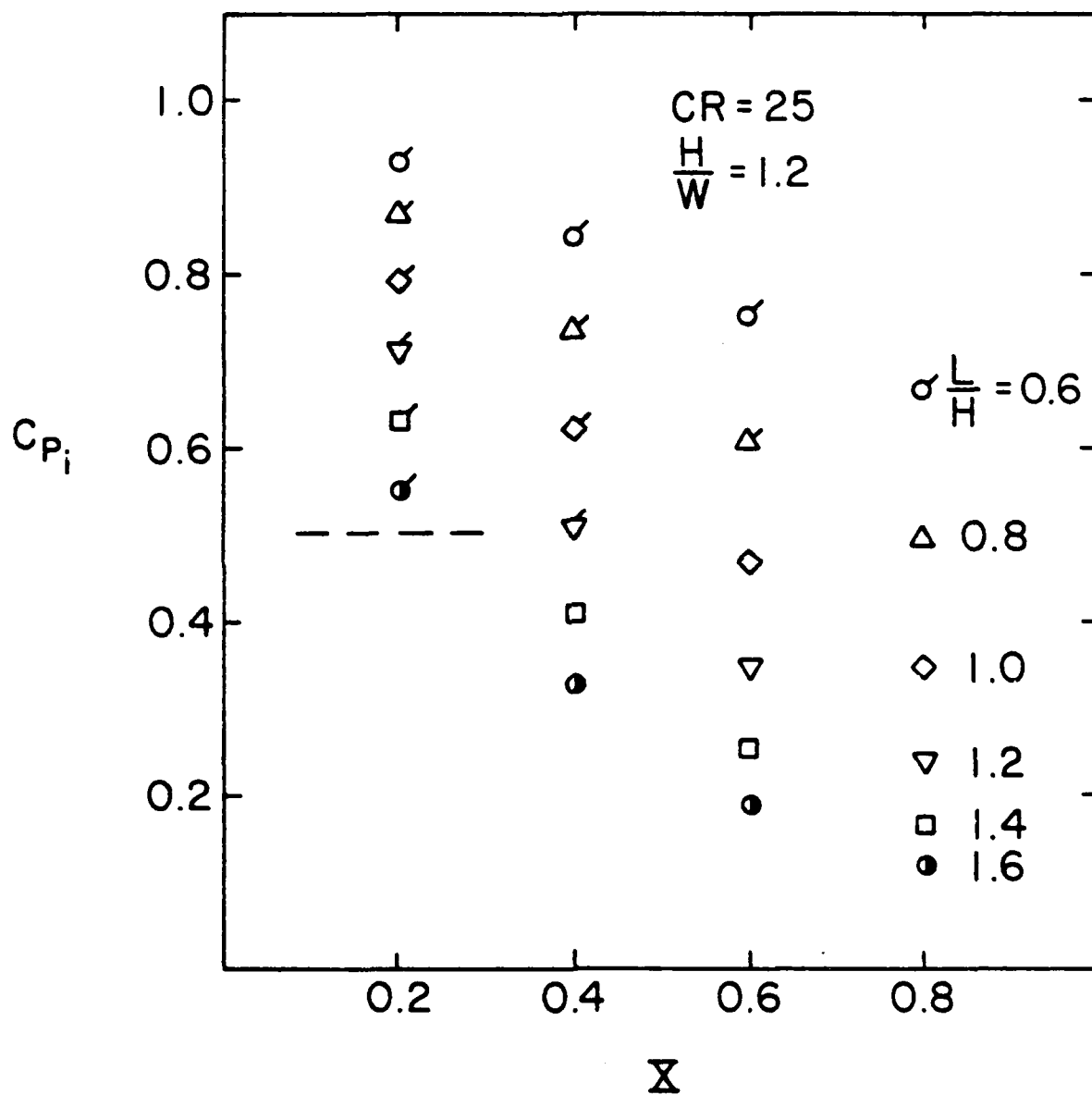
a. \tilde{u}_i vs X

Figure 49. Inlet Design Charts, CR = 25, H/W = 1.20



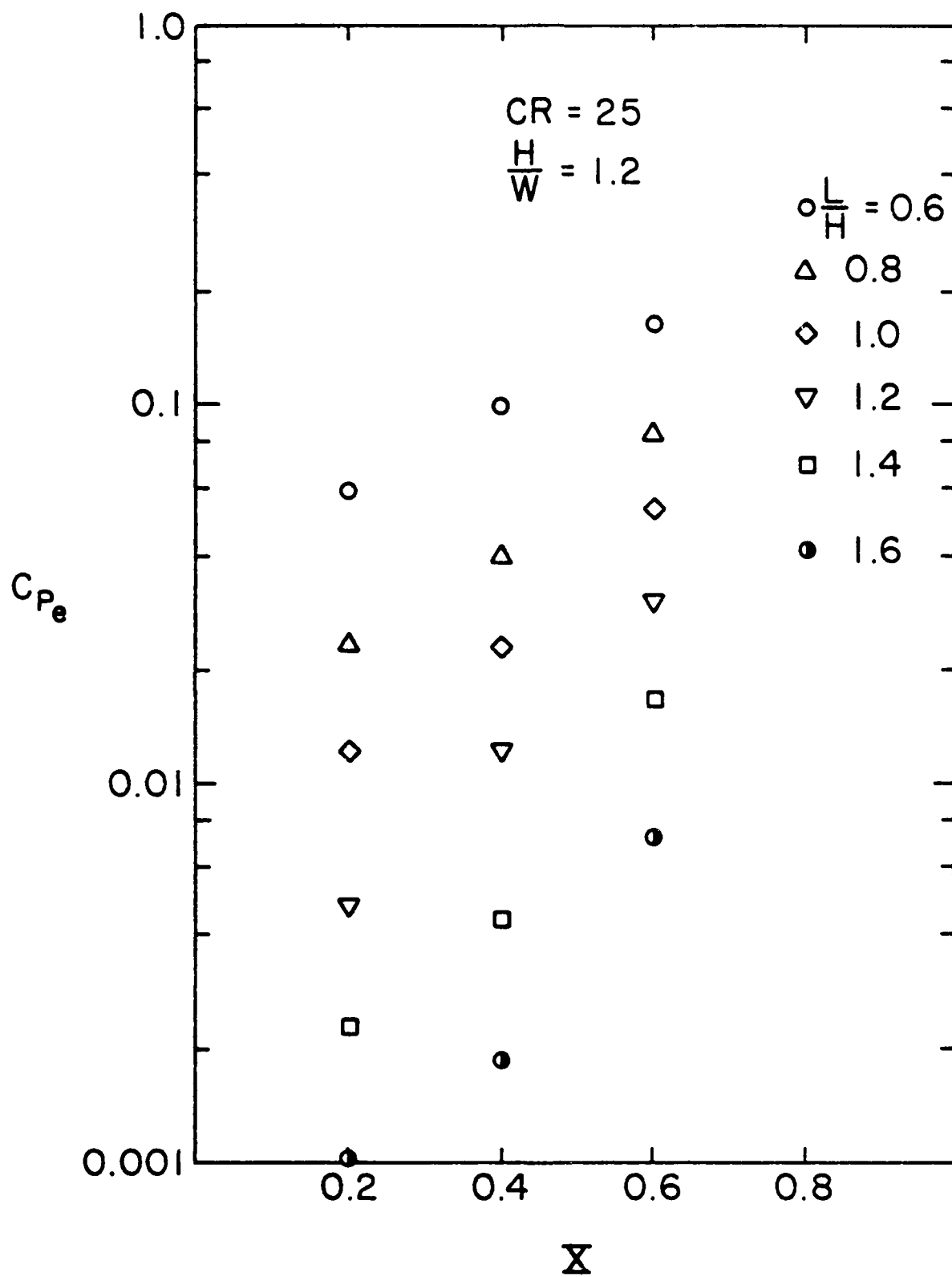
b. \tilde{U}_e vs X

Figure 49. Inlet Design Charts, CR = 25, H/W = 1.20



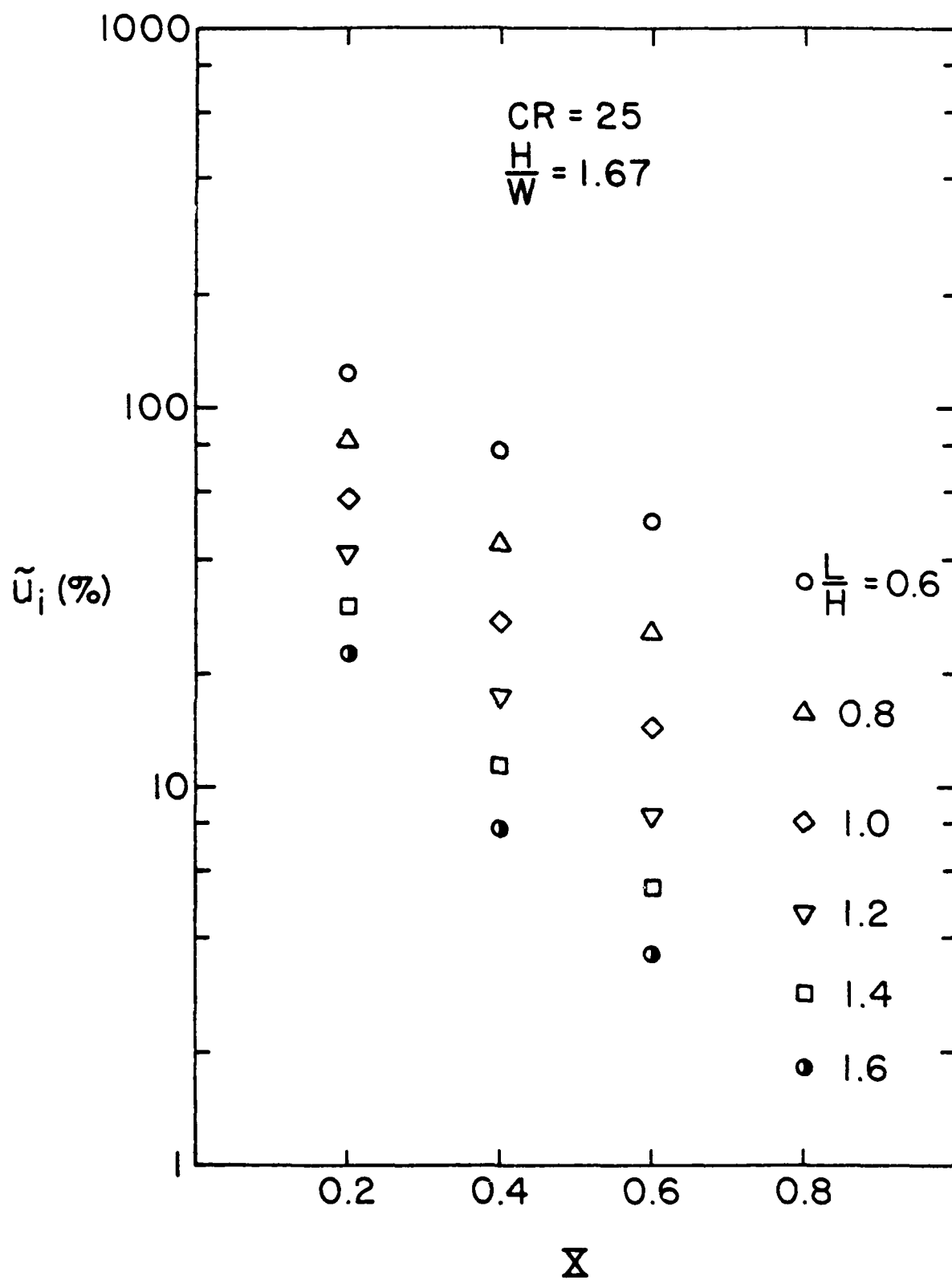
c. C_{P_i} vs X

Figure 49. Inlet Design Charts, CR = 25, H/W = 1.20



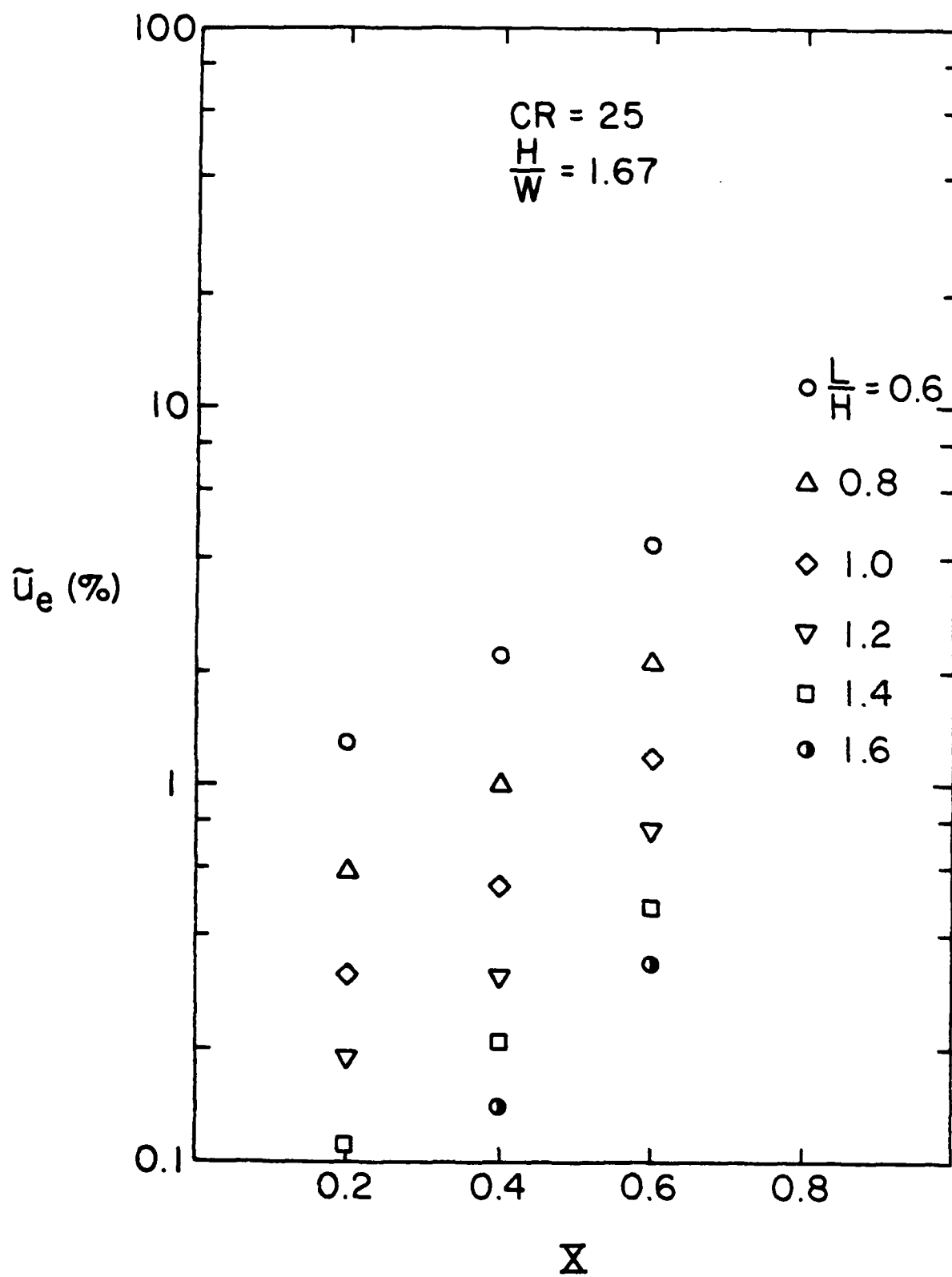
d. C_{Pe} vs X

Figure 49. Inlet Design Charts, CR = 25, H/W = 1.20



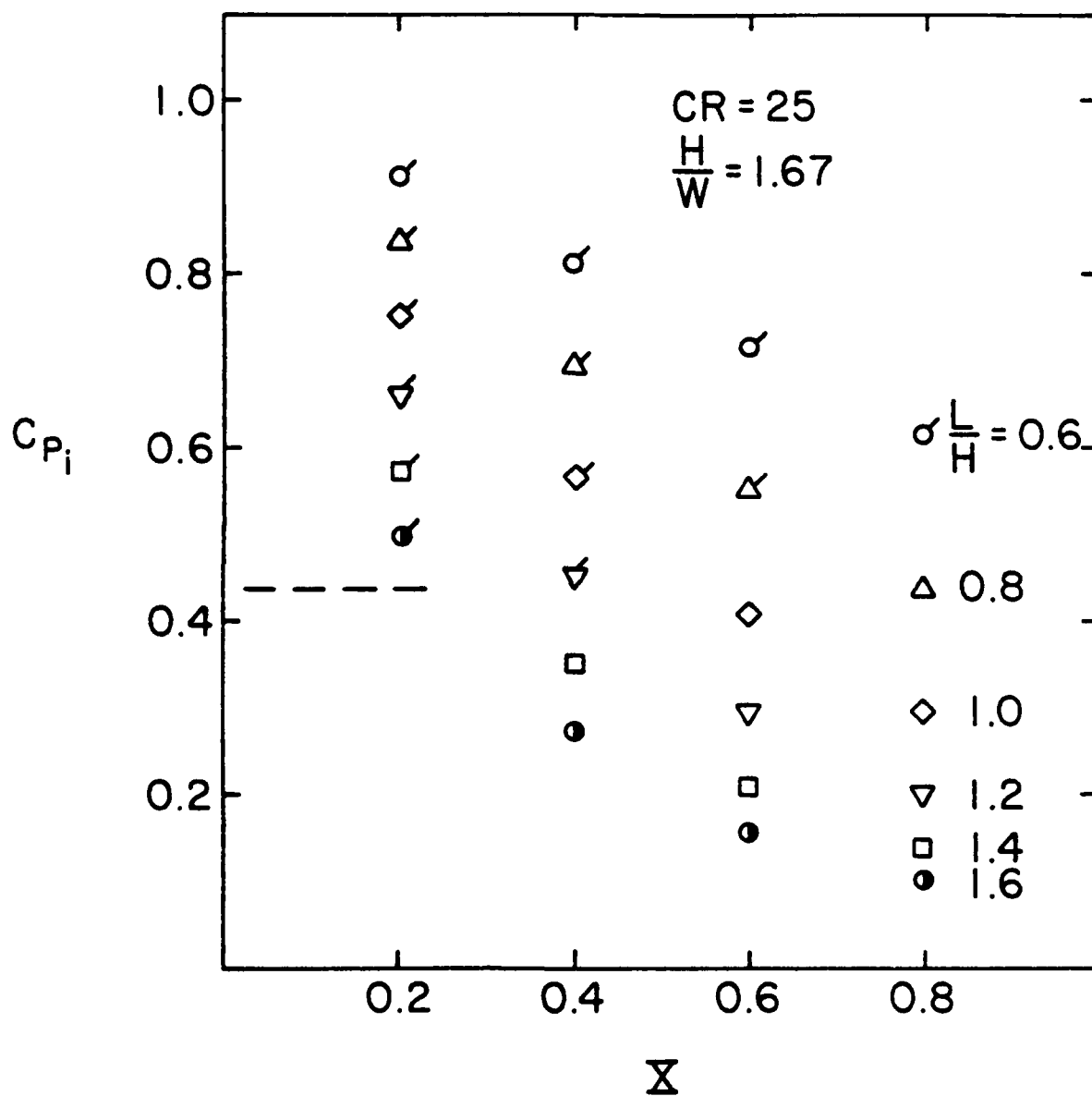
a. \tilde{u}_i vs X

Figure 50. Inlet Design Charts, CR = 25, H/W = 1.67



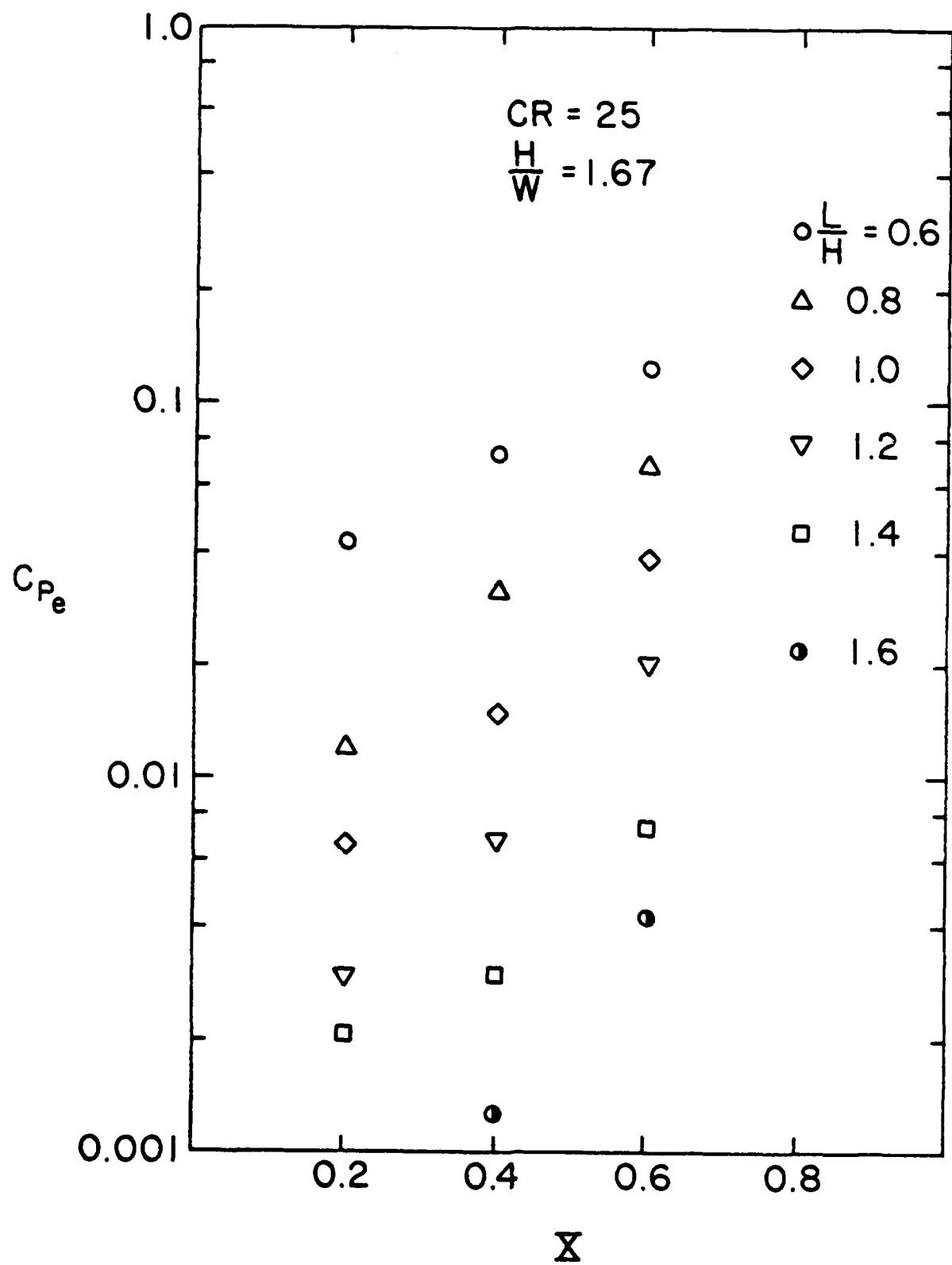
b. \tilde{u}_e vs X

Figure 50. Inlet Design Charts, CR = 25, H/W = 1.67



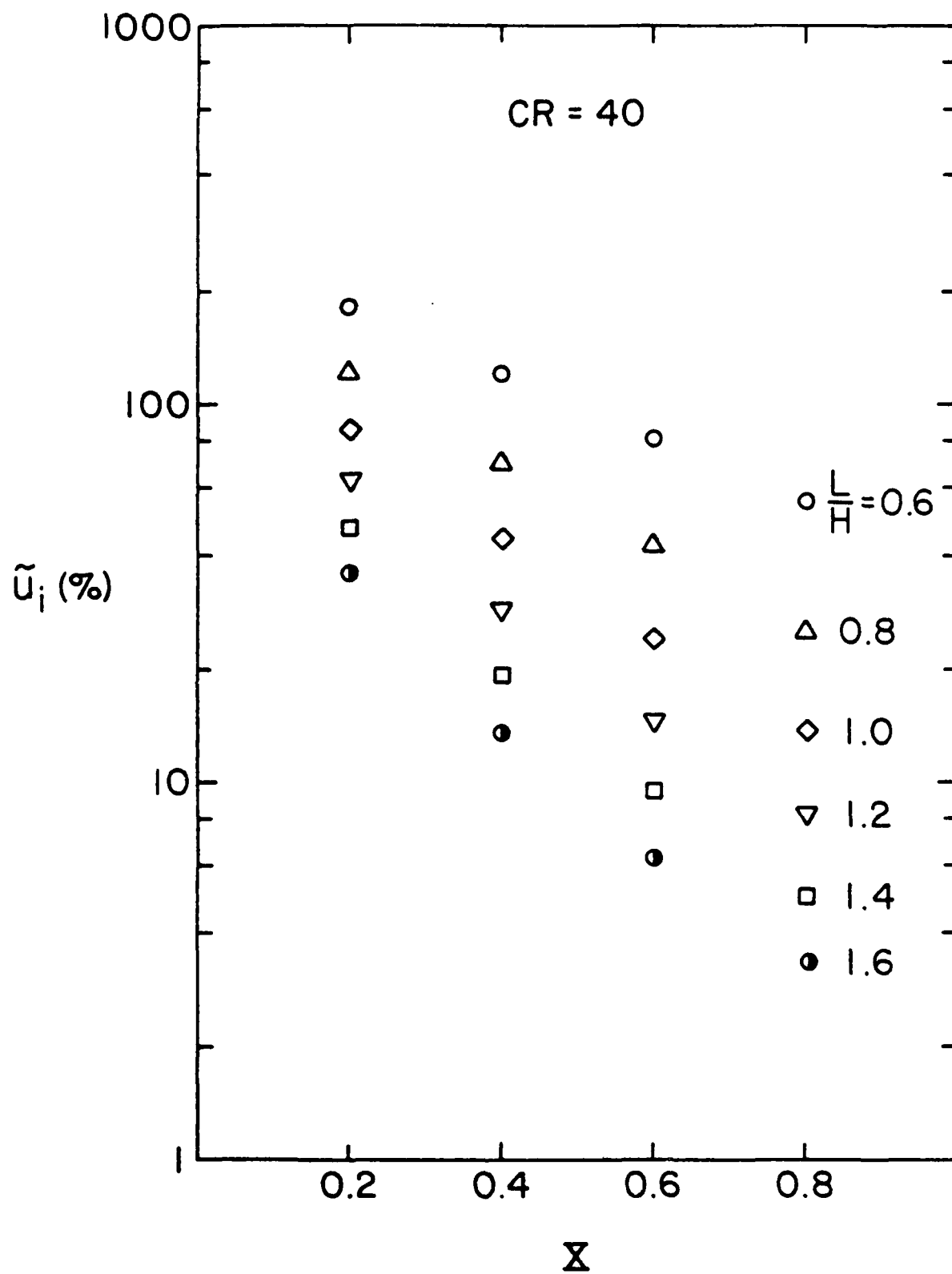
c. C_{Pi} vs X

Figure 50. Inlet Design Charts, CR = 25, $H/W = 1.67$



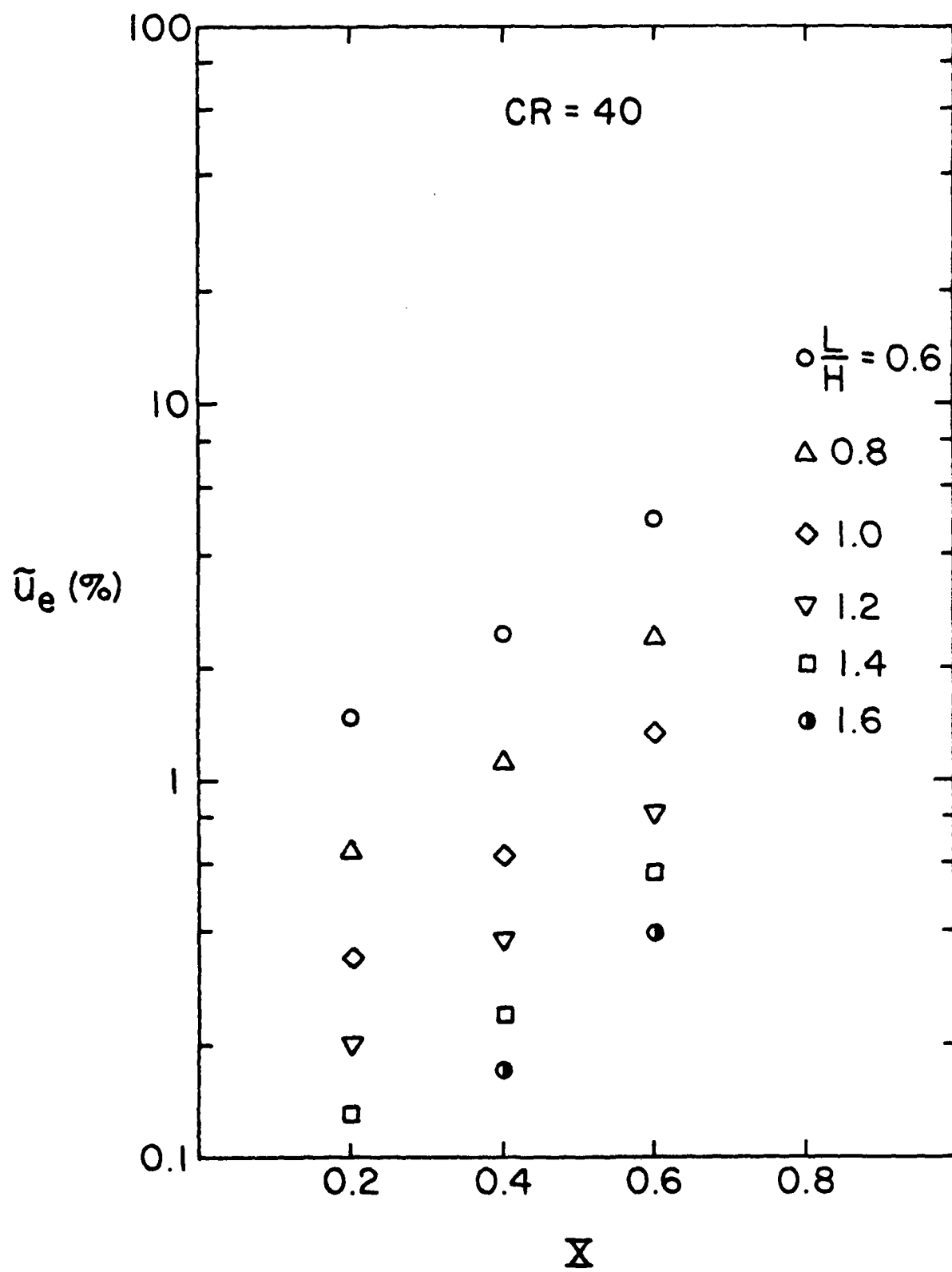
d. C_{Pe} vs X

Figure 50. Inlet Design Charts, CR = 25, H/W = 1.67



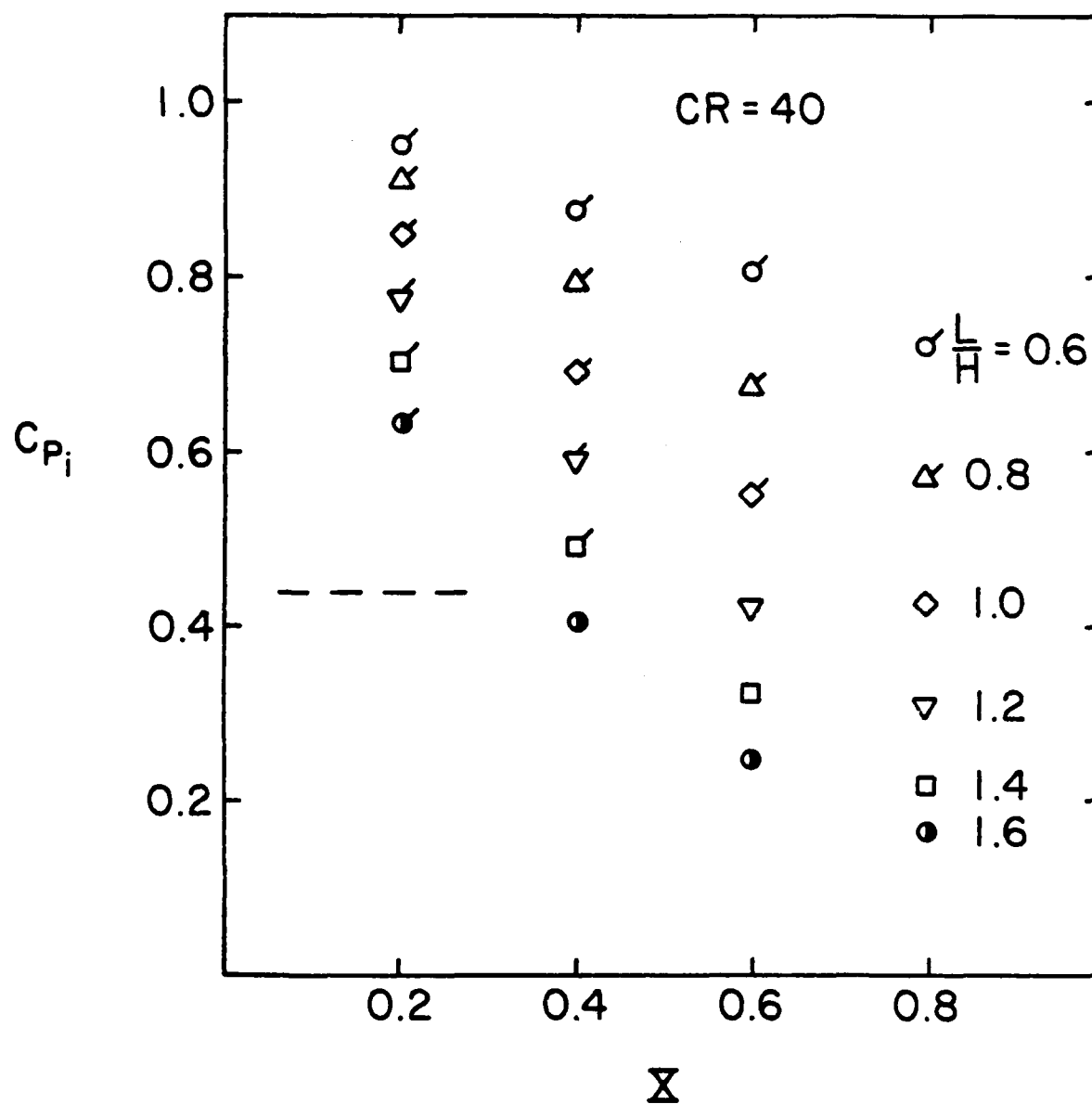
a. \tilde{u}_i vs X

Figure 51. Inlet Design Charts, CR = 40, H/W = 1.0



b. \tilde{u}_e vs X

Figure 51. Inlet Design Charts, CR = 40, H/W = 1.0



c. C_{Pi} vs X

Figure 51. Inlet Design Charts, CR = 40, H/W = 1.0

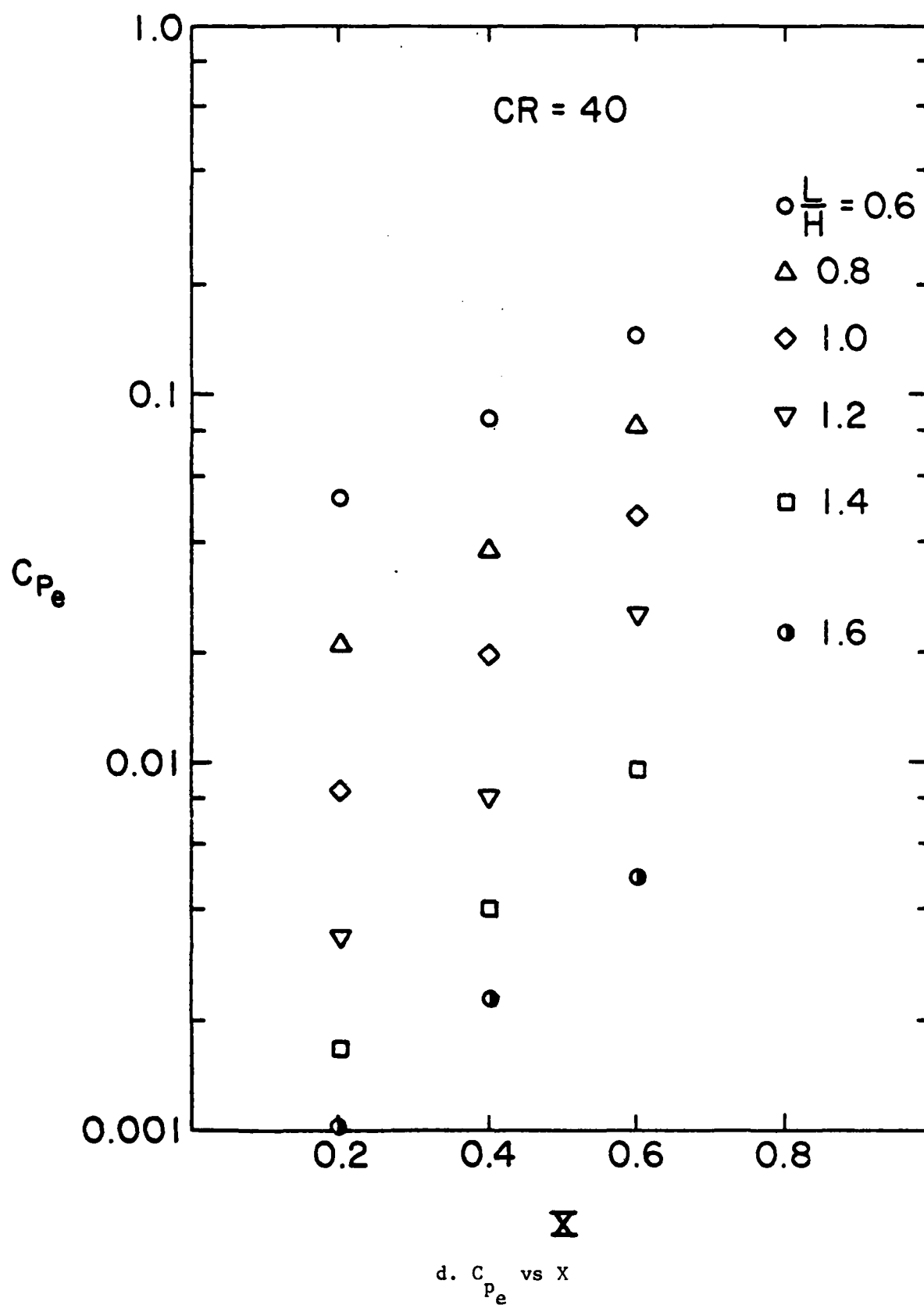


Figure 51. Inlet Design Charts, $CR = 40$, $H/W = 1.0$

END

FILMED

4-84

DTIC